Quantification of Performance of Wildfire Chemicals using a Custom-Built Sensible Enthalpy Rise Calorimeter

by

Razim Refai

A thesis submitted in partial fulfillment of the requirements for the degree of

Master of Science

Department of Mechanical Engineering

University of Alberta

ABSTRACT

A simple and effective laboratory experiment was developed to investigate the relationship between coverage level, fuel load, and fire intensity for different vegetative fuels. The experiment consisted of a fuel bed consisting of known quantities of fuel load and applied coverage, and an electric-powered radiant heater as a heat source. Fire intensities from controlled laboratory experiments were statistically examined using analysis of variance and Tukey's Post Hoc tests to evaluate which coverage levels and fuel loads produced significantly different fire intensities. It was found that the effect of coverage level and fuel load variation on fire intensity was dependent on the water retention characteristics of the fuel bed. Information from these experiments was used as input to develop a new laboratory test methodology to evaluate the performance of wildland forest fire chemicals. The proposed custom-built thermal calorimeter, referred to as the "Thermal Canister" in this study, consisted of a rectangular aluminum enclosure that was used to house vegetative fuel beds, and a radiant heater that was used to supply a uniform heat load to ignite the fuel. Temperature data gathered from the thermocouples attached to the surfaces of the enclosure was used as input to a one-dimensional heat conduction model to estimate the heat release rate from the vegetative fuels during combustion. Water, foam, and two types of gels were used as wildfire chemicals to control ignition and combustion of the fuels. The test results indicated that the Thermal Canister was able to characterize the performance of the different fire chemical treatments by comparing the respective heat release rates that were measured by the device. Narrow standard deviation, coefficient of variation, and repeatability standard deviation values suggested that the test methodology was repeatable. The Thermal Canister test methodology can be considered as an alternative, low-cost approach to evaluate the performance of wildfire chemicals.

ACKNOWLEDGMENTS

I would like to express my appreciation to a number of people who have supported me along this journey. I would like to thank my supervisor, Dr. André McDonald for his unwavering support and constant encouragement throughout this graduate program experience. I have learned far more than just technical knowledge from your guidance and for this, I will always be grateful.

I would like to thank Rex Hsieh for his countless hours of company, both as a friend and as a mentor. You have made this project an enjoyable experience for which I will always be indebted. I would also like to thank the FPInnovations team: Ray Ault, Greg Baxter, Jim Thomasson, and Mark Ackerman for providing support along the way. Special thanks to my friends and colleagues in Edmonton who have stood by me through the two years that I have been here.

Last, but not least, I'd like to thank my parents Shamir and Waheeda Refai, as well as my brother Rehan for always being there for me. Your support and sacrifices have been imperative in getting me to where I am today and I will always be grateful for that.

TABLE OF CONTENTS

LIST OF FIGURES

LIST OF TABLES

NOMENCLATURE

A	area, m^2
Bi	Biot number
C_p	specific heat at constant pressure, J/kg K
d	depth, m
D	diameter, m
h	convection heat transfer coefficient, W/m^2 K
k	thermal conductivity, W/m K
L	length, m
l	characteristic length, m
m	mass flow rate, kg/s
p	pressure, N/m^2
q'	heat transfer rate, W
q''	heat flux, W/m^2
Re	Reynolds's number, $\mathrm{Re} = \frac{ul}{\nu}$
T	temperature, $^{\circ}C$
t	time, s
u	velocity, m/s
V	fluid velocity, m/s
W	thermal canister plate thickness, m
x, y, z	rectangular coordinates, m

Greek Symbols

α	thermal diffusivity (m^2/s)
ε	emissivity
ρ	density (kgm^{-3})
λ	separation constant (m^{-1})
ν	kinematic viscosity, m^2/s
σ	Stefan-Boltzmann constant, 5.67×10^{-8} W/m^2K^4
τ	function dependent on *t*, only
Φ	function dependent on *x*, only
Ψ	function dependent on *x* and *t*
ω	error variable
∞	ambient

Subscripts

c	cross-section
e	exhaust
i	initial
s	surface
t	total

1 INTRODUCTION

1.1 WILDLAND FOREST FIRES

High intensity wildland forest fires are a common occurrence in many forested areas of the world and have played an integral role in influencing the structure and function of forest ecosystems [1]. Recently, there has been a significant increase in wildland fire activity in different parts of the world [2]. Climate change factors such as increased temperatures, variability in atmospheric moisture conditions, and forest disturbances such as insects have been cited as reasons for an increase in the frequency of forest fire activity [2, 3-5]. Current trends in climate change towards warmer, drier summers suggest that a further increase in wildland fire activity is expected. Consequently, it is likely that an increased risk of significant damage caused by these wildfires is imminent [6-8].

Forest fires can be caused naturally by lightning or volcano activity [9, 10]. Studies have shown that lighting accounts for 80% of Canada's documented large fires between 1959 and 1997 [7]. Due to increased human activity in forested areas, the frequency of human-caused fires has also increased and represents a majority cause of ignition [7]. Expansion of residential developments into wildland-urban interfaces dramatically increase the threat posed by forest fires to the human population [11-12]. Forest fires are a substantial threat to the safety of communities around the world and have adverse environmental and economic impact [1]. Fire agencies in Canada and the United States have annually spent CAD $500 million and $1 billion on fire management and suppression, respectively, and with extreme fire weather conditions projected in the near future, these costs are expected to rise [13-14]. Of particular interest are the fires that occurred recently in Fort McMurray, AB and in several locations across the state of California that have resulted in a

significant rise in awareness of the damage that forest fires are capable of causing [15-16]. Extensive research in wildland forest fires would be highly beneficial towards improving wildfire mitigation practices and reducing the damage caused by it. An important aspect of this research is studying the energy exchange between wildland forest fires and the surroundings.

Taking into consideration the growing frequency of wildland forest fires as well as the threat that they pose to humans and their properties, it has become necessary to understand the complexity of wildland forest fires and their interaction with the surroundings in greater depth. An important step to understand this complexity is to distinguish between the different types of fires that occur in wildland forests. Forest fires are categorized into ground fires, surface fires, and crown fires [17]. Ground fires are slow moving fires that burn vegetative fuels such as peat, roots, organic soils, etc. underneath the surface of the ground [17]. Surface fires are the combustion of fuels near the surface such grass, leaves, and forest needles [17]. Crown fires are associated with extreme fire behavior where fire spread includes combustion of the top of trees [17-18]. Wind speed and direction are also variables that make prediction of fire behavior difficult [17]. Another important variable that determines forest fire behavior is the type of vegetative fuel that is available for the fire to consume. The various fuel types found in forests, each with its own flammability characteristics, have an extensive impact on fire behavior and consequently, on the intensity of forest fires.

1.2 WILDLAND FIRE FUEL CHARACTERISTICS

A forest ecosystem typically consists of different types of vegetation, all of which can serve as fuel in a forest fire. The size, shape, compactness, arrangement, quantity, moisture content, organic composition, and flammability, to name a few parameters, all play an important role in influencing

the intensity of a fire [17]. Several of these characteristics are interdependent; for example, the organic composition and moisture content can play a decisive role in determining the flammability of a vegetative fuel. While each individual vegetative fuel has its own characteristics, they are often present among other vegetative fuels in a forest environment and therefore require a broader classification. There are three categories that are used to differentiate among vegetative fuels based on their presence in a forest environment: ground fuels, surface fuels, and aerial fuels (see Figure 1-1). Ground fuels consist of roots and duff that are present below the surface of the ground [17]. The compact packing of ground fuels results in fires that have low rate of spread. Ground fires are particularly dangerous since smoldering can occur over long periods of time and are capable of restarting a fire that appears to have been extinguished. Surface fuels consist of moss, logs, leaves, and grass whereas aerial fuels consist of trees and tree branches [17]. The three different types of forest fires based on the fuel that they consume are all dangerous to any structures or personnel within its vicinity due to the amount of energy released to the surroundings during the combustion process. Thus, understanding the combustion process of these vegetative fuels is an important step in an attempt to measure the energy emitted from the combustion of these fuels.

Holton, *et al.* [19] discussed the several stages of the combustion process of forest vegetative fuels. In the pre-ignition phase, the vegetative fuel is heated and its temperature rises towards the ignition temperature. The ignition temperature is typically above the boiling temperature of water and is about 390°C for fuels composed mainly of cellulose (an organic polymer and important structural component in cells walls of vegetative fuels). Therefore, moisture present in

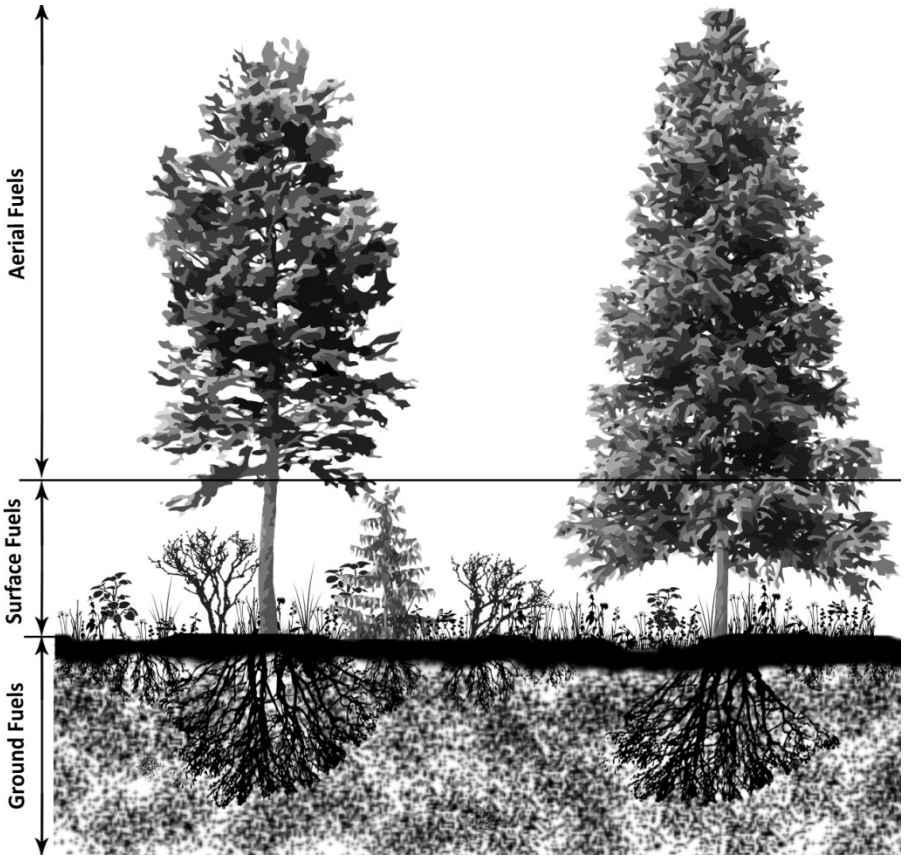

Figure 1-1: Categories of vegetative fuel types [18]

the vegetative fuel vaporizes before ignition of the fuel occurs. At high temperatures (200-340°C), the vegetative fuel undergoes thermal decomposition or pyrolysis (also called thermolysis). The products of pyrolysis are flammable gasses, solid char, and semi-volatile tar. Holton, *et al*. [19] further stated that ignition is the transition from the pre-ignition phase to the combustion phase, at a temperature at which external heating is no longer required. Once ignition has occurred, the heat generated by combustion of the fuel results in the ignition of the surrounding fuels, and the combustion process of surrounding fuels carries on. The heat generated during the combustion process of the fuel was found to be an important property in understanding the energy transfer of combusted vegetative fuels and is discussed later in Section 1.6 of this thesis. In order to minimize the combustion of these vegetative fuels and consequently mitigate wildland forest fires,

firefighting agencies work towards wildfire suppression by attempting to either keep vegetative fuels at a temperature that is below its ignition temperature or reducing oxygen available for combustion, thereby restraining the combustion process. Prior to studying details about wildfire suppression, it is important to understand energy transfer in forest fires.

1.3 MEASURING ENERGY TRANSFER IN WILDLAND FIRES

A fire requires three components for its sustenance: oxygen, heat, and fuel, which together make the fire triangle. In wildland fires, the fire behavior is influenced by the amount and arrangement of fuel, the weather, and the topography. These three components together make the fire behavior triangle. In order to translate observable fire behavior to useful information for the purposes of fire mitigation, structural protection, and development of safety protocol, energy emitted from a wildland fire must be quantified. An understanding of energy transfer from forest fires remains relatively rudimentary, partially due to the limitations of measuring devices for wildland fires [20]. Kremens, *et al.* [21] showed that there have been several methods developed to quantify energy released from a fire. The limitations of these available methods are often associated with the requirement of multiple measurements at a large scale in order to obtain data resolution that is able to provide sufficient information. One common method to measure the intensity of a forest fire is to use Byram's fireline intensity, which is defined as the rate of heat released per unit time per unit length of fire front, and is measured is kW/m [22]. Fireline intensity represents the radiant and convective energy of the flame front. Information about the fireline intensity is useful in fire suppression activities since it combines several factors of the fire such as rate of spread, fuel load, and heat of combustion into a single parameter [23-24]. The rate of spread of a fire is the linear rate of advance of a fire front in a direction perpendicular to it. The fuel load is the mass of available

fuel per unit area and the heat of combustion is the total energy released as heat when a substance undergoes complete combustion. Based on fire intensities, fires are often classified into several classes ranging from 1 to 6, where class 1 fires are smoldering surfaces with intensities less than 10 kW/m while class 6 represents fires with intensities greater than 10,000 kW/m [25]. While fireline intensity is a good indication of fire behavior, it is not helpful in quantifying the exact energy emitted from the fire that is incident on an object. Therefore, for the purposes of protection of objects from the energy emitted from wildfires, transfer of energy measured in terms of heat flux (in kW/m^2) would be more informative. Heat flux is the rate at which energy is transferred per unit area perpendicular to the direction of that transfer. This energy can be released or absorbed by the object or surface, and can be transferred by conduction, convection, and/or radiation. Measuring heat flux would provide a single parameter that can be measured with several devices such as a mass loss cone calorimeter or a heat flux sensor for the testing of materials or products against the incident energy of a wildfire. While there are several existing methods to measure energy transfer from wildfires, industry practitioners are still working on finding the ideal method to measure energy from wildfires that would further research in structure protection as well as help improve operations involving wildfire suppression.

1.4 WILDFIRE SUPPRESSION

Firefighting agencies employ different tactics in an effort to prevent or suppress wildland forest fires. Operations can include direct attacks where a treatment, either in the form of water or fire chemicals, is directly applied to the burning fuel, or indirect attacks involving the application of fire chemicals in advance of the fire front to create control lines [26]. Other indirect attack tactics include vegetative fuel reduction, contingency firelines, backburning, and wetting of unburnt fuels.

The application of water or fire chemicals is often done aerially using airtankers or helicopters to help reach areas that are inaccessible by road to cover the maximum possible area in limited available time. Wildfire industry practitioners use the term "coverage level" to quantify the volume of water or fire chemical applied on the vegetative fuel. One coverage level is defined as one U.S. gallon of fluid per 100 ft^2 of area [27].

There have been several drop tests conducted to evaluate the drop patterns from airtankers and helicopters with focus on the mapping of the area covered by the drop as well as the coverage quantity delivered to the ground [28-29]. Field experiments have also been conducted to improve the delivery systems of airtankers [27, 30-35]. While it is important to improve the effectiveness of delivery of water or fire chemicals to a wildfire, it is equally important to understand the effect of water or fire chemicals in reducing the intensity of a wildfire. Firefighting efforts are resource intensive operations where there is a limited availability of airtankers and helicopters, consequently resulting in a limited volume of water or fire chemicals that can be dropped on a fire. Therefore, effective resource management is imperative during wildfire mitigation operations [36]. A common practice to enable the effective allocation and use of resources is the reduction of the intensity of a fire to a fire intensity class that can be handled by ground crews [37]. Airtankers drop water or fire chemicals on high intensity wildfires, thereby reducing its intensity, but not completely extinguishing it. The reduced intensity fire can then be managed by ground crews while aerial delivery systems can be reassigned to different drop sites. It should be noted that at very high intensities, water and/or fire chemicals are not effective to suppress wildfires due to the magnitude of energy released during the combustion process.

Despite this form of resource management that occurs in practice, there have been no studies on the relationship between coverage level from an aerial drop and the reduction of fire intensity

brought about by it. Quantifying the reduction of fire intensity brought about by different coverage levels would be beneficial in strategic planning for combatting wildland fires. This relationship can be evaluated from an alternate approach where fuel load (mass of vegetative fuel per unit area), an important variable in determining the intensity of a fire, is assessed for a fixed volume of coverage applied on it. Therefore, investigating the relationship between coverage level, fuel load, and fire intensity in a controlled environment where external variables such as wind speed and wind direction are absent or constrained could help provide information that would be useful during wildfire direct attack operations.

Firefighting agencies in Canada use water as a fire suppressant or retardant during aerial operations due its abundance [38]. Water can be effective to suppress wildfires if sufficient quantities can be applied to the fuel. This is often dependent on the availability and capacity of aerial vehicles to deliver water to the burning fuel, and therefore renders it as an impractical option. Water in low quantities is not very effective as a fire suppressant or retardant due to the low film thickness that it forms, its viscosity, and its relatively high surface tension [39]. The film that water forms on the surface of vegetative fuels is not sufficiently thick to behave as an insulating barrier between the fuel and the heat from the surrounding fire. The low viscosity of water causes the water to be ineffective in adhering to vegetative surfaces properly and also increases its dispersion in air when dropped on to fuel during aerial applications. Its relatively high surface tension results in reduced surface coverage of vegetative fuels. Therefore, it was found necessary to change the properties of water to improve its effectiveness as a suppressant or retardant. This has given rise to the manufacture of fire chemicals that alter the properties of water to improve its performance as a suppressant or retardant.

1.5 WILDFIRE SUPPRESSION CHEMICALS

The use of fire suppression chemicals to contain and extinguish wildland fires has become increasingly popular among several firefighting agencies. Various types of fire chemicals have been developed for the purpose of containment and extinguishing of wildland forest fires. Fire chemicals have been proven to be effective at retarding the rate of spread of fires as well as lowering fire intensities [40]. Combustion recovery tests have also shown that the application of fire chemicals was successful in reducing the recurrence of flaming combustion due to their greater "knockdown" capabilities [41], which describe the ability of a treatment to diminish the intensity of a fire by increasing the fuel moisture. Increasing fuel moisture of the vegetative fuel results in more energy required to dry the fuel before they can ignite.

There are two main classifications of fire chemical additives: retardants and suppressant water-enhancers. Fire chemical retardants are often used in indirect attack treatments where the application of the fire chemicals is done in advance of the fire front to create control lines [42]. Fire chemical retardants are capable of inhibiting combustion, and can slow fire progression even after the vaporization of the water-based matrix [43-44]. They are commonly made of ammonium phosphates and corrosion inhibitors, which have a negative impact on water quality, aquatic organisms, and land vegetation [45]. This concern has led to the development of environmentally safe fire suppressant chemicals. Suppressant enhancers are used to improve the suppression effectiveness of water by modifying its physical properties. They can be further sub-classified into two main sub-categories: foaming agents and water enhancing gels. Foaming agents reduce the surface tension of water [46-47], thus increasing fuel coverage as well as forming an insulating barrier of air between the fuel and the fire [48-49]. Water enhancing gels increase the viscosity of water, thereby increasing adherence to the fuels and minimizing dispersion during application from

aircrafts [50]. Fire suppressant chemicals can be used in both direct attack treatments as well as short term indirect attack treatments.

There has been an increase in the use of fire chemicals in recent years [51-52], supplemented by the improvement in effectiveness and efficiency of aerial firefighting [53]. Consequently, the availability of fire chemicals has also increased, with different products being commercially available in a range of mixing ratios. While test methodologies have been standardized to evaluate properties of these fire chemicals such as biodegradability, toxicity, corrosivity, and adherence to surfaces [47, 50, 54-55], there is no standardized method to evaluate their relative performance to mitigate or inhibit ignition of the fuel. The availability of a standard test methodology would help to assess the relative performance of different fire chemicals at different mixing ratios, thereby helping to distinguish between the several commercially available products that are on the market.

1.6 EVALUATION OF WILDFIRE CHEMICALS

There are several analytical methods that are used to evaluate the performance of wildland fire chemicals. These include thermal gravimetric analysis, mass spectroscopy, and gas chromatography-Fourier transform infrared spectroscopy analysis, among others [56-60]. However, such methods use small test samples, which can result in erroneous interpretation of the resulting data when scaled up to forest fuel flammability applications in real, practical situations [61]. Therefore, analytical methods of evaluating the performance of wildland fire chemicals should be supported by larger laboratory-scale empirical tests. Empirical field experiments would be ideal for the evaluation of wildfire chemicals since they are able to represent a real wildfire scenario closely. However, field burns in controlled experiments are impractical to conduct due to

many external variables such as relative humidity, temperature, wind direction and speed that are difficult to control. Field burns also demand extensive logistical requirements which can be challenging.

Several laboratory-scale tests have been developed to determine the effectiveness of fire chemicals. Blakely [62] developed a flame spread method using a fuel bed of forest species for determining the effectiveness of forest fire retardants. These tests were found to be tedious and had low reproducibility. Plucinski [63] constructed a fuel bed in a wind tunnel and used an overhead nozzle to spray the fire chemicals. This method considered the volume of the fire chemical and used it as a parameter to gauge the performance of the fire chemicals; however, the test method has the potential to release more chemical suppressant than required, thus leading to erroneous data. The cone calorimeter, a common apparatus that measures the heat release rate, has also been used to test fire chemicals [64-65]. The equipment, however, is expensive and uses solid materials such as wood rather than foliar samples [61]. The wildfire industry uses the ASTM E1321-13 Standard Test Method for Determining Material Ignition and Flame Spread Properties [66]. The US Forest Service has used this standard to develop the Lateral Ignition and Flame Spread (LIFT) test [67]. However, this LIFT test uses a plywood substrate for evaluation and, hence, is not indicative of performance of the chemical in a wildland forest of vegetative fuel.

Numerous laboratory and field experimental ignition studies have been conducted on various materials [68-71]. In relation to wildfire chemicals, Tafreshi and Marzo [68] conducted ignition studies with foams and gels as the wildfire chemicals. The time-to-ignition data in these studies were primarily based on visual measurements, and therefore may prove to be onerous and prohibitive to collect. In addition, visual determination of time–to-ignition can result in negative health and safety issues due to the high heat fluxes generated in flash fires [72]. These studies also

used non-foliar vegetative samples, and thus cannot provide a true representation of the interaction between the wildfire chemical and the vegetative fuels in real fire scenarios. Thus, Anderson and McDonald [73] developed an experimental assembly that used foliar vegetative fuels and a custom-built heat flux sensor to quantify the heat released from the combustion of the fuel. The incident heat flux on the sensor may vary based on the orientation and position of the heat flux sensor relative to the burning fuel, and therefore did not capture the total heat flux, which may create errors in the comparison of the performance of the fire chemicals.

Janssens [74] regarded rate of heat release as the primary variable that facilitates a comprehensive understanding of the combustion and fire characteristics of materials. There are numerous methods that have been developed to determine the heat release rate [74]. These methods for determining the heat release rate are fundamentally based on oxygen consumption measurements and sensible enthalpy rise [74]. Techniques that utilize oxygen consumption measurements to estimate heat release rates are often considered to be the most accurate [74]. The heat release rate is estimated from the oxygen concentration and flow rates of the exhaust products. Both flow rate and composition of the gas are measured at an appropriate distance downstream in the exhaust duct that allows for sufficient mixing of the exhaust gas. Thornton [75] documented that a constant net amount of heat is released per unit mass of oxygen consumed for complete combustion. Based on the information from the energy released per unit mass of oxygen consumed for complete combustion as well as the oxygen concentrations and flow rate, the heat release rate based on the oxygen consumption principle can be expressed as [74]:

$$q'_{\mathrm{oc}} = E_{\mathrm{O_2}} (\dot{m}_{\mathrm{a}} Y^{\mathrm{a}}_{\mathrm{O_2}} - \dot{m}_{\mathrm{e}} Y^{\mathrm{e}}_{\mathrm{O_2}}) , \tag{1-1}$$

where E is the heat release per unit mass of oxygen consumed, $\dot{m}_a$ is the mass flow rate of the inlet air, $\dot{m}_e$ is the mass flow rate of the combustion products, $Y_{O_2}^a$ is the mass fraction of oxygen in the combustion dry air, and $Y_{O_2}^e$ is the mass fraction of oxygen in the combustion products. The accuracy of the heat release rate estimates can be further improved by measuring the concentrations of carbon monoxide, carbon dioxide, and water in the exhaust gas [74]. However, the oxygen consumption method does have its limitations and these include the fact that the oxygen analyzer measures the mole fraction and not the mass fraction of oxygen in a gas sample as well as the flow meters that measure volumetric flow rates rather than mass flow rates [74]. The conversion from mole fraction to mass fraction can often be erroneous due to the approximations made to the molecular weight of the exhaust gas due to variability in the compounds present in the exhaust gas as a result of the combustion process. Changes in density and temperature of the exhaust gas can result in inaccurate data when flow meters measure volumetric flow rates rather than mass flow rates. The oxygen consumption method also requires the use of high quality oxygen analyzers and rigorous calibration, resulting in high cost of instrumentation and frequent maintenance [74]. These disadvantages make the sensible enthalpy rise method of estimating heat release rates more convenient due to its simplicity.

Fire calorimeters that are based on the sensible enthalpy rise estimate heat release rates by measuring the temperature change of the system during the combustion process. Anderson [76] developed a cost effective laboratory test methodology that uses the concept of sensible enthalpy rise to determine the heat release rate of treated foliar samples during combustion. The test methodology consisted of fuel samples that were located inside a metal box enclosure where combustion occurred. By monitoring the temperature of the enclosure walls, as well as the flue

gases from the combustion process, the total heat released by a sample of fuel can be determined. The test methodology does not rely on time-to-ignition measurements, and can be used to quantify the heat release rates of both vegetative and non-vegetative samples. Anderson's methodology was mathematically developed, but not experimentally validated. The assessment of this mathematical model and its experimental validation will provide a low-cost, robust, flexible device to help evaluate the performance of chemically-treated fuels.

1.7 OBJECTIVES

The overall objectives of this study were to:

1. Investigate the relationship between coverage level, fuel load, and fire intensity by collecting data using laboratory scale prescribed experimental burns.
2. Validate the theoretical model of a low-cost sensible enthalpy rise calorimeter by:
    i. Assessing the mathematical model design of the sensible enthalpy rise calorimeter to produce more accurate heat release rate estimates.
    ii. Conduct experimental burns using the sensible enthalpy rise calorimeter test methodology.
    iii. Compare the data obtained from the sensible enthalpy rise calorimeter test methodology to show its ability to characterize the performance of the wildland fire chemicals.
    iv. Evaluate the repeatability of the sensible enthalpy rise calorimeter test methodology.
    v. Assess the functionality and capability of the sensible enthalpy rise calorimeter assembly.

1.8 THESIS ORGANIZATION

This thesis document is organized into several chapters. Chapter 2 presents the mathematical heat conduction model used to develop the sensible enthalpy rise calorimeter. Design modifications that resulted in modifications made to the mathematical model are also presented. Chapter 3 describes the experimental methods for two different test assemblies. The first test assembly discussed consists of the fuel bed and radiant panel setup that was used to investigate the relationships between the coverage level, fuel load, and fire intensity. The second test assembly discussed is the sensible enthalpy rise calorimeter assembly used to test the performance of wildland fire chemicals. Details about the preparation and applications of the fire chemicals as well as data collection methods are also described. Chapter 4 presents results and analysis from the two experimental assemblies. Statistical data analysis as well as inferences from the coverage level, fuel load, and fire intensity experimental burns is presented. The validity and repeatability of the sensible enthalpy rise calorimeter test methodology based on heat release rate estimates are discussed. A discussion about the functionality and capabilities of the sensible enthalpy rise calorimeter assembly is also explored. Chapter 5 presents the conclusions of this study and Chapter 6 discusses the possible future work that may be extended from this thesis study.

2 MATHEMATICAL MODEL

2.1 THERMAL CANISTER HEAT CONDUCTION MODEL

A metal enclosure, hereafter known as the “Thermal Canister”, was developed to estimate the total heat release rate from burning vegetative fuels based on the principle of sensible enthalpy rise. A heat conduction model based on Anderson’s [76] original theoretical model was developed to determine the temperature distribution in the Thermal Canister. The heat conduction model was based on the assumption of uniform heating of a rectangular-shaped body. The model was idealized as a one-dimensional, finite-length scale problem with the assumption that the heat transfer across the exposed walls of the canister was relatively uniform. Use of aluminum to build the thermal canister facilitated the reduction of thermal fluctuations that may occur due to its high thermal diffusivity.

The temperature distribution in each plate was solved using the separation of variables method. Data from the temperature distribution was used to calculate the total indecent heat flux on all the places. The enclosure walls were subdivided into two even different sections along the lines of symmetry in order to model the Thermal Canister. Consider the following plate with thickness, W as shown in Fig. 2-1b:

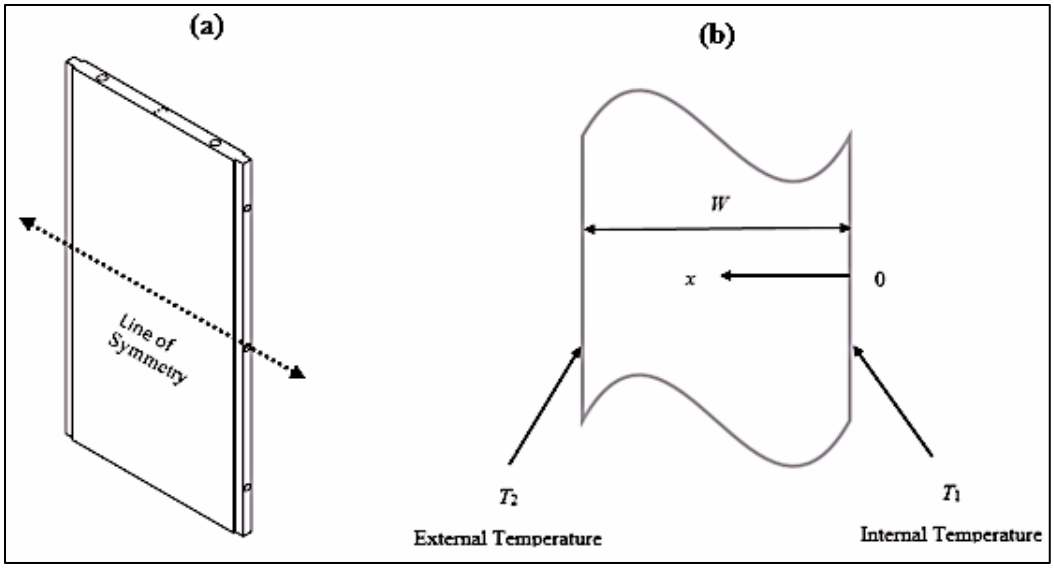

Figure 2-1: (a) Representation of the thermal canister wall showing line of symmetry and (b) schematic for the mathematical model. [76]

The Biot number (Bi) was calculated to determine whether the enclosure walls could be assumed to be one-dimensional. The problem can be modeled as one-dimensional if the Biot number is less than 0.1 [77]. The Biot number is defined as:

$$Bi = \frac{h\delta}{k}, \tag{2-1}$$

where h is the heat transfer coefficient, k is the thermal conductivity, and δ is the half thickness. Aluminum 6061 was chosen as the material for the Thermal Canister walls based on its high thermal diffusivity, high thermal conductivity, high melting point, and relatively constant thermal conductivity at elevated temperatures [78]. The heat transfer coefficient, h, was estimated to be 13.3 W/m^{2}K, based on the assumption of free convective flow over a vertical plate subjected to uniform heat flux as determined by Sullivan and McDonald for the maximum temperature differences expected in wildland fire conditions [79]. The thermal conductivity of the material, k,

was 167 W/mK [80] and the half thickness, δ was calculated to be 0.0095 m. Therefore, the Biot number is:

$$\mathrm{Bi} = \frac{13.3\ \mathrm{W/m^2K} \times 0.0095\mathrm{m}}{167\ \mathrm{W/m^2K}} = 0.00076.$$

Since Bi = 0.00076 <<< 0.1, the one dimensional model assumption is justified.

The one-dimensional governing equation for the temperature distribution in the Thermal Canister plate is given as follows:

$$\frac{\partial^2 T}{\partial x^2} = \frac{1}{\alpha}\frac{\partial T}{\partial t}, \tag{2-2}$$

where α is the thermal diffusivity of the material, which is defined as $\alpha = k/\rho C_p$, and is a measure of the rate of transfer of heat through a material medium.

The boundary and initial conditions are given by:

$$T(0,t) = T_1(t), \tag{2-3}$$

$$T(W,t) = T_2(t), \tag{2-4}$$

$$T(x,0) = T_i. \tag{2-5}$$

The total energy transfer to and from the walls of the enclosure due to conduction, convection, and radiation is indicated by the measured values of the transient temperatures that were used in the boundary conditions presented in Eq. 2-3 and 2-4. Therefore, conductive, convective, and radiative boundary conditions are not explicitly necessary. In addition, implicit inclusion of heat transfer by

conduction, convection, and radiation in the mathematical model results in linear boundary conditions, thus making the mathematical problem easier to solve.

Since the boundary conditions of Eqs. (2-3) and (2-4) are non-homogeneous, the method of superposition and separation of variables was used directly to solve the governing equation. Therefore, a solution of the form

$$T(x,t) = \Psi(x,t) + \Phi(x)\,, \tag{2-6}$$

was assumed, where Ψ depends on x and t for the homogenous solution and Φ depends on x, only for the particular solution.

Equation (2-6) was substituted into the governing equation of Eq. (2-2) to produce

$$\frac{\partial^2 \Psi}{\partial x^2} + \frac{\partial^2 \Phi}{\partial x^2} = \frac{1}{\alpha}\frac{\partial \Psi}{\partial t}\,. \tag{2-7}$$

The homogenous and non-homogeneous terms of Eq. (2-7) were separated into two different equations, one for $\Psi(x,t)$ and the other for $\Phi(x)$ to yield

$$\frac{\partial^2 \Psi}{\partial x^2} = \frac{1}{\alpha}\frac{\partial \Psi}{\partial t}\,, \tag{2-8}$$

$$\frac{\partial^2 \Phi}{\partial x^2} = 0\,. \tag{2-9}$$

Boundary conditions to solve $\Psi(x,t)$ and $\Phi(x)$ were obtained by substituting Eq. (2-7) into the boundary and initial conditions. Therefore, the boundary condition at $x = 0$ in Eq. (2-3) gives

$$\Psi(0,t) + \Phi(0) = T_1(t)\,. \tag{2-10}$$

For a simple homogeneous problem, assume

$$\Psi(0,t) = 0\,. \tag{2-11}$$

Consequently,

$$\Phi(0) = T_1(t)\,. \tag{2-12}$$

Similarly, substituting the boundary condition at $x = W$ in Eq. (2-4) gives

$$\Psi(W,t) + \Phi(W) = T_2(t)\,. \tag{2-13}$$

Assume

$$\Psi(W,t) = 0\,. \tag{2-14}$$

Therefore

$$\Phi(W) = T_2(t)\,. \tag{2-15}$$

The initial condition gives

$$\Psi(x,0) + \Phi(x) = T_i\,. \tag{2-16}$$

Rearranging Eq. (2-16) yields

$$\Psi(x,0) = T_i - \Phi(x)\,. \tag{2-17}$$

The linear ordinary differential equation, Eq. (2-9) was solved by integration, giving

$$\Phi(x) = Ax + B\,, \tag{2-18}$$

where A and B are the constants of integration. Application of the boundary conditions of Eqs. (2-12) and (2-15) to Eq. (2-18) gives the two constants of integration as

$$B = T_1,$$

$$A = \frac{1}{W}(T_2 - T_1).$$

Therefore, the solution to Eq. (2-9) becomes

$$\Phi(x) = \frac{1}{w} X(T_2 - T_1)x + T_1. \tag{2-19}$$

The solution of $\Psi(x,t)$ in Eq. (2-8) is obtained using the method of separation of variables. Therefore, a product solution of the form

$$\Psi(x,t) = X(x)\tau(t), \tag{2-20}$$

was assumed, where X depends on x, only and τ depends on t, only.

Equation (2-8) was substituted into Eq. (2-20) to give

$$\frac{d^2X}{dx^2}\tau = \frac{1}{\alpha}\frac{d\tau}{dt}X. \tag{2-21}$$

Separating the variables and setting the resulting equation equal to a constant, $\pm\lambda_n^2$, gives

$$\frac{d^2X_n}{dx^2} \mp \lambda_n^2 X_n = 0, \tag{2-22}$$

$$\frac{d\tau_n}{dt} \mp \alpha\lambda_n^2\tau_n = 0 \qquad . \tag{2-23}$$

The eigenvalue for the *x*-variables is positive since the *x*-variable has two homogeneous boundary conditions. Therefore, Eqs. (2-22) and (2-23) become

$$\frac{d^2X_n}{dx^2} + \lambda_n^2 X_n = 0, \tag{2-24}$$

$$\frac{d\tau_n}{dt} + \alpha\lambda_n^2\tau_n = 0\,. \tag{2-25}$$

For the case $n = 0$ ($\lambda_n = 0$), the equations become

$$\frac{d^2X_0}{dx^2} = 0, \tag{2-26}$$

$$\frac{d\tau_0}{dt} = 0\,. \tag{2-27}$$

The ordinary differential equations of Eqs. (2-26) and (2-27) were solved by direct integration, which yields

$$X_0(x) = A_0 x + B_0\,, \tag{2-28}$$

$$\tau_0(t) = C_0\,. \tag{2-29}$$

where A_0, B_0, and C_0 are the constants of integration. Applying the boundary conditions of Eq. (2-11) and (2-14) and the initial condition (2-17) to Eqs. (2-26) and (2-27) gives a trivial solution

$$X_0(x) = 0\,,$$

$$\tau_0(t) = 0.$$

When n is greater than zero, integration of Eqs. (2-24) and (2-25) yields

$$X_n(x) = A_n \sin \lambda_n x + B_n \cos \lambda_n x, \tag{2-30}$$

$$\tau_n(t) = C_n e^{-\alpha \lambda_n^2 t}, \tag{2-31}$$

where A_n, B_n, and C_n are the constants of integration. Then applying the boundary condition from Eq. (2-11) yields

$$B_n(x) = 0.$$

Also, applying the boundary condition from Eq. (4-14) gives

$$A_n \sin \lambda_n W = 0.$$

Therefore, the characteristic equation for λ_n is

$$\lambda_n = \frac{n\pi}{W}, \qquad \text{where } n = 1, 2, 3\ldots \tag{2-32}$$

Therefore, the complete homogeneous solution becomes

$$\Psi(x,t) = \sum_{n=1}^{\infty} a_n e^{-\alpha \lambda_n^2 t} \sin \lambda_n x, \tag{2-33}$$

where $a_n = A_n C_n$.

Applying the initial condition of Eq. (2-17) gives

$$T_i - \Phi(x) = \sum_{n=1}^{\infty} a_n \sin \lambda_n x \,. \tag{2-34}$$

To solve for a_n, the concept of orthogonality was applied [81]. The characteristic function, $\sin \lambda_n x$ in Eq. (2-34) are solutions to Eq. (2-24). Equation (2-24) was compared with the Sturm Liouville equation shown in Eq. (2-35) [81]:

$$\frac{d}{dx}\left[p(x)\frac{dT_n}{dx} \right] + \left[q(x) + \lambda_n^2 w(x) \right] T_n = 0 \ , \tag{2-35}$$

where $p(x) = e^{\int a_1 dx}, q(x) = a_2 dx, w(x) = a_3 p(x)$.

For this problem, $a_1 = a_2$, $a_3 = 1$, $p(x) = w(x) = 1$, and $q(x) = 1$, and $q(x) = 0$. Multiplying both sides of Eq. (2-34) by $\sin \lambda_n x$, integrating from $x = 0$ to $x = W$, and invoking orthogonality gives

$$\int_0^W [T_i - \Phi(x)] \sin \lambda_n x dx = a_n \int_0^W \sin^2 \lambda_n x dx,$$

$$a_n = \frac{\int_0^W [T_i - \Phi(x)] \sin \lambda_n x dx}{\int_0^W \sin^2 \lambda_n x dx},$$

$$a_n = \frac{\int_0^W [T_i - \frac{1}{w}(T_2 - T_1)x - T_1] \sin \lambda_n x dx}{\int_0^W \sin^2 \lambda_n x dx},$$

$$a_n = \frac{\frac{-\lambda_n W (T_i - 2T_1 - T_2)\cos \lambda_n W + \lambda_n W (T_i - T_1) + (T_1 - T_2)\sin \lambda_n W}{{\lambda_n}^2 W}}{\frac{2\lambda_n W + \sin(2\lambda_n W)}{4\lambda_n}},$$

$$a_n = \frac{-4\left[\lambda_n W(T_i - 2T_1 - T_2)\cos\lambda_n W + \lambda_n W(T_i - T_1) + (T_1 - T_2)\sin\lambda_n W\right]}{\lambda_n W\left[2\lambda_n W + \sin(2\lambda_n W)\right]}. \tag{2-36}$$

Substituting a_n into Eq. (2-33), the temperature distribution in the section becomes

$$T(x,t) = \frac{1}{W}(T_2 - T_1)x + T_1 + \sum_{n=1}^{\infty} a_n e^{-\alpha\lambda_n^2 t}\sin\lambda_n x. \tag{2-37}$$

The series solution of Eq. (2-37) decays rapidly as n and λ_n increase due to the exponential decay function. Therefore, for times greater than approximately two seconds, the term $\sum_{n=1}^{\infty} a_n e^{-\alpha\lambda_n^2 t}\sin\lambda_n x$ has negligible effect on the final solution and was neglected. The reduced solution then becomes

$$T(x,t) = \frac{1}{W}[T_2(W,t) - T_1(0,t)]x + T_1. \tag{2-38}$$

Finally, the heat flux is given by

$$q''(t) = -k\frac{dT(x,t)}{dx}. \tag{2-39}$$

Substituting Eq. (2-38) into Eq. (2-39) gives

$$q''(t) = -k\left[\frac{1}{W}[T_2(W,t) - T_1(0,t)]\right]. \tag{2-40}$$

The heat flux that can be calculated from Eq. (2-40) is a function of time and is spatially independent. This dependence stems from the temperature measurements being a function of time.

2.2 ESTIMATION OF LOSSES

2.2.1 Radiation Losses

Radiation losses will occur from the walls of the Thermal Canister enclosure. Equation (2-40) does not take into account radiation heat transfer and therefore has to be corrected for the radiation reflected from the surface as well as the radiation emitted as the temperature of the enclosure wall increases. Sullivan and McDonald [79] performed an energy balance, as shown in Fig 2-2, on the thermal cube sensor, a custom-built heat flux sensor that is based on a similar one dimensional heat conduction model. The net heat flux measured by the sensor based on the energy balance is given as the incident heat flux minus the reflected and emitted heat flux,

$$q''_{\text{net}}(t) = q''_{\text{incident}}(t) - q''_{\text{reflected}}(t) - q''_{\text{emitted}}(t). \tag{2-41}$$

The reflected heat flux will depend on the absorptivity of the surface, and it will be assumed to be equal to the emissivity [79]. Furthermore, radiation will not transmit through the body since the body is opaque. Therefore, the reflected heat flux is

$$q''_{\text{reflected}}(t) = (1-\varepsilon) q''_{\text{incident}}(t). \tag{2-42}$$

The incident heat flux was found by substituting Eq. (2-42) into Eq. (2-41) to give

$$q''_{\text{incident}}(t) = \frac{1}{\varepsilon}\left[q''_{\text{net}}(t) + q''_{\text{emitted}}(t)\right] \quad . \tag{2-43}$$

The Thermal Canister lacks a cooling mechanism and therefore, the temperature of the walls of the enclosure will increase over the duration of the test. This will result in energy loss due to radiation from the canister walls to the ambient surroundings. To compensate for this radiation

heat loss due to the increased temperature of the canister walls, the Stefan-Boltzmann law [81] was included in the model. It is

$$q''_{\text{emitted}}(t) = \sigma\varepsilon(T(x,t)^4 - T_\infty^4). \tag{2-44}$$

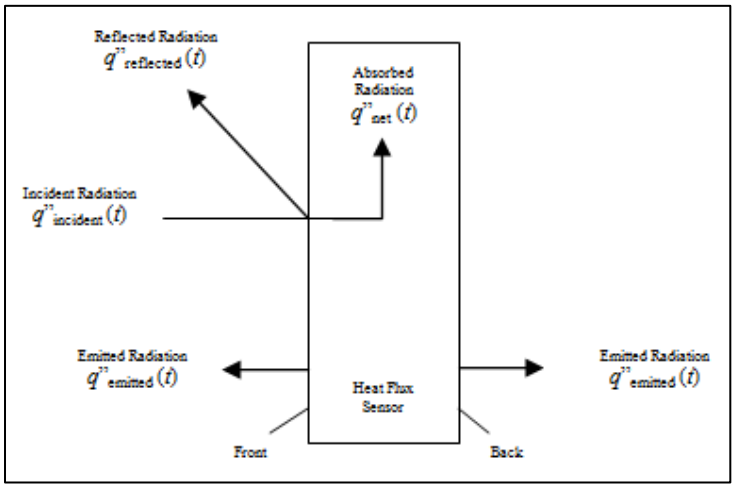

Figure 2-2: The absorption and reflection of incident radiation and emitted radiation of the thermal cube sensor [79]

Therefore, the incident heat flux on the surface of each of the canister walls becomes

$$q''_{incident}(t) = \frac{1}{\varepsilon}\left(-\frac{k}{W}\left[T_2(W,t) - T_1(0,t)\right] + \sigma\varepsilon\left[T_2(W,t)^4 + T_1(0,t)^4 - 2T_\infty^2\right]\right). \tag{2-45}$$

2.2.2 Combustion Exit Losses

Exit energy losses from the combustion process were quantified by conducting an energy balance on the exhaust pipe of the Thermal Canister by assuming a steady state, steady flow system. A

schematic of the flow of exhaust gases that enter and exit a control volume sectioned from the exhaust pipe is shown in Fig. 2-3.

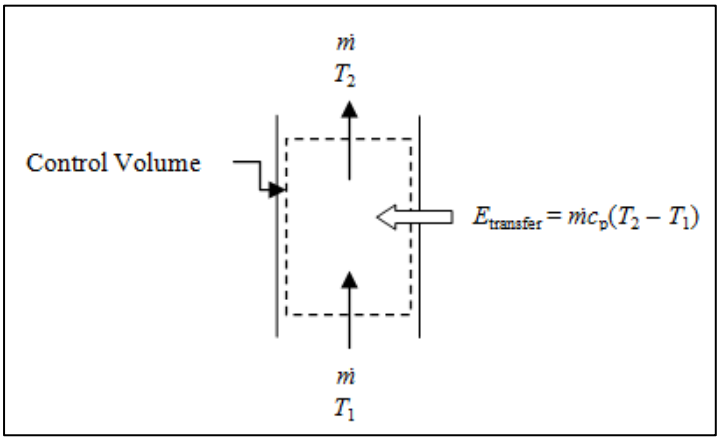

Figure 2-3: Control volume of the energy through the exhaust pipe [76].

The flow of exhausts gases through the exhaust pipe of the Thermal Canister was assumed to be one-dimensional. The properties of the exhaust gas were assumed to be uniform at any cross section normal to the flow direction. Based on the one-dimensional flow approximation, the mass flow rate of the exhaust gases through the exhaust pipe is given as

$$\dot{m} = \rho V A_c , \tag{2-46}$$

where $\dot{m}$ is the mass flow rate of the exhaust gases, A_c is the cross-sectional area of the pipe, ρ is the gas density, and V is the velocity of the exhaust gas. When the changes in kinetic and potential energies are negligible, there is no work, and the energy balance for the steady-flow system reduces to the expression for internal energy,

$$q'(t) = \dot{m}c_p T = \rho c_p V A_c \Delta T_e , \tag{2-47}$$

where q' (t) is the rate of net heat transfer out of the control volume corresponding to the energy losses from the combustion process, c_p is the specific heat capacity of air, and ΔT_e is the temperature difference between the control volume. To determine the losses experimentally, Anderson suggested the use of a Pitot tube. The Pitot formula of Eq. (2-48) can be substituted into Eqn. (2-47), as shown in the equations below:

$$V = \sqrt{\frac{2(P_t - P_s)}{\rho}}\,, \tag{2-48}$$

where, P_t is the total pressure and P_s is the stagnation pressure. ($P_t - P_s$) is determined using the Pitot tube. Therefore,

$$q'(t) = \rho c_p A_c \sqrt{\frac{2(P_t - P_s)}{\rho}} \Delta T_e\,. \tag{2-49}$$

However, preliminary experimental tests based on Anderson's original design did not produce pressure values when the Pitot tube was used. Pitot tubes are ineffective for measuring low fluid velocities, and therefore, direct measurement of the velocity of the exhaust gas was done by using an anemometer.

2.2.3 Total Heat Release Rate

To determine the total heat released from the combustion process, the heat flux incident on each wall section of the Thermal Canister wall must be converted to heat flow, q'. The heat flow is defined as

$$q'(t) = q''(t) A_s\,, \tag{2-50}$$

where A_s is the surface area of the canister wall. Therefore, substituting Eq. (2-45) into Eq. (2-50) gives

$$q'(t) = \frac{A_s}{\varepsilon}\left\{\left(-\frac{k}{W}[T_2(W,t) - T_1(0,t)] + \sigma\varepsilon[T_2(W,t)^4 + T_1(0,t)^4 - 2T_\infty{}^4]\right)\right\}. \tag{2-51}$$

The Thermal Canister enclosure was divided into ten sections along the line of symmetry. This included eight sections for the four vertical walls and two sections for the enclosure lid. Therefore, the total heat flow to the thermal canister is given by

$$\sum_{i=1}^{10} q'(t) = \sum_{i=1}^{10} \frac{A_s}{\varepsilon}\left\{\left(-\frac{k}{W}[T_2(W,t) - T_1(0,t)] + \sigma\varepsilon[T_2(W,t)^4 + T_1(0,t)^4 - 2T_\infty{}^4]\right)\right\}_i. \tag{2-52}$$

The total heat release rate from the entire system is found by taking the sum of the energy incident on the walls of the canister and adding the energy lost via the exhaust gases. Therefore, the total heat release rate was found by adding Eq. (2-52) and (2-47) which gives

$$q'_{Total}(t) = \rho c_p A_c V \Delta T_e + \sum_{i=1}^{10} \frac{A_s}{\varepsilon}\left\{\left(-\frac{k}{W}[T_2(W,t) - T_1(0,t)] + \sigma\varepsilon[T_2(W,t)^4 + T_1(0,t)^4 - 2T_\infty{}^4]\right)\right\}_i. \tag{2-53}$$

The thermocouples used in the Thermal Canister measurement system were differentially wired, similar to Anderson's modifications on the thermal cube design [82]. This design modification was done to limit the propagation of errors that arise due to the manufacturer-associated error of the thermocouples. The thermocouples used to measure the enclosure wall temperatures was therefore given by,

$$\Delta T_W = T_2(W,t) - T_1(0,t). \tag{2-54}$$

Therefore, the total heat release rate in the thermal canister is given as

$$q'_{Total}(t) = \rho c_{\mathrm{p}} A_c V \Delta T_{\mathrm{e}} + \sum_{i=1}^{10} \frac{A_{\mathrm{s}}}{\varepsilon} \left\{ \left(-\frac{k}{W} \Delta T_{\mathrm{W}} + \sigma \varepsilon [T_2(W,t)^4 + T_1(0,t)^4 - 2T_\infty{}^4] \right) \right\}_i . \qquad (2\text{-}55)$$

3 EXPERIMENTAL METHODS

3.1 COVERAGE LEVEL AND FUEL LOAD EXPERIMENTS

3.1.1 Fuel Bed Assembly

The experimental assembly consisted of a fuel bed holder, a wire mesh, a catchment tray, and an electric-powered radiant panel, all placed on a portable skid. Figure 3-1 shows the individual components of the setup assembled together. The fuel bed holder, of dimensions 60 cm x 31 cm x 5 cm, was fabricated using sheet metal and was used to provide a consistent boundary and location for the fuel to be placed. A steel woven wire mesh (0.0075" wire diameter) was used as the base of the fuel bed holder. The purpose of the mesh was to provide a surface for supporting the fuel while simultaneously allowing any excess water or chemicals from the applied coverage to pass through. Seepage of excess water or chemicals was considered while designing the experimental assembly in order to measure the effective coverage level in a fuel bed. A catchment tray made from sheet metal was placed underneath the fuel bed to enable collection of excess water or chemicals that seep through the fuel bed. The fuel bed holder along with the catchment tray was placed on a portable skid for easy movement of the assembly. The portable skid consisted of an attachable radiant heater, which provided a uniform heat flux to the width of the fuel bed.

The heat source used in the experimental assembly was an electric-powered radiant heater (Omegalux QH-121250, Omega Engineering Inc., Laval, QC, Canada). The radiant heater was rated at 240 VAC, 1 phase, 1660-8640 watts, and allowed for incident heat fluxes of up to 90 kW/m^2, with a maximum surface temperature rating of up to 980°C. The heater was connect to a Si-controlled rectified (SCR) power controller (SCR390 – 24-040, Omega Engineering Inc., Laval, QC, Canada), a 1/32 DIN temperature controller (CN7533, Omega Engineering Inc., Laval, QC,

Canada), and an AC current indicator (DP450-HACC, Omega Engineering Inc., Laval, QC, Canada) to monitor and control the power output, all of which were securely mounted inside a NEMA (National Electrical Manufacturers Association) 13 enclosure located at 2.44 m (8 ft.) from the heater [76]. Figure 3-2 shows a complete wiring diagram of the system.

Two thermal heat flux sensors were placed underneath the fuel bed and wire cloth, at 22 cm and 52 cm from the radiant panel. The heat flux sensors were used in the experiment to collect temperature for use in calculating heat fluxes and to determine the rate of spread. The entire assembly was placed under a ventilation hood. The ventilation in the hood was switched off to enable natural convection of air during the experimental burns. A video camera (Sony HDR-XR 200, Sony Corporation, Minato, Tokyo, Japan) was used to record the experimental burns in order observe the fire behavior and rate of spread.

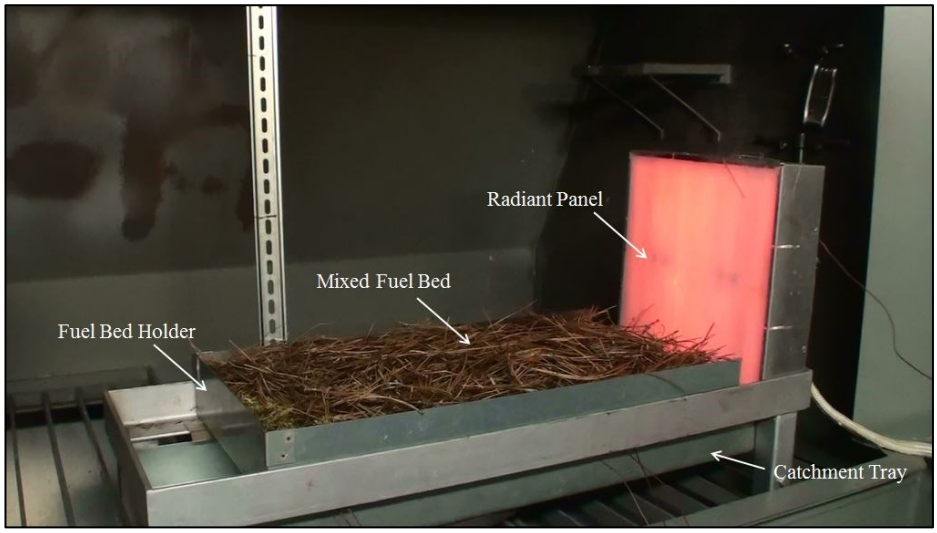

Figure 3-1: Fuel bed assembly with radiant panel

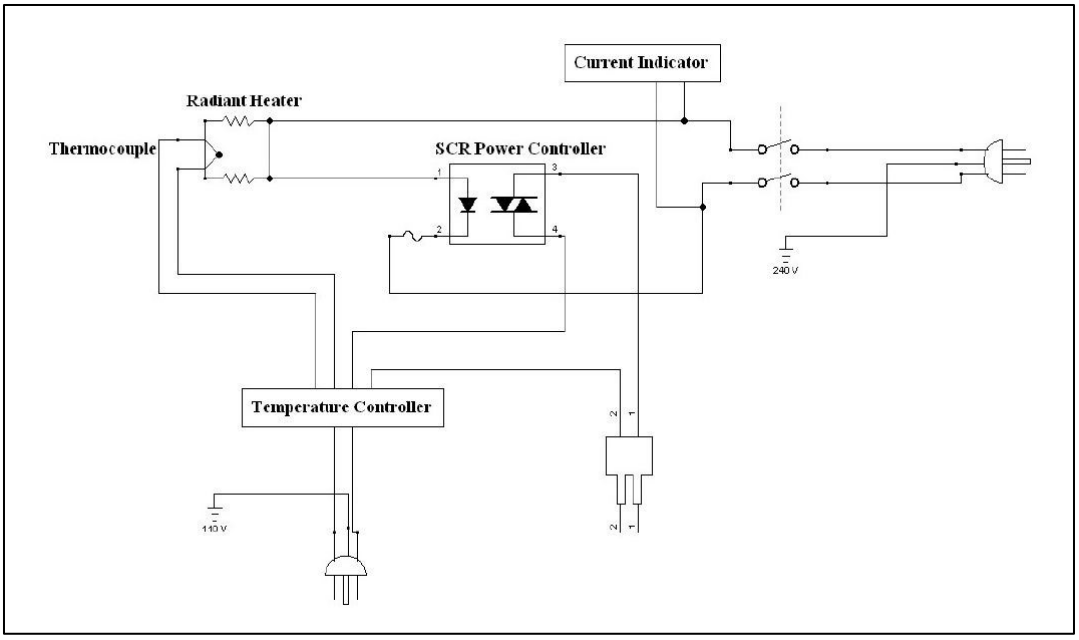

Figure 3-2: Radiant heater panel wiring diagram [76].

3.1.2 Heat Flux Sensor Assembly

The two heat flux sensors were connected to a data acquisition system (DaqProTM 5300, Fourier Systems Inc., Mokena, IL, USA) that was placed below the ventilation hood. The heat flux sensors were fitted with differential thermocouple wiring in order to reduce the propagation of uncertainty errors [82]. The output from the data acquisition system was processed using the heat conduction model developed by Sullivan and McDonald [79] to obtain the heat flux data. The heat flux estimates were calculated by using the following equation:

$$q''_{incident}(t) = \frac{1}{\varepsilon}\left(\frac{k\Delta T}{(L-d)} + \sigma\varepsilon\left[T(d,t)^4 + T_1(t)^4 - 2T_\infty^4\right]\right). \quad (3\text{-}1)$$

When the fuel located above the heat flux sensors combusted, a sharp rise in heat flux should be seen. This method was developed and evaluated for wildland fire chemical evaluation by Anderson

[76]. The difference in time between the maximum heat fluxes is indicative of the time required for the fire to travel from over one sensor to the other. The rate of spread can be calculated using this time duration and the known distance between the two sensors.

3.1.3 Testing Methodology

The fuels used in the experiments were dried using a convection oven to prevent any variability due to the moisture present in the fuel. The fuels were weighed at three time periods: before the drying process, after three hours of drying, and after four hours of drying. Moisture content of the fuel was calculated based on loss of mass of the fuel during the drying process and was ensured to be less than 5% in accordance with ASTM Standard D4442 [83]. The fuels were stored in a laboratory space in plastic containers in order to minimize the influence of external variables on the properties of the fuel. The fuels were stored for 24 hours before being used in experimental burns. During this storage period, it is possible that moisture from the air in the storage environment can increase the moisture content of the fuels and could therefore potentially add variability to the experimental results.

For every iteration of the experiment, the fuel mass was first measured by using a weigh scale, placed in the fuel bed holder and on the steel mesh. The fuel was uniformly placed throughout the fuel bed and was allowed to sit naturally. To obtain consistency in fuel height, any fuel of irregular height was cut to ensure fuel beds of the same fuel type and fuel load had the same fuel height. The fuel bed was placed such that the stand-off distance (distance between the radiant panel and the specified location in fuel) was zero. A spray bottle was used to apply the desired coverage level of water uniformly on the top surface of the fuel bed. One coverage level is defined as 1 U.S. gallon of product (water / chemical) per 100 ft^2 of area. The fuel bed was divided into 10 segments of equal area with care taken to ensure that each segment received equal coverage based on the

number of spray strokes from the spray bottle used to apply the desired coverage level. During the application of coverage, 7 cm tall sheet metal strips were placed along the perimeter of the fuel bed to ensure all coverage was applied within the perimeter of the fuel bed. It should be noted that this method of application of coverage can be improved on by developing an automated delivery system that is able to uniformly apply the product on to the fuel bed. Table 3-1 shows the coverage levels that were explored in this study. Higher coverage levels that reflect actual aerial tanker drops were used during preliminary test fires and were found to be very effective at suppressing combustion. Due to high coverage levels being effective at suppression combustion, a propagating fire front was not observed. Without a propagating flame front, the rate of spread of the fires could not be measured. Consequently, the calculation of fire intensity using Byram's fire intensity equation was not possible. Therefore, lower coverage level values (presented in Table 3-1) were used in this study.

Table 3-1: Coverage level quantities used for a fuel bed of area 1860 cm^2

Coverage Level (unit)	Coverage Level (mL)
0	0
0.2	15.2
0.4	30.4
0.6	45.6
0.8	60.8
1	76
2	152
3	228
4	304

The radiant panel was programmed for a set-point temperature of 600°C. A sheet metal plate was placed between the fuel bed and the surface of the radiant panel to shield any radiation from the panel during its heating up phase. Upon reaching 600°C, the sheet metal plate was removed, and the fuel bed was exposed to the incident radiant energy.

The fire behavior of three different fuel bed types namely, pine needles (*pinus palustris*), red-stemmed feather moss (*Pleurozium schreberi*), and a mixed bed of a feather moss base and pine needle upper surface, was studied individually. These vegetative fuels were selected since they

would provide a rough representation of vegetative fuels found in surface fires. The fuels were sourced from industrial suppliers to ensure consistent levels of product quality. Multiple iterations of the experiment were carried out wherein data of fire intensity for various coverage levels and fire intensity for various fuel loads were collected separately.

The fire intensity values were calculated using Byram's fireline intensity formula [84]:

$$I = Hwr\,, \tag{3-2}$$

where I is the fire intensity (kW/m), H is the fuel heat of combustion (kJ/kg), w is the fuel load (kg/m^2), and r is the rate of spread. The fuel heat of combustion for different fuels was experimentally obtained by using an oxygen bomb calorimeter, as discussed in Section 3.1.4. The fuel load was calculated by measuring the mass of the fuel being placed on the fuel bed of a known area. A video camera was placed perpendicular to the fuel bed to capture the propagation of the flame front in order to estimate its rate of spread. The rate of spread was calculated with measured values of the distance travelled by the fire from the radiant panel and the time taken to do so. Ignition of the fuel bed (as shown in Fig. 3-3) indicated the time at which collection of measurements of the transient rate of spread calculations were initiated.

Figure 3-3: Steady flame front (start of rate of spread measure)

3.1.4 Bomb Calorimetry Tests for Heat of Combustion

An oxygen bomb calorimeter (1341 Plain Jack Bomb Calorimeter, Parr, Illinois, USA) was used to obtain heat of combustion values for the fuels used in the fire intensity calculations. Half-gram samples were placed in the holder along with a nickel chromium fuse wire (45C10, Parr, Illinois, USA), which was connected to ignition wire leads. The fuse wire was 34 B&S Gauge and 10 cm diameter. The holder was placed in a pressurized oxygen combustion vessel at 30 atm, which was in turn placed in a water-filled oval bucket located in a calorimeter jacket as shown in Fig. 3-4. A motorized stirrer was used to ensure the circulation of water in the bucket. A thermistor was used to track the temperature measurements of the water in the bucket.

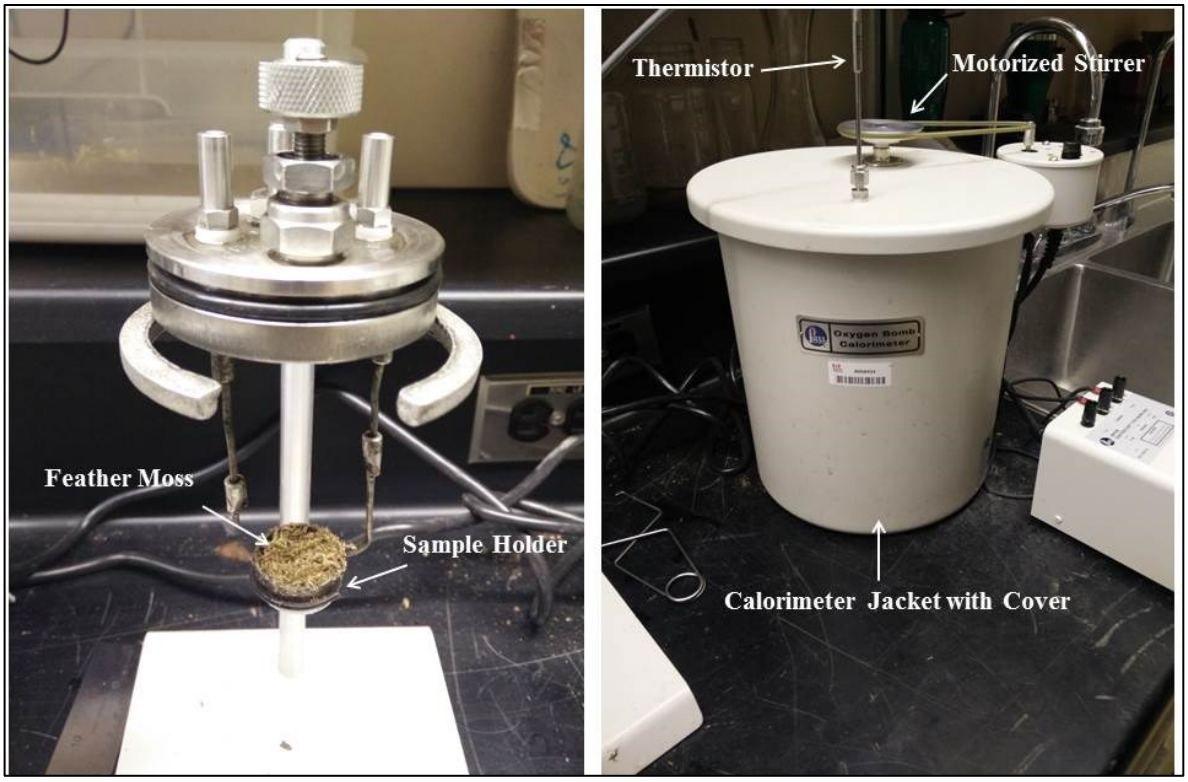

(a) **(b)**

Figure 3-4: Images showing: (*a*) 0.5 g of feather moss in the sample holder, and (*b*) the calorimeter jacket with cover.

The net corrected temperature rise of water in the bomb calorimeter assembly was calculated by using the following equation:

$$T = t_c - t_a - r_1(b-a) - r_2(c-b), \tag{3-3}$$

where T is the net correct temperature rise, a is the time of firing, b is the time when the temperature reaches 60% of total rise, c is the time at beginning of period in which the rate of temperature change has become constant, t_a is temperature at time of firing, t_c is temperature at time c, r_1 is rate (temperature units per minute) at which the temperature was rising during the period before firing,

r_2 is the rate (temperature units per minute) at which the temperature was rising during the period after time c. The selection of 60% mark of the total temperature rise was based on ASTM D240-17 [85].

The gross heat of combustion, H_g (in calories per gram), was the calculated by the following equation:

$$H_g = \frac{TW - e_1 - e_2 - e_3}{m}, \tag{3-4}$$

where W is the energy equivalent of the calorimeter, determined from standardization or calibration of the calorimeter using a calorific grade one gram benzoic acid pellet (2426 calories/°C), e_1 is the correction in calories for heat of formation of nitric acid (HNO_3), e_2 is the correction in calories for heat of formation of sulphuric acid (H_2SO_4), e_3 is correction in calories for heat of combustion of fuse wire, and m is the mass of sample in grams.

3.2 THERMAL CANISTER TEST METHODOLOGY

3.2.1 Thermal Canister Fabrication

The Thermal Canister was fabricated from 6061 aluminum plates. The enclosure was comprised of four vertical walls and a horizontal lid. The dimensions of each vertical wall and the horizontal lid were 0.508 m long x 0.279 m wide x 0.01905 m thick and 0.295 m x 0.295 m x 0.020 m thick, respectively. Socket head cap screws were used to facilitate easy assembly of the Thermal Canister as well as disassembly for the purpose of mounting of the fuel. An exhaust pipe of diameter 0.076 m and length 0.85 m was attached to the enclosure lid to enable transport of the flue gases from the Thermal Canister (see Figure 3-5(a)). The internal faces of the enclosure walls and lid were

painted with a high-temperature black spray paint (Krylon 1618 BBQ and Stove Paint, The Sherwin-Williams Company, Cleveland, OH, USA) in order to increase the surface emissivity to approach that of a black body. Holes of 1.98 mm diameter were drilled in the walls and lid of the Thermal Canister, as shown in Figure 3-6. The placement of the holes was similar to that of the Thermal Cube Heat Flux Sensor developed by Anderson, *et al.* [76]. These holes served as housing for thermocouples, which were used to obtain transient temperature data at the front and back surfaces of the walls and the lid.

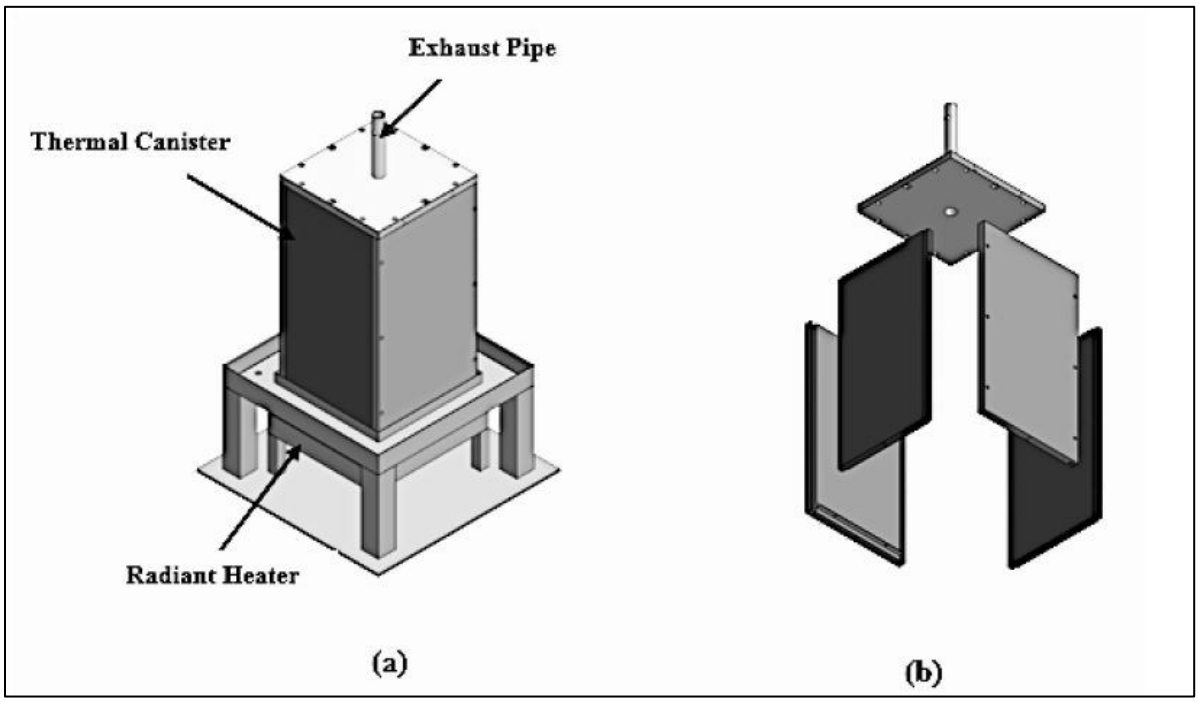

Figure 3-5: (a) Assembled view and (b) exploded view of the Thermal Canister. [76]

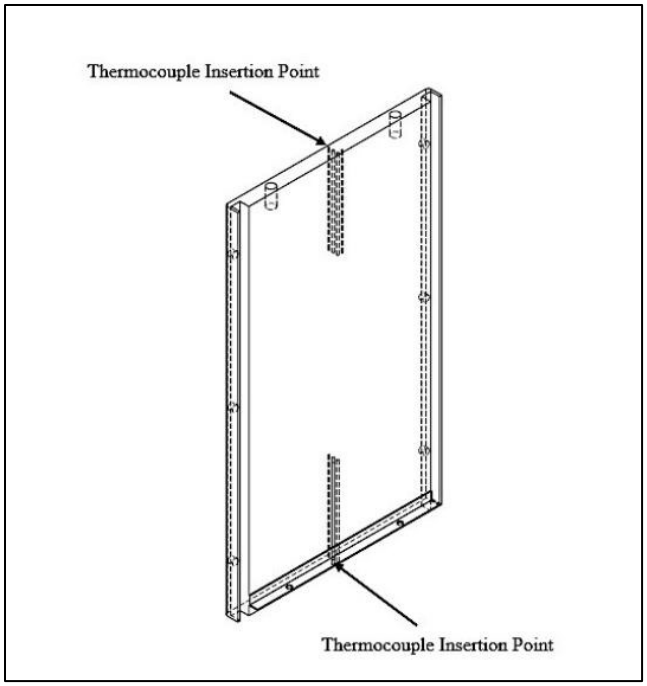

Figure 3-6: Schematic of a typical Thermal Canister Wall. [76]

3.2.2 Thermal Canister Experimental Assembly

Figure 3-7 shows the Thermal Canister that was vertically mounted on a steel stand with the open end facing the ground. The stand served as a platform for the enclosure to rest, and provided clearance below the enclosure to accommodate the heat source. The heat source used in this experiment was an electric-powered radiant panel (Omegalux QH-121260, Omega Engineering Inc., Laval, QC, Canada) that emitted a uniform heat transfer rate across the bottom of the enclosure into the Thermal Canister. This radiant panel was placed on a secondary stand to minimize the distance between the face of the radiant panel and the open end of the Thermal Canister. Minimizing this distance increased the heat flux projected vertically upward towards the interior of the Thermal Canister while simultaneously reducing heat loses in the other directions. A small gap was maintained between the radiant panel and the opening of the Thermal Canister to enable air flow. The radiant panel was programmed to attain and maintain a temperature of 500°C.

J-Type 30 gauge thermocouples (Omega Engineering Inc., Laval, QC, Canada) were used to measure the temperature of the walls, lid, and exhaust flue gases of or from the Thermal Canister. A total of 30 thermocouples were fitted in the holes that were drilled in the walls and lid of the enclosure. The thermocouples were differentially wired to minimize the propagation of error [82]. An additional thermocouple was inserted at the inlet of the exhaust pipe to measure the temperature of the flue gases. Two data loggers were used to collect data from these thermocouples. The 30 thermocouples that were fitted in the walls and lid of the Thermal Canister were connected to a multi-channel data acquisition unit (34970A Data Acquisition/Data Logger Switch Unit, Keysight Technologies Inc., Santa Rosa, California, USA), and the thermocouple in the exhaust pipe was connected to a stand-alone data logger (DaqProTM 5300, Fourier Systems Inc., Mokena, IL, USA). An anemometer (2G-2948 EDRA Anemometer, Airflow Developments Ltd., Richmond Hill, ON, Canada) was placed above the exhaust pipe outlet to measure the velocity of the flue gases. Natural ventilation of air during the experimental burns was the predominant mode of air movement.

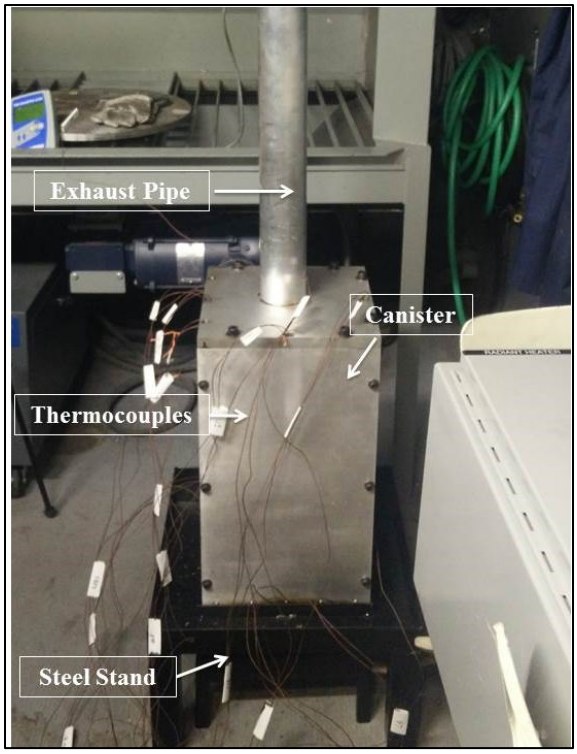

Figure 3-7: Thermal Canister experimental assembly.

Anderson's original design was modified to include an exhaust pipe with an increased length. A 0.85 m long sheet metal pipe was used to replace the existing 0.012 m long pipe. This modification was done in order to restrict the developing flow region at the entrance of the pipe, reducing the hydrodynamic length of the pipe, so that fully-developed flow could be assumed along the length of the entire pipe. The hydrodynamic entry length of the pipe was estimated by using the following formula [86]:

$$\frac{L_{\mathrm{h,laminar}}}{D} \cong 0.06\mathrm{Re}, \tag{3-5}$$

where L_{h} is the length of the circular pipe, D is the diameter of the circular pipe, and Re is the Reynold's number. When the hydrodynamic length is much smaller than the length of the pipe,

entrance effects are negligible and the flow tends to be fully-developed. The properties of the flue gas were assumed to be that of air to calculate the Reynold's number and the total heat release rate. This approximation was based on the fact that the fuel gas consisted primarily of air that did not participate in the combustion process. The experimental burn consisted of 45 grams of fuel burned during the combustion process, with volumetric flow rates of the flue gas averaging 0.003 m^3/s towards the end of the burn cycles for different fuel treatments. This high volumetric flow rate of flue gas implies that the mass of air used in each burn cycle was also high, specifically in comparison to the mass of fuel that was used in the experiment. The high air-to-fuel ratio suggests that only a small amount of air that entered the enclosure was used in the combustion process. The flue gas emitted from the enclosure consisted mainly of air that was not used in the combustion process and therefore the properties of the flue gas were taken to be those of air.

3.2.3 Thermal Canister Experimental Procedure

Red-stemmed feather moss (*Pleurozium schreberi*) was selected as the fuel to be used in the experimental burns. Feather moss was chosen as the preferred fuel due to its ability to absorb and retain water efficiently as well as other water-based chemical products (foams, gels, and other fire suppressant and retardants). The moss was dried to a moisture content of less than 5% in accordance with ASTM Standard D4442 [83]. The drying process removed moisture, thus preventing any variability in the measurements of heat release rate of the fuel due to the moisture content in the fuel. The process of drying and storage of the moss has been outlined in Section 3.1.3. A woven steel wire mesh (0.0075" wire diameter) of dimensions 25 cm x 25 cm was used to contain the fuel during the experiments. Forty-five (45) grams of feather moss was measured and placed on the steel mesh. The treatment of the fuel was applied prior to placement of the fuel in the Thermal Canister assembly.

3.2.3.1 Preparation of Fire Chemicals. The performance of five different types of treatments was used to evaluate the Thermal Canister assembly. The names of the products used as treatments have been intentionally excluded from this study for proprietary reasons. The different treatments were: zero coverage level (no water/fire chemicals applied), water, a Foam Product, and two gel (water enhancer) products, A and B, all at coverage level 0.8. The mixing ratios used have been presented in Table 3-2, and the ratios for the preparation of the foam and gel products were selected as per the manufacturers' recommendations. Dry chemical concentrates were mixed by weight and wet chemical concentrates were mixed by volume. The foam and gel products were thoroughly mixed by using a high performance blender (Ninja, Euro-Pro Operating LLC, Ville St. Laurent, QC, Canada). A Marsh funnel (Fann Instrument Company, Houston, Texas, USA) was used to determine the time required for a fixed volume of the foam and gel products to flow through the funnel. The flow time was indicative of the viscosity of the product, where the higher the flow time, the larger the viscosity of the product. The Marsh funnel test was carried out to ensure the viscosity of the mixed product that was prepared in the laboratory was similar to the viscosity values obtained by industry practitioners. One thousand, five hundred (1500) mL of foam and gel products was used in the Marsh funnel test, with each test repeated three times ($n = 3$). The results from the Marsh funnel test are presented in Table 3-3 and were found to be consistent with the time measurements recorded by industry practitioners. The standard deviation is presented with the average values of all parameters that were measured in this study.

Table 3-2: Fire chemical product mixing ratios.

Chemical Product	Mixing Ratio

Foam Product	0.65%
Gel Product A	0.65%
Gel Product B	3%

Table 3-3: Fire chemical product flow time through a Marsh funnel.

Chemical Product	**Time, (s)**
Foam Product	24 ± 1
Gel Product A	63 ± 2
Gel Product B	22 ± 1

3.2.3.2 Experimental Burns. The Thermal Canister lid was removed to allow for the placement of the fuel bed by way of the top of the assembly. This ensured that the physical placement of the radiant panel at the open end of the Thermal Canister was not disturbed. The lid was replaced after the successful placement of the fuel, and fastened to the walls of the enclosure using socket head cap screws. The data loggers were programmed to record the temperatures and differential voltages at three-second intervals. The data recording process was initiated when the radiant panel was switched on. The experiments were repeated three times (n = 3) for each type of fuel treatment under the same parametric conditions mixing ratio, mass of fuel, and heat flux. Data obtained from the experiments was extracted and Eq. 2-55 was used to calculate the heat release rate.

3.2.3.4 Data Analysis for Repeatability Evaluation. ASTM E177 [87] states that the precision of a new test methodology can be evaluated by calculating the repeatability and reproducibility of the quantitative results produced by it. The precision of an instrument depends on random errors and

does not relate to an accepted reference value. The measures of precision are often expressed in terms of imprecision and are computed using the standard deviation of the test results. When the test results produce large standard deviations, the test methodology is said to be less precise. Precision is evaluated under repeatability and reproducibility conditions. ASTM E456 [88] defines repeatability conditions as "conditions where independent test results are obtained with the same method on identical test items in the same laboratory by the same operator using the same equipment within short intervals of time," and defines reproducibility conditions as "conditions where test results are obtained with the same method on identical test items in different laboratories with different operators using different equipment." Reproducibility evaluation was excluded from this study due to the lack of availability of alternate identical laboratory assemblies and different operators.

The Thermal Canister experiments followed the stipulated conditions required to evaluate the repeatability of a test method. Five time periods were selected to calculate the standard deviation of the heat release rates from three test burns for each treatment type. The selected time periods were 201, 300, 399, 501, and 600 seconds for the untreated fuel beds, and 300, 399, 501, 600, and 699 for the treated fuel beds. This difference in selected time periods between untreated and treated fuels was due to the prolonging of the ignition time by the fire chemicals as well as the time taken for the complete combustion of the treated fuel beds. The intervals between the selected time periods were not precisely 100-second intervals due to the recording of data points at three-second intervals by the data logger. The repeatability standard deviation and coefficient of variation were used as measures of repeatability in accordance with ASTM E177 [87]. The repeatability standard deviation, s_r, is given as the square root of the average variances obtained from the time periods. The lower the repeatability standard deviation, the higher is the repeatability of the test method.

The coefficient of variation, *CV*, is the ratio of the standard deviation and the mean of a population and it describes the precision relative to the test result available.

4 RESULTS AND DISCUSSIONS

4.1 COVERAGE LEVEL AND FUEL LOAD EXPERIMENTS

4.1.1 Rate of Spread Measurements using Heat Flux Sensor

Data from the heat flux sensors was analyzed to determine if the sensors were capable of measuring the rate of spread of a fire accurately. This method of rate of spread measurements was conducted to evaluate the capability of the thermal heat flux sensors to function as rate of spread loggers. Figure 4-1 shows heat flux as a function of time, for a pine needle fuel bed with zero coverage level and 0.538 kg/m^2 fuel load. The two nearly singular increases in the heat flux represent the combustion of the fuel that was above the respective sensors. The difference in time between the maximum heat fluxes were selected as indicative of the time required for the fire to travel atop one sensor to the other. The noise levels in the estimated heat flux sensor data was documented by Anderson in the heat flux sensor's evaluation, citing a combined result of convection at the surface of the sensors and the absence of signal filters are its source.

The measurement of rate of spread using the heat flux sensors was estimated three times (n = 3) from three experimental burns and was compared to the measurements made from the same three experimental burns by using a video camera. The estimated average rate of spread from the three experimental burns using the heat flux sensors was 0.00672 m/s while the estimated average rate of spread using the video camera was 0.00647 m/s. The standard deviation in the rate of spread measurements using the heat flux sensor was 7.14 x 10^{-5} m/s and that using the video camera was 6.54 x 10^{-5} m/s. Based on the similar rate of spread values and low standard deviation, it was found that the heat flux sensors are capable of measuring rate of spread values that are in close agreement with the visual method of measurement that uses a camera to find the distance and time travelled

by the fire. It should be noted that this method of measurement is possible only when there is a uniform and even flame front. The heat flux sensors were used to estimate the rate of spread in experimental burns involving different fuels, fuel loads, and coverage levels. It was observed that due to the progression of a non-uniform flame front along the length of the fuel bed for experimental burns involving any applied coverage, the singular increases in heat flux did not correspond to the actual rate of spread values, but instead resulted in lower rate of spread values. This highlighted the limitations of the heat flux sensors as rate of spread logger devices.

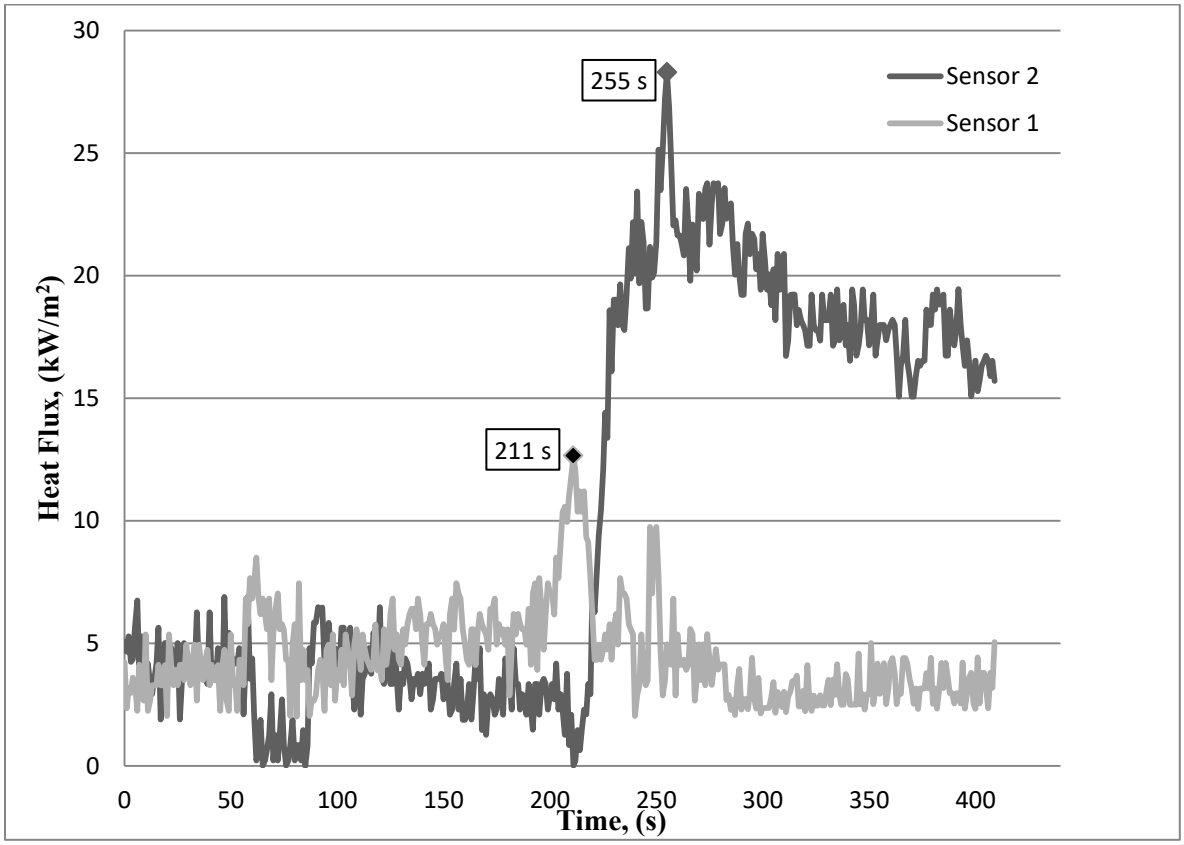

Figure 4-1: Heat flux data from the two sensors for a pine needle fuel bed with zero coverage level and 0.538 kg/m^2 fuel load for the first experimental burn.

4.1.2 Heat of Combustion from Bomb Calorimetry

Heat of combustion data was obtained using a bomb calorimeter and used the fire intensity calculations for the coverage level and fuel load variation experimental burns described in Section 4.1.3 and 4.1.4. The bomb calorimeter test with each fuel type was repeated five times to provide sufficient data for statistical analysis. The heat of combustion values obtained are shown in Table 4-1:

Table 4-1: Heat of Combustion values from oxygen bomb calorimetry.

Fuel Type	Heat of Combustion (kJ/kg)
Pine Needles	17733 ± 314 (n = 5)
Feather Moss	14503 ± 292 (n = 5)
Mixed Fuel	16625 ± 372 (n = 5)

4.1.3 Coverage Level Variations

The purpose of the coverage level variation experimental burns was to map the relationship between coverage level and fire intensity for a fixed fuel load. Different fuel beds were used in the experimental burns to understand how the characteristics of the fuel affect the relationship between the coverage level and fire intensity. Data from the experimental burns with different fuel beds would also help with the selection of fuel type that would be used in the Thermal Canister experimental burns.

4.1.3.1 Pine Needle Fuel Bed (constant Fuel Load)

Figure 4-2 shows the relationship between fire intensity and coverage level for a pine needle fuel bed at a constant fuel load of 0.538 kg/m^2. The coverage levels used were 0, 1, 2, 3, and 4, with each test burn repeated three times (n = 3) in order to determine average values and variations. The average fire intensities for each coverage level are present in Fig. 4-2 with the error bars indicating the standard deviations of fire intensities. The graph suggests that the fire intensity produced in the fuel bed decreases with an increase in coverage level. A comparison between the fire intensities produced at coverage level 0 and coverage level 1 is indicative of the fact that application of water on the fuel bed helps significantly reduce the fire intensities. However, a comparison between the intensities produced at coverage levels 1, 2, and 3 indicate that while there is a reduction in the resulting intensities, the magnitude of reduction is not as large as that between coverage levels 0 and 1 (i.e. no water application vs. water application). To verify whether the mean fire intensities obtained are statistically significant, a one-way ANOVA (analysis of variance) test was conducted using Statistica (Dell Inc., Texas, USA). A significance level, a, of 5% was selected for the ANOVA test based on statistical convention [89]. The ANOVA test produces a *p-value* which, if less than 0.05, suggests that the means of the fire intensities are statistically different. If the *p-value* produced is greater than 0.05, the differences in the means of the fire intensities are insignificant. The test produced a *p-value* of 9.45 x 10^{-9} which is less than 0.05, suggesting that the means of fire intensities are statistically different. To understand which coverage levels produced intensities whose means are statistically different from each other, a Tukey's honest significant difference (HSD) Post Hoc Test was conducted. The results from Tukey's HSD Post Hoc Test are presented in Table 4-2.

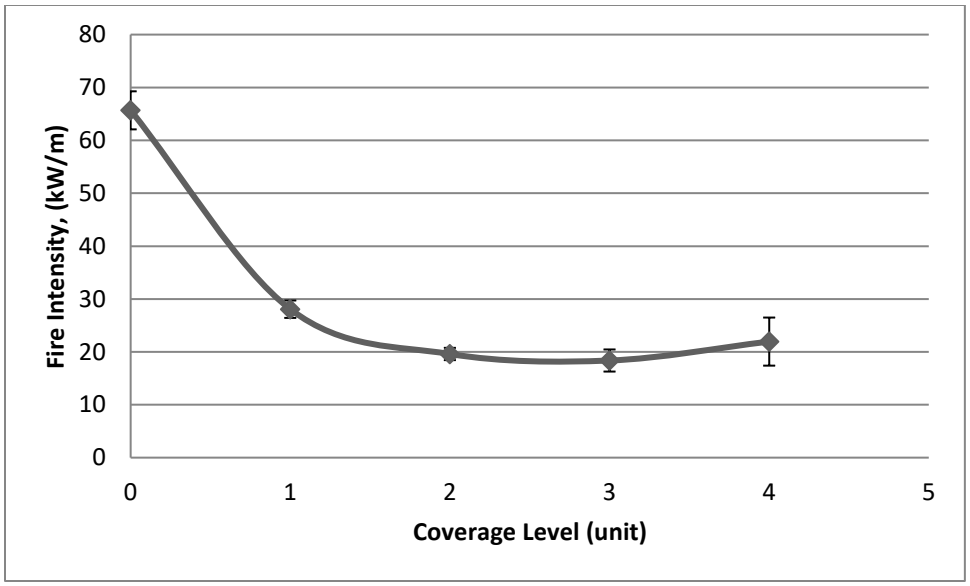

Figure 4-2: Fire intensity versus coverage level at constant fuel load for a pine needle fuel bed.

Table 4-2: Tukey's HSD Post Hoc Test for a pine needle fuel bed of varying coverage level and constant fuel load.

Coverage Level (unit)	**0**	**1**	**2**	**3**	**4**
0		0.000176	0.000176	0.000176	0.000176
1	0.000176		0.032184	0.014486	0.146614
2	0.000176	0.032184		0.983205	0.854055
3	0.000176	0.014486	0.983205		0.578489
4	0.000176	0.146614	0.854055	0.578489	

The results from the Tukey's Post Hoc Test support the conclusion that the application of water results in a significant reduction of fire intensity. The results also suggest that the change in fire intensities produced at coverage levels 2 and 3 are not significantly different; therefore, any coverage level beyond 2 would not reduce the fire intensity significantly. It is of significance to mention that water seeped through the pine needle fuel bed when coverage levels 3 and 4 were applied. This seepage loss was not observed for coverage levels 1 and 2. This suggests that the pine needle fuel bed is unable to retain water completely for coverage levels 3 and above due to its water retention characteristics which describe the ability a fuel to retain water when applied on it. This inability to retain water completely for coverage levels 3 and above could explain the lack of significantly different fire intensities produced on application of coverage levels 3 and 4. The water retention characteristics also explain the increase in fire intensity for coverage level 4 (shown in Fig. 4-2). Since water was collected in the catchment tray on application of coverage level 4, the effective coverage level on the pine needle fuel bed was less than the applied coverage level, thus producing a fire intensity corresponding to a lower coverage level.

4.1.3.2 Feather Moss Fuel Bed (constant Fuel Load)

Figure 4-3 shows the relationship between fire intensity and coverage level for a feather moss fuel bed at a constant fuel load of 0.538 kg/m^2. The coverage levels used were 0, 0.2, 0.4, 0.6, and 0.8, with each test burn repeated three times ($n = 3$) for statistical reliability. The average fire intensities for each coverage level were plotted in Fig. 4-3 with the error bars indicating standard deviation. The graph suggests that the fire intensity produced in the fuel bed decreases with an increase in coverage level. The application of water on a feather moss fuel bed caused a reduction in the

intensity of the fire significantly. This can be seen at the data points corresponding to coverage level 0 (no water) and 0.2, where the fire intensity produced for coverage level 0 was 202.18 kW/m and the fire intensity produced for coverage level 0.2 was 72.63 kW/m. Coverage levels 0.2, 0.4, 0.6, and 0.8 further reduced the fire intensity produced. To ensure the mean fire intensities of the different burns are statistically significant, a one-way ANOVA test was carried out using a significance level of 5%. A *p-value* of 1.04×10^{-7} was obtained which is less than 0.05, implying that the means of the fire intensities are statistically different from one another and did not occur due to chance. A further investigation of the mean fire intensities was carried out in order to individually compare each of the mean fire intensities to each other. This was done using Tukey's HSD Post Hoc Test, the results of which are presented in Table 4-3.

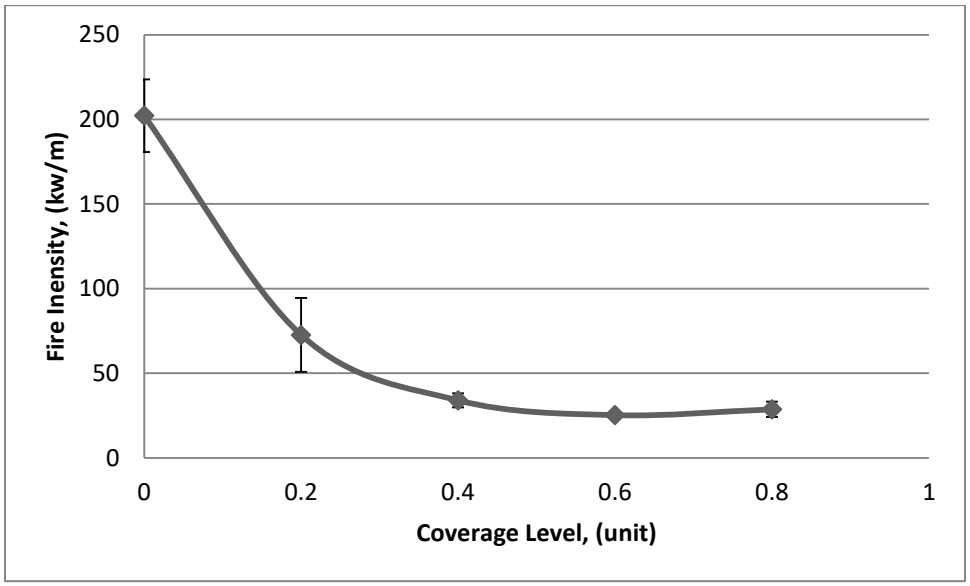

Figure 4-3: Fire intensity versus coverage level at constant fuel load for a feather moss fuel bed.

Table 4-3: Tukey's HSD Post Hoc Test for a feather moss fuel bed of varying coverage level and constant fuel load

Coverage Level (unit)	**0**	**0.2**	**0.4**	**0.6**	**0.8**
0		0.000176	0.000176	0.000176	0.000176
0.2	0.000176		0.043131	0.013309	0.020890
0.4	0.000176	0.043131		0.934724	0.988554
0.6	0.000176	0.013309	0.934724		0.998057
0.8	0.000176	0.020890	0.988554	0.998057	

The results from Tukey's Post Hoc Test suggested that the mean fire intensities produced when water was applied (i.e., data points corresponding to coverage levels 0.2, 0.4, 0.6, and 0.8) are significantly different from the mean fire intensity produced when no water is applied. This can be attributed to the water retention capabilities of feather moss. This hypothesis regarding water retention capabilities of the feather moss was further supported when it was observed that no water was collected in the catchment tray upon application of different coverage levels, indicating that all water applied was retained by the feather moss. Increasing the coverage level from 0.4 to 0.8 decreased the intensity of fires produced. However, the reduction in magnitude is not as notable as a reduction in fire intensity produced between coverage levels 0 and 0.2, and coverage levels 0.2 and 0.4. The Tukey's Post Hoc Test shows that the differences in mean fire intensities for coverage levels 0.4, 0.6, and 0.8 are not significant from each other.

It should be noted that in an effort to maintain consistency with the pine needle fuel bed experimental burns, coverage levels 0 to 4 were initially chosen for the feather moss fuel beds. However, coverage levels 1 and 2 resulted in fires that spread less than 10 cm from the radiant panel before extinguishing. This behaviour is due to the ability of feather moss to retain the applied water. Therefore, coverage levels 0, 0.2, 0.4, 0.6, and 0.8 were selected for the feather moss fuel bed burns.

4.1.3.3 Mixed Fuel Bed (constant Fuel Load)

Figure 4-4 shows the relationship between fire intensity and coverage level for a mixed fuel bed at a constant fuel load of 1.076 kg/m^2. The coverage levels used were 0, 1, 2, 3, and 4, with each test burn repeated three times (n = 3) for statistical reliability. The average fire intensities for each coverage level were plotted in Fig. 4-4, with the error bars indicating standard deviation. The graph shows that there is a noticeable reduction in fire intensity upon application of water. This can be seen when comparing data points representing coverage level 0 (i.e., no water) to data points representing coverage levels 1, 2, 3, and 4. The graph also shows that coverage levels 1, 2, and 3 resulted in approximately the same fire intensity values. A discussion of the increase in fire intensity values for coverage level 4 has been presented after the following analysis. The different mean fire intensities were checked for statistical significance using an ANOVA test with a significance level of 5%. The *p-value* obtained from the ANOVA test was 4.03 x 10^{-8} which is less than 0.05, suggesting that the mean fire intensities are statistically different. A Tukey's HSD Post Hoc Test was carried out to compare the statistical significance of the mean fire intensity values with each other. The results of Tukey's HSD Post Hoc Test are presented in Table 4-4.

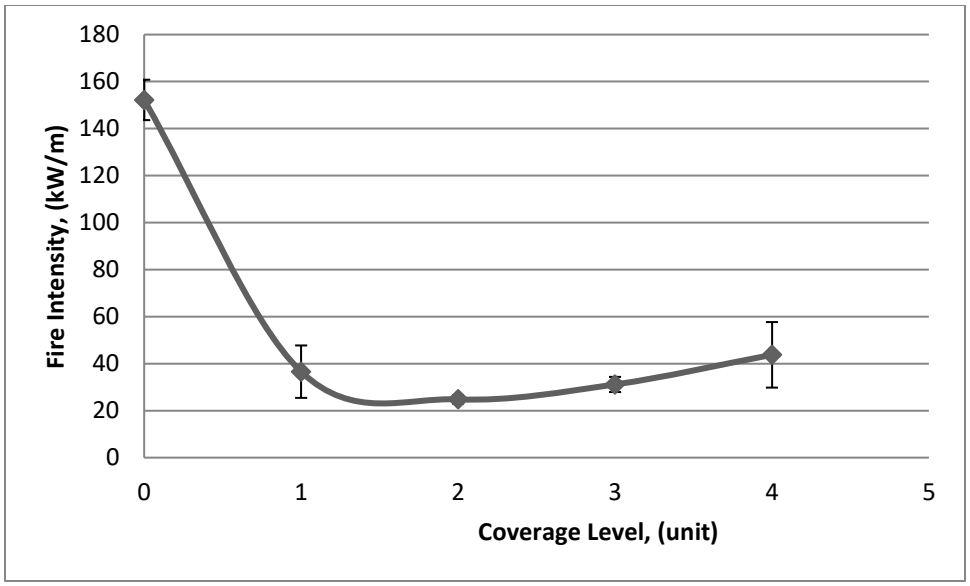

Figure 4-4: Fire intensity versus coverage level at constant fuel load for a mixed fuel bed.

Table 4-4: Tukey's HSD Post Hoc Test for a mixed fuel bed of varying coverage level and constant fuel load

Coverage Level (unit)	**0**	**1**	**2**	**3**	**4**
0		0.000176	0.000176	0.000176	0.000176
1	0.000176		0.528210	0.941989	0.861712
2	0.000176	0.528210		0.904526	0.149513
3	0.000176	0.941989	0.904526		0.468942
4	0.000176	0.861712	0.149513	0.468942	

The results from Tukey's Post Hoc Test support the conclusion that application of water on the mixed fuel bed significantly reduces the fire intensity. However, as coverage levels were increased, there was no significant reduction in fire intensities. Also, despite an increase in mean fire intensity produced at coverage level 4, the quantitative increase is not significant enough to consider that data point as a start of an upward trend.

Certain physical observations were noted during the mixed fuel bed burns:

1. When the mixed fuel bed was exposed to the radiant energy from the radiant panel, it was observed that the upper pine needle layer had a greater rate of spread than the lower feather moss layer. This occurrence can be attributed to feather moss having better water retention capabilities than pine needles and hence required more energy to ignite and spread.
2. During the burns, a primary fire in the pine needle layer would traverse the length of the fuel bed followed by a delayed secondary fire that occurred in the feather moss layer. The delay and occurrence of the secondary fire in the feather moss layer was due to the feather moss layer retaining more water and thus requiring more energy to enable ignition of the fuel. It should be noted that the fire intensities were calculated using the rate of spread values from the primary fire.
3. The distance traversed by the primary fire in the pine needle layer in the fuel bed was greater than the distance traversed by the secondary fire in the feather moss layer (seen in Fig. 4-5). This occurred as a result of the pine needle layer having a greater rate of spread as well as requiring less energy for ignition.

Since primary fires predominantly occurred in the pine needle layer of the mixed fuel bed, it was expected that the fire behaviour produced would be similar to that of the pine needle fuel bed. Figure 4-4 shows an increase in fire intensity for coverage levels 3 and 4, which can be attributed

to the water retention characteristics of pine needles discussed in Section 4.1.3.1. It was also observed that the fire front was patchy and uneven due to the random orientation of the pine needles in the fuel bed. This uneven fire front could also contribute to an increase in fire intensity.

Figure 4-5: Mixed fuel bed of with a fuel load of 0.941 kg/m^2 and coverage level 3.

Discussion on Coverage Level Experimental Burns

Based on the experimental burns involving the application of various coverage levels on different vegetative fuel types, it was observed that the relationship between fire intensity and coverage level resembled a negative exponential curve. The experimental burns showed that application of water on to the fuel bed helped reduce the fire significantly, thus representing the rapidly decaying

section of the negative exponential curve. The burns also showed that the effect of water at higher coverage levels did not result in significant changes in fire intensity, thereby representing the slow decaying section of the negative exponential curve. The fire behaviour observed in response to the different coverage levels applied was found to depend on the water retention characteristics of the vegetative fuel. Addition of excess water (i.e., high coverage level) to the pine needle fuel bed was not effective in significantly reducing fire intensity due to the relatively poor water retention characteristics of the pine needles. Feather moss fuel bed was found to require significantly less water for changes in fire behaviour to be observed. This was due to the ability of the feather moss to absorb and retain water that was applied on it. Fire behaviour in the mixed fuel bed was found to be more complex to interpret due to the presence of two fuels with significantly different water retention characteristics in the fuel bed. However, since experimental burns involving mixed fuel beds is a closer representation of actual surface fuels than the pine needle and feather moss fuel beds, it is necessary to pursue these experimental burns to help develop a deeper understanding of the relationship between coverage level and fire intensity in real surface fire scenarios. Addition of more surface fuels to increase the accuracy of the fuel bed representing surface fuels would result in increased difficulty using an analytical approach to this investigation. Therefore, more empirical tests in the form of laboratory or field prescribed burns will have to be conducted to investigate the relationship between coverage level and fire intensity further.

The information gathered from the experimental burns involving the different fuel types helped select the fuel type to be used for the Thermal Canister experimental burns. Data in Section 4.1.3.1 suggested that pine needles were not efficient at retaining water. The pine needle fuel bed was also found to have excess water seep through the fuel bed. For the Thermal Canister assembly, this seepage of water or chemicals through the fuel bed would result in the water or chemicals falling

directly on the radiant heater. The risk of water or chemicals influencing the heat source is not ideal and would add variability to the experiment. Therefore, pine needles were rejected as the fuel type to be used in the Thermal Canister experiment. Data from Sections 4.1.3.1 and 4.1.3.2 showed that pine needles and feather mosses have different water retention capabilities and therefore required different amounts of water to reduce the fire intensity significantly. The mixing of these two fuel types would result in fire behaviour that is challenging to interpret, as indicated in Section 4.1.3.3 where experimental burns with a mixed fuel bed were conducted. Therefore, to eliminate further complexity while validating the Thermal Canister test methodology, a mixed fuel bed was rejected as the fuel type for the Thermal Canister experiments. The selection of a feather moss fuel bed was affirmed based on its water retention characteristics as well as its relatively denser fuel arrangement that would help to reduce seepage, if any.

It should be noted that the experimental procedure that was used to investigate the relationship between coverage level and fire intensity as well as fuel load and fire intensity that is presented in Section 4.1.4 did not include fuel consumption as part of the data analysis and interpretation. During the experimental burns, secondary fires were observed in unburned parts of the fuel bed. These secondary fires occurred while waiting to reset the test assembly once the experimental burn was over and were caused due to prolonged exposure to the radiant panel. These secondary fires consumed fuel, thereby resulting in a mass of remaining fuel that did not accurately reflect the mass of fuel consumed in the primary fire. Therefore, fuel consumption was not considered while evaluating and interpreting data from the experimental burns. This can be considered as a disadvantage of the current experimental procedure. It is recommended that a strain gauge-based load cell is installed in the experimental assembly to provide transient mass loss data measurements to circumvent this issue.

4.1.4 Fuel Load Variations

4.1.4.1 Pine Needle Fuel Bed (constant Coverage Level)

Figure 4-6 shows the relationship between the fire intensity and fuel load for an evenly distributed pine needle fuel bed at constant coverage level of 3. The fuel loads used were 0.538, 0.672, 0.806, 0.941, and 1.076 kg/m^2, with each test burn repeated three times (n = 3) to generate a reliable average fuel intensity. The average fire intensities for each fuel load were presented in Fig. 4-6 with the error bars indicating standard deviation. The graph suggests a nearly positive linear trend between fire intensity and fuel load. The different mean fire intensities were verified for statistical significance using a one-way ANOVA test. The *p-value* obtained was 1.09 x 10^{-5} which is less than 0.05, implying that the differences in mean fire intensities are significant. A Tukey's HSD Post Hoc Test was conducted to compare mean fire intensities of different fuel loads. The results from the Tukey's HSD Post Hoc Test are presented in Table 4-5.

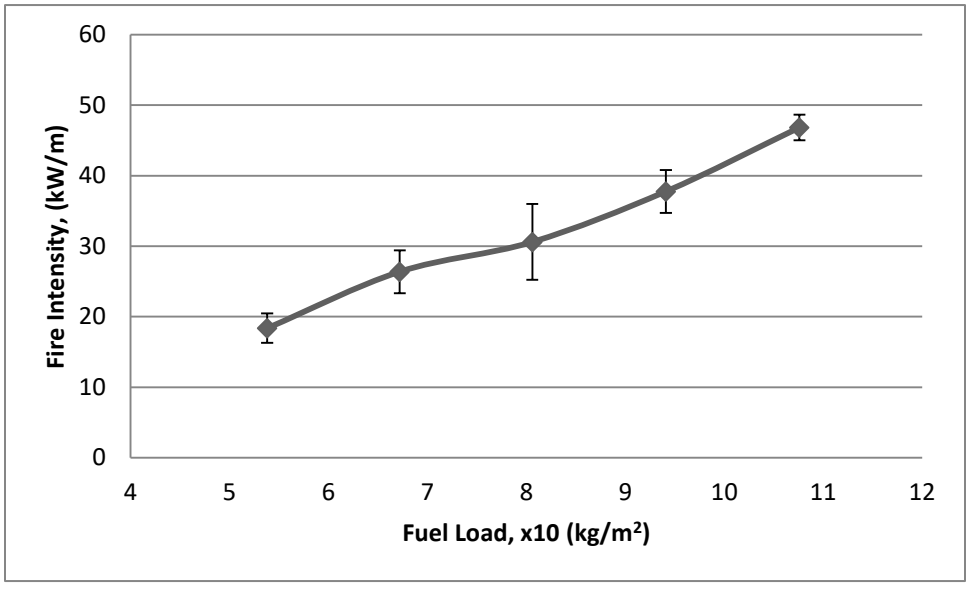

Figure 4-6: Fire intensity versus fuel load at constant coverage level for a pine needle fuel bed

Table 4-5: Tukey's HSD Post Hoc Test for a pine needle fuel bed of varying fuel load and constant coverage level

Fuel Load (kg/m^2)	**0.538**	**0.672**	**0.806**	**0.941**	**1.076**
0.538		0.084071	0.007814	0.000360	0.000178
0.672	0.084071		0.552225	0.012375	0.000283
0.806	0.007814	0.552225		0.134517	0.001100
0.941	0.000360	0.012375	0.134517		0.045672
1.076	0.000178	0.000283	0.001100	0.045672	

The results from Tukey's Post Hoc Test suggest that an addition of 0.134 kg/m^2 of pine needles to a fuel load of 0.538 kg/m^2 was not enough to produce a significant change in fire intensity. This suggests that the effect of the coverage level applied was the dominant parameter that influenced the resultant fire behavior while the fuel load was the auxiliary parameter. However, 0.134 kg/m^2 increases in fuel loads from 0.672 kg/m^2 and upward was found to be enough to produce significantly different fire intensities. This suggests that the increase in fuel load was the dominant parameter in influencing the resultant fire behavior while the applied coverage level was the auxiliary parameter. Thus, for a pine needle fuel bed that has coverage level 3 applied on it, there exists a point between the fuel loads of 0.538 kg/m^2 and 0.672 kg/m^2 where the resultant fire behavior observed is equally influenced by the fuel load and the coverage level applied. Below

this point, the coverage level is the dominant parameter in influencing fire behavior while fuel load is the auxiliary parameter and above this point, the fuel load is the dominant parameter in influencing fire behavior while coverage level is the auxiliary parameter.

4.1.4.2 Feather Moss Fuel Bed (constant Coverage Level)

Figure 4-7 shows the relationship between the fire intensity and fuel load for an evenly distributed feather moss needle fuel bed at constant coverage level of 0.6. The fuel loads used were 0.538, 0.672, 0.806, 0.941, and 1.076 kg/m^2, with each test burn repeated three times (n = 3) for statistical reliability. The average fire intensities for each fuel load were plotted in Fig. 4-7 with the error bars indicating the standard deviation. The graph indicates that there was no noticeable change in the fire intensity for fuels loads of 0.538, 0.672 and 0.806 kg/m^2. However, with fuel loads of 0.941 and 1.076 kg/m^2, the fire intensities increased. In order to ensure that the mean fire intensities are significantly different, an ANOVA test was carried out with a chosen significance level of 5%. The ANOVA test resulted in a *p-value* of 0.000347 which is less than 0.05, implying that there is statistical significance in the difference in means of fire intensities for different fuel loads. To identify which mean fire intensities were statistically different from each other, a Tukey's HSD Post Hoc Test was done. The results of Tukey's HSD Post Hoc Test are presented in Table 4-6.

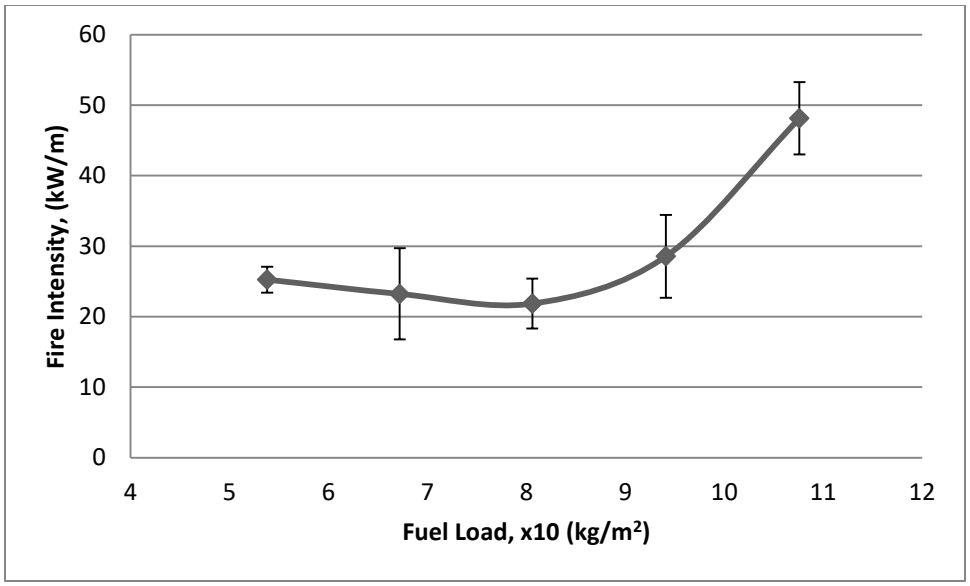

Figure 4-7: Fire intensity versus fuel load at constant coverage level for a feather moss fuel bed

Table 4-6: Tukey's HSD Post Hoc Test for a feather moss fuel bed of varying fuel load and constant coverage level

Fuel Load (kg/m^2)	**0.538**	**0.672**	**0.806**	**0.941**	**1.076**
0.538		0.984596	0.907161	0.914440	0.001473
0.672	0.984596		0.996468	0.674269	0.000810
0.806	0.907161	0.996468		0.482263	0.000570

0.941	0.914440	0.674269	0.482263		0.004368
1.076	0.001473	0.000810	0.000570	0.004368	

The results from Tukey's Post Hoc Test suggest that an addition of 0.134 kg/m^2 to fuel loads of 0.538, 0.672, and 0.806 kg/m^2 was not enough to produce a significant change in fire intensity. This suggests that the applied coverage level was the dominant parameter that influenced the resultant fire behavior while the fuel load was the auxiliary parameter. However, addition of 0.134 kg/m^2 to a fuel load of 0.941 kg/m^2 was able to produce significantly different fire intensity, thereby suggesting that fuel load was the dominant parameter in influencing fire behavior while the applied coverage level was the auxiliary parameter. Thus, there exists a point between the fuel loads 0.806 and 0.941 kg/m^2 where the resultant fire behavior observed is equally influenced by the fuel load and the coverage level applied. Below this point, the coverage level is the dominant parameter in influencing fire behavior while fuel load is the auxiliary parameter and above this point, the fuel load is the dominant parameter in influencing fire behavior while coverage level is the auxiliary parameter.

4.1.4.3 Variation of Fuel Load in Mixed Fuel Bed (constant Coverage Level)

Figure 4-8 shows the relationship between the fire intensity and fuel load for an evenly distributed mixed fuel bed at constant coverage level of 3. The fuel loads used were 0.806, 0.941, 1.076, 1.210, and 1.344 kg/m^2, with each test burn repeated three times (n = 3) for statistical reliability. The average fire intensities for each fuel load were plotted in Fig. 4-8 with the error bars indicating standard deviation. The graph shows a positive trend; an increase in fuel load results in an increase

in fire intensity. It is evident that the increase in fire intensity is marginal between fuel loads of 0.806 and 0.941 kg/m^2. However, the fire intensity increases as more fuel is added to the fuel bed. To statistically quantify the increase in fire intensities across the different fuel loads in order to see which increases in intensities are significant, an ANOVA test was carried out with a significance level of 5%. The *p-value* obtained from the ANOVA test was 0.000349, which is greater than 0.05, implying that within this set of data, a significant difference in mean fire intensities occurs. A Tukey's HSD Post Hoc Test was done to individually compare the mean fire intensities to each other. The results of Tukey's HSD Post Hoc Test are presented in Table 4-7.

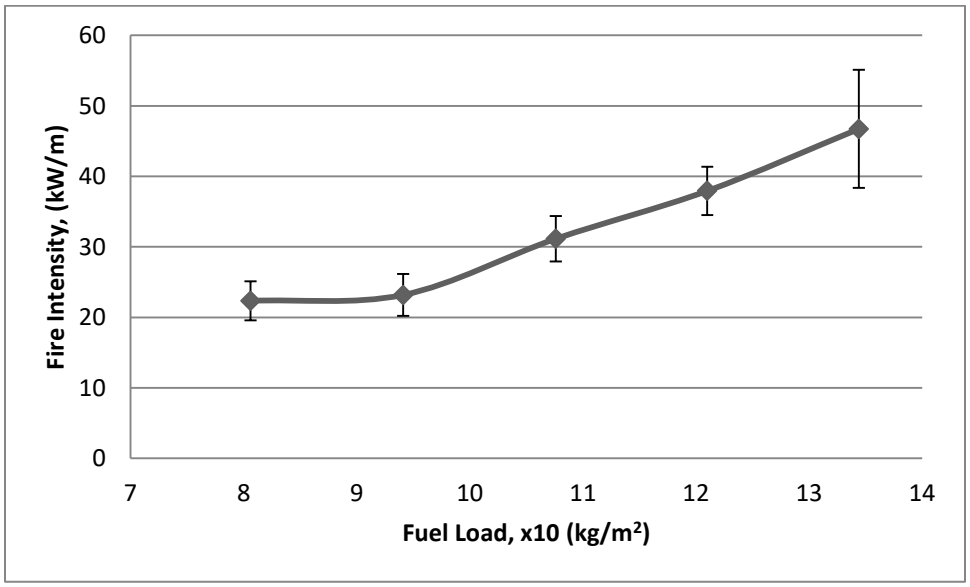

Figure 4-8: Fire intensity versus fuel load at constant coverage level for a mixed fuel bed

The results from Tukey's Post Hoc Test suggest that an addition of 0.134 kg/m^2 to fuel loads of 0.806 and 0.941 kg/m^2 was not enough to produce a significant change in fire intensity. This suggests that the applied coverage level was the dominant parameter that influenced the resultant fire behavior while the fuel load was the auxiliary parameter. However, addition of 0.134 kg/m^2 to fuel loads of 1.076 and 1.210 kg/m^2 was able to produce significantly different fire intensities,

thereby suggesting that fuel load was the dominant parameter in influencing fire behavior while the applied coverage level was the auxiliary parameter. Thus, there exists a point between the fuel loads 0.941 and 1.076 kg/m^2 where the resultant fire behavior observed is equally influenced by the fuel load and the coverage level applied. Below this point, the coverage level is the dominant parameter in influencing fire behavior while fuel load is the auxiliary parameter and above this point, the fuel load is the dominant parameter in influencing fire behavior while coverage level is the auxiliary parameter.

Table 4-7: Tukey's HSD Post Hoc Test for a mixed fuel bed of varying fuel load and constant coverage level

Fuel Load (kg/m^2)	**0.806**	**0.941**	**1.076**	**1.210**	**1.344**
0.806		0.999415	0.217884	0.014476	0.000690
0.941	0.999415		0.294153	0.020229	0.000874
1.076	0.217884	0.294153		0.430926	0.014547
1.210	0.014476	0.020229	0.430926		0.218625
1.344	0.000690	0.000874	0.014547	0.218625	

Discussion on Fuel Load Experimental Burns

Based on the information gathered from the fuel load variation experimental burns with different fuel types, it was inferred that there exists a quantifiable fuel load for which the effects of the applied coverage level and fuel load equally influence the fire behavior. This quantifiable fuel load was found to be different for the different vegetative fuel beds that were used in the experimental burns. The relationship between fuel load and fire intensity can be intensively mapped at different coverage levels for different fuel types by conducting more experimental burns. This would create a database of information which can be used in real life surface fire scenarios. By knowing the fuel load of a specific area, the information from these experiments would be able to suggest which coverage levels would be able to result in non-significant fire intensities that can therefore be controlled.

4.2 THERMAL CANISTER TEST METHODOLOGY

4.2.1 Validation of Test Methodology

The purpose of the Thermal Canister was to develop a methodology to evaluate the relative performance of wildland fire chemicals. Heat released during the combustion process of the fuel beds was considered as a measure of the performance of the chemical treatment. By measuring and comparing the heat release rates from the combusted fuel beds during experimental burns, the relative performance of the fire chemicals was assessed. Treated fuel beds that produced lower heat release rates during experimental burns were considered to have better performance due to their ability to suppress the combustion process better. Therefore, heat release rate was considered to be the performance characteristic of the Thermal Canister test methodology.

The heat release rate of a given fuel bed depends on the heat of combustion of the fuel as well as the rate of combustion of the fuel bed. In the event of a treated fuel, the performance of the chemical treatment and its interaction with the fuel will have to be considered while estimating the heat release rate. To study the performance of the fire chemicals exclusively, the type of fuel (feather moss) was kept constant for all experimental burns. The heat of combustion of the fuel was therefore no longer an influencing factor, which enabled proper assessment of the relative performance of the fire chemicals with the Thermal Canister device.

4.2.1.1 Evaluation of Relative Performance of Fire Chemicals.

To examine the ability of the Thermal Canister to evaluate the relative performance of fire chemicals, four different treatments were selected: water, Foam Product, Gel Product A, and Gel Product B, with all treatments done at coverage level 0.8. The performance of the different fuel treatments was evaluated by studying the average heat release rates from three experimental burns for each fuel treatment. Due to the difference in performance of the fire chemicals, the duration of the combustion process differed for the different treatments. Experimental burns with untreated fuel lasted for a duration of 10 minutes, water and foam-treated fuels burned for 15 minutes, and gel-treated fuels burned for 18 minutes. This difference in the duration of the combustion process for different fuel treatments can serve as a quantitative estimate of the relative performance of the chemicals. However, this estimate cannot distinguish between the relative performances of the chemicals when the duration of the combustion process of the chemicals being compared is similar.

Figure 4-9 shows the average heat release rates of the different fuel treatments: water, Foam Product, Gel Product A, and Gel Product B. The average heat release rate of water at coverage

level 0.8 was used as a control measure to gauge the relative performance of the fire chemicals. Fire chemicals are used in wildland fire suppression since they have better combustion suppression capabilities than water [41]. Therefore, to evaluate the relative performance of the fire chemicals, water was considered as the control measure in this study. The performance of the fire chemicals was evaluated in terms of the percentage increase or decrease in average heat release rates in comparison to the average heat release rate of water-treated fuels. This percentage value was calculated at five time periods, namely 300, 450, 600, 750, and 900 seconds. Table 4-8 shows the relative performance the fire chemicals at these five times.

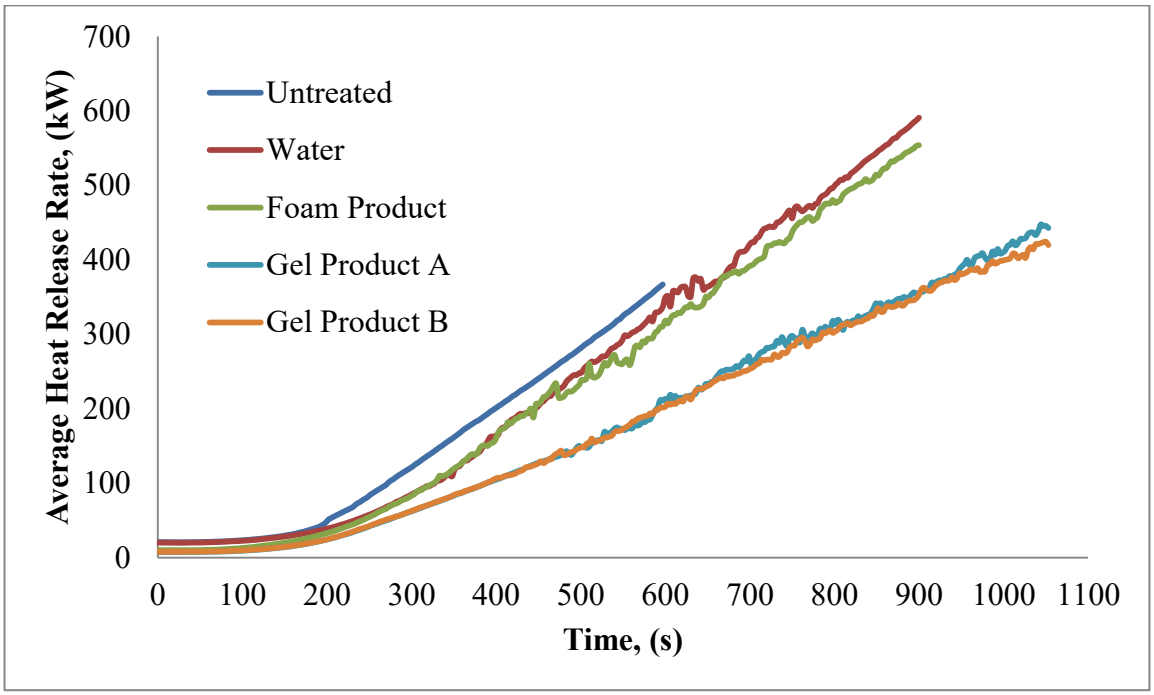

Figure 4-9: Transient average heat release rates of the untreated and treated fuels

Table 4-8: Relative performance of fire chemicals in comparison to water-treated fuel beds.

Treatment / Time	Foam Product	Gel Product A	Gel Product B
300 seconds	1.9%	26.7%	26.0%
450 seconds	-1.5%	37.6%	37.9%
600 seconds	8.9%	39.0%	42.0%
750 seconds	4.0%	34.6%	37.5%
900 seconds	6.2%	39.8%	40.3%

From Table 4-8, it is observed that the use of all three fire chemicals resulted in lower average heat release rates in comparison to the use of water, indicating that they were more effective than water in suppressing combustion. The Foam Product resulted in lower heat release rates in comparison to water; however, the reduction in heat release rates produced was marginal at all five times and therefore, its performance cannot be considered to be a significant improvement in comparison to the performance of water. The Gel Product A and Gel Product B produced significantly lower heat release rates in comparison to those with water and the Foam Product. This indicates that the gel product treatments were the most effective at suppressing the combustion of the fuel. In addition, the two gel products had the longest experimental burn duration (time from start of experimental burn to the time when no smoke is seen in the exhaust indicating end of combustion of the fuel bed) of all treatments, further supporting the inference that the two gel products are more effective at suppressing combustion in comparison to other treatments. The Thermal Canister test methodology was therefore able to characterize the performance of the different fire chemical treatments by comparing the respective heat release rates that were measured by the device.

4.2.1.1 *Evaluation of Repeatability of Test Methodology*

Zero Coverage Level. Figure 4-10 shows the heat release rates as functions of time for three different experimental burns of dry, untreated feather moss fuel. The figure shows the heat lease rates as functions of time for three different burns of dry, untreated feather moss fuel. The five time periods selected to evaluate the repeatability were 201, 300, 399, 501, and 600 seconds. These time periods were selected since they cover both pre-combustion and combustion periods of the experimental burn. Table 4-9 shows the standard deviation and coefficient of variation of the five time periods, for the three experimental burns that were conducted under identical conditions.

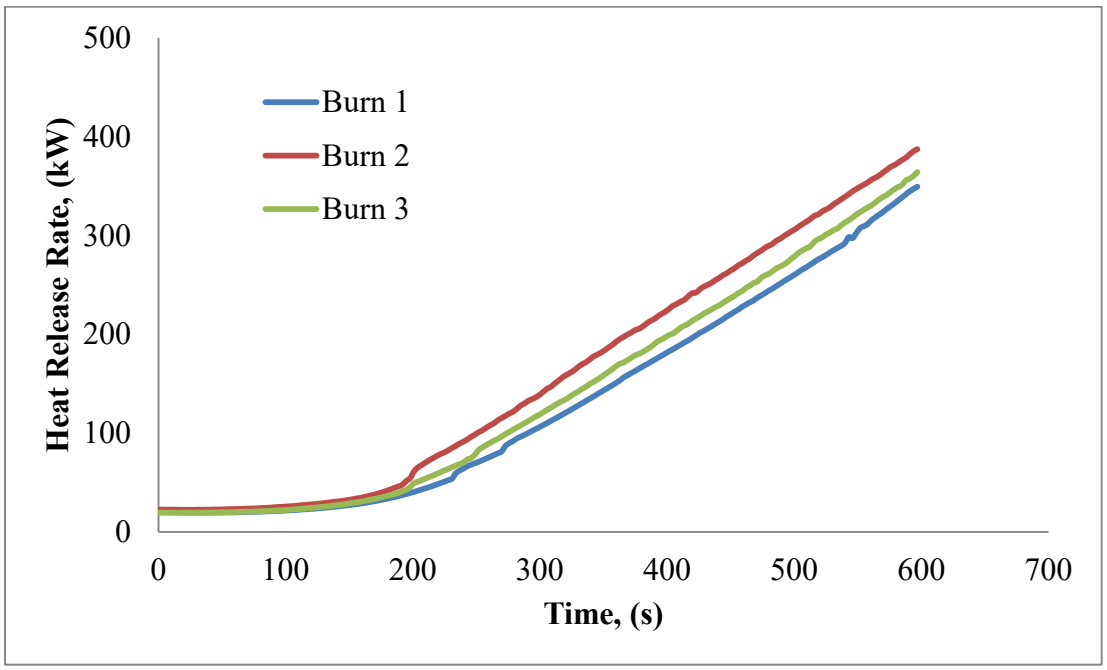

Figure 4-10: Heat release rate from burns of a dry, untreated feather moss fuel bed (zero coverage level).

Table 4-9: Standard deviation and coefficient of variation of heat release rates from burns of dry, untreated feather moss fuel bed (zero coverage level).

Time Period (s)	Standard Deviation (kW)	Coefficient of Variation
201	10.3	20.5%
300	16.4	13.5%
399	21.3	10.6%
501	23.0	8.1%
600	19.0	5.1%

Heat release rate data from the three experimental burns showed low standard deviation values at different time periods of the experiment (seen in Table 4-9). The repeatability standard deviation calculated from the standard deviation data was 18.4 kW, suggesting good repeatability of the test method. The coefficient of variation was calculated at each time period in order to evaluate the standard deviation values relative to the absolute average heat release rate at that time period. The low percentage values of the coefficient of variation at different time periods further suggested that the test methodology had good repeatability.

Water at Coverage Level 0.8. Figure 4-11 shows the transient heat release rates from three different experimental burns of a feather moss fuel bed treated with water at coverage level 0.8. It was observed that the heat release rates for all experimental burns involving treated vegetative fuels produced non-smooth curves. This suggests that the presence of the treatment products affected the combustion of the vegetative fuels, resulting in an irregular combustion process. The suppression of combustion caused by the different treatments resulted in combustion occurring in different sections of the fuel bed at different times during the experimental burns. The interaction

of the treatment products with the random orientation of the fuel bed also contributed to the irregular combustion process. Therefore, sudden fluctuations were observed in the heat release rate data that was plotted.

Table 4-10 shows the standard deviation and coefficient of variation that was calculated from the heat release rate data obtained from the experimental burns. The repeatability standard deviation was calculated from the standard deviation values and found to be 24.5 kW. This low repeatability standard deviation and reasonable coefficient of variation values suggest that this test method is repeatable for water-covered fuel beds.

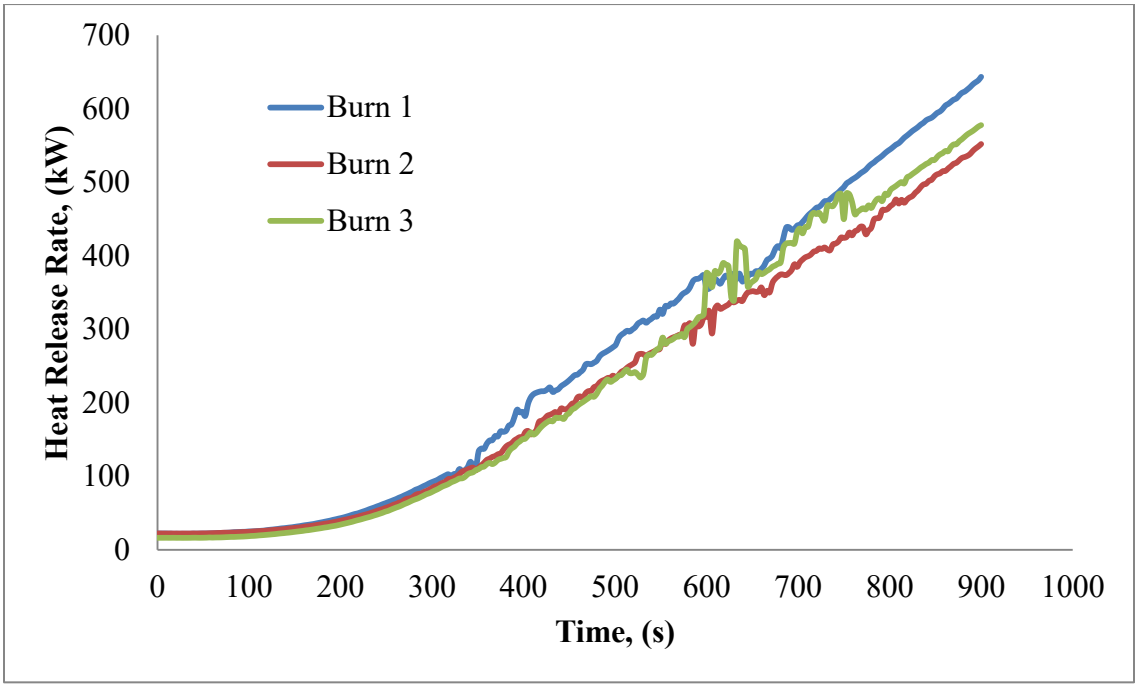

Figure 4-11: Heat release rate from burns of feather moss fuel bed covered with water at coverage level 0.8.

Table 4-10: Standard deviation and coefficient of variation of heat release rates from burns of feather moss fuel bed covered with water at coverage level 0.8.

Time Period (s)	Standard Deviation (kW)	Coefficient of Variation
300	6.8	8.0%
399	20.8	12.7%
501	26.4	10.6%
600	30.1	8.6%
699	30.3	7.2%

Foam Product at Coverage Level 0.8. Figure 4-12 shows the heat release rates as functions of time for three different experimental burns of a feather moss fuel bed treated with the Foam Product at coverage level 0.8. The occurrence of non-smooth curves due to the fluctuations in heat release rate during the combustion process caused by the foam treatment was observed. Standard deviation data (presented in Table 4-11) suggests an increase in deviation from the mean during the combustion process. However, the decrease in coefficient of variation implies that these increasing standard deviations relative to the absolute heat release rates is not significant. The repeatability standard deviation was calculated from the standard deviation values and was found to be 28.4 kW, suggesting that the Thermal Canister has reasonable repeatability. Visual observation of Fig. 4-12 suggests that the heat release rate from Burn 3 is lower than those of Burns 1 and 2, consequently causing an increase in the standard deviation values. The change in heat release rate values observed in Burn 3 implies a change in the performance of the Foam Product. This change in suppression capabilities can be attributed the physical properties of the Foam Product.

The Thermal Canister lacks a cooling mechanism, and therefore required that each experimental burn was complete so that the enclosure walls could cool to the initial temperature. The time period

allowed for this cooling phase was 24 hours. This time period between two successive experimental burns allowed the physical properties of the Foam Product to change. The performance of foam as a surfactant is highly dependent on the properties of the bubbles that are formed during its mixing process [48]. The gas fraction and bubble size of a foam mixture are known decrease until equilibrium is reached [49]. Gardiner *et al.* [48] found that it is necessary to keep all variables such as surface tension, bubble size, and liquid phase viscosity constant throughout the experiments in order to avoid variability in performance of the foam. This time-dependent change in foam properties affected the performance of the foam as a surfactant when the same mixed product is used over extended periods of time.

The Foam Product used in the three experimental burns was prepared as a batch on the day of the first burn. This batch preparation was done to avoid any variability in mixing ratios. The Foam Product was stored in air-tight containers and used for burns 2 and 3. Since the properties of the foam used in Burn 1 was different from that of Burn 2 and Burn 3, the stipulated conditions for repeatability were not met. Therefore, the data from the experimental burns that used the Foam Product should not be considered towards evaluating the repeatability of the Thermal Canister as a device for measuring the heat release rates of the burning fuel beds. The time period required for the Thermal Canister to return to its initial temperature was considered as a negative feature of this test methodology.

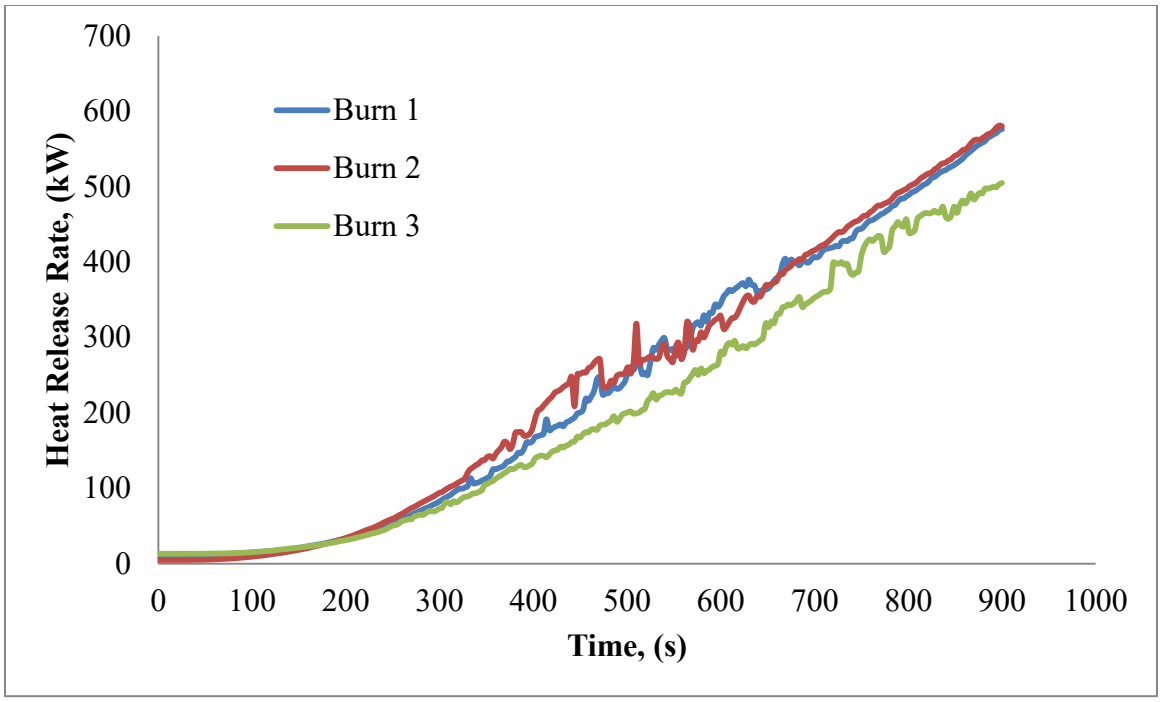

Figure 4-12: Heat release rate from burns of feather moss fuel bed covered with the Foam Product at coverage level 0.8.

Table 4-11: Standard deviation and coefficient of variation of heat release rates from burns of feather moss fuel bed covered with the Foam Product at coverage level 0.8.

Time Period (s)	Standard Deviation (kW)	Coefficient of Variation
300	10.5	12.6%
399	23.2	14.7%
501	32.9	13.8%
600	33.4	10.5%
699	34.5	8.8%

Gel Product A and Gel Product B, at Coverage Level 0.8. Figures 4-13 and 4-14 show the transient heat release rates from different experimental burns of feather moss fuel beds treated with Gel

Product A and Gel Product B respectively, at coverage level 0.8. Visual observation of Fig. 4-13 and 4-14 of the minimal dispersion among the heat release rate curves combined with standard deviation and coefficient of variation data found in Tables 4-12 and 4-13 suggest that the test methodology is capable of producing repeatable results. The repeatability standard deviation calculated from the standard deviation at the five selected time periods was found to be 11.9 kW and 1.2 kW for Gel Product A and Gel Product B respectively, reinforcing that the test methodology has reasonable repeatability. Non-smooth heat release rate curves were once again observed, indicating the effect of Gel Product A and Gel Product B on the respective combustion processes. Heat release rate data showed no drop or change in performance across the three experimental burns for both gel products, unlike what was observed in Burn 3 of the Foam-treated experimental burns. Since there were no changes in the performance of the fire chemicals, it was assumed that the physical properties of Gel Product A and Gel Product B remained constant for all three respective experimental burns, and therefore met the repeatability criteria of unchanged test conditions and parameters.

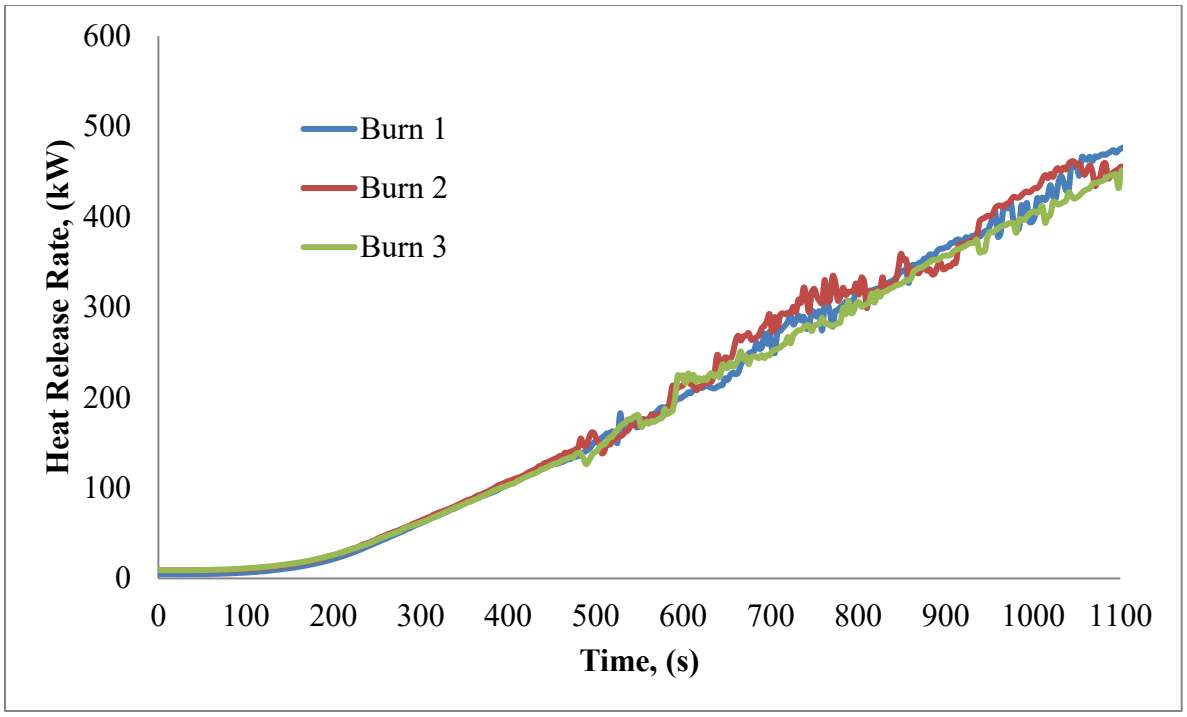

Figure 4-13: Heat release rate from burns of feather moss fuel bed covered with Gel Product A at coverage level 0.8.

Table 4-12 : Standard deviation and coefficient of variation of heat release rates from burns of feather moss fuel bed covered with Gel Product A at coverage level 0.8.

Time Period (s)	Standard Deviation (kW)	Coefficient of Variation
300	1.5	2.4%
399	2.4	2.3%
501	7.1	4.8%
600	11.6	5.4%
699	22.7	8.4%

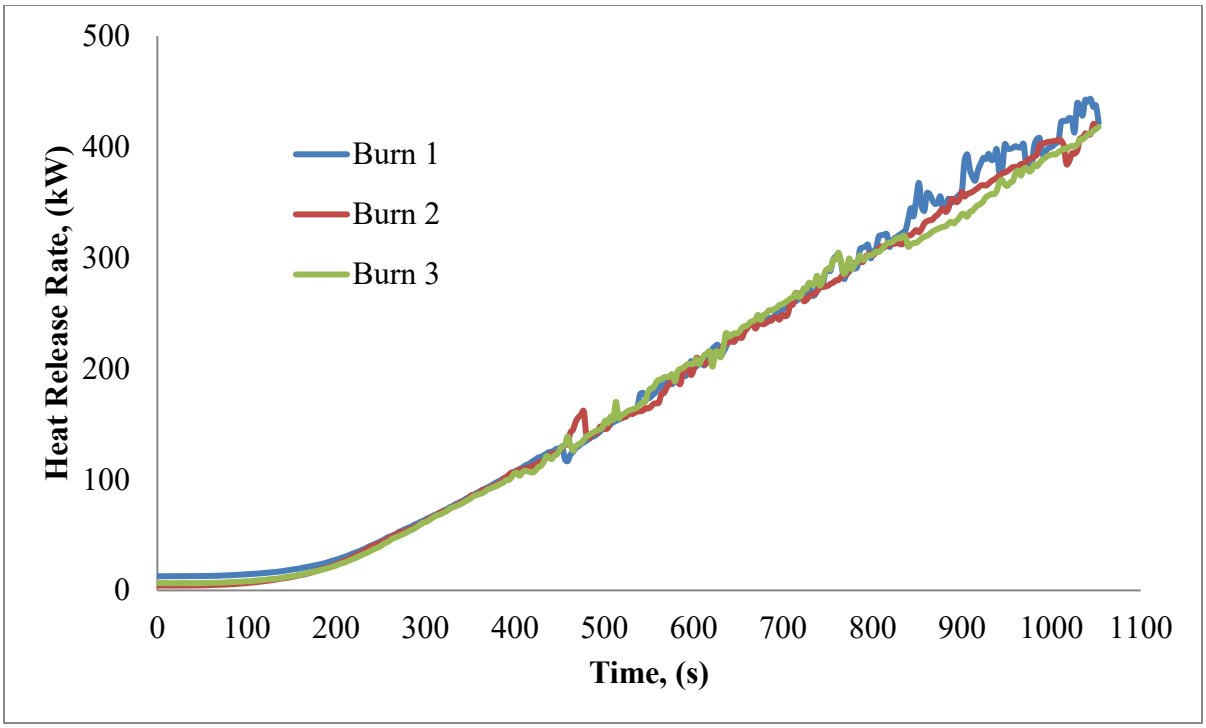

Figure 4-14: Heat release rate from burns of feather moss fuel bed covered with Gel Product B at coverage level 0.8.

Table 4-13: Standard deviation and coefficient of variation of heat release rates from burns of feather moss fuel bed covered with the Gel Product B at coverage level 0.8.

Time Period (s)	Standard Deviation (kW)	Coefficient of Variation
300	1.2	1.8%
399	0.8	0.8%
501	4.3	2.9%
600	3.1	1.6%
699	4.8	1.9%

The low standard deviation, coefficient of variation, and repeatability standard deviation values for the experimental burns involving untreated fuel beds, water-covered fuel beds, Gel Product A-

treated fuel beds, and Gel Product B-treated fuel beds suggest that the test methodology is capable of producing repeatable results within reasonable heat release rate value deviations for the purpose of testing wildland fire chemicals. Data from the experimental burns involving the Foam Product-treated fuel beds was excluded from the repeatability evaluation due to the change in physical properties of the chemical product. The Foam Product experimental burns, however, show that the Thermal Canister test methodology is capable of testing changes in the performance of a product, and can thus be used in the quality assessment of products and evaluation of time-dependent performance of products.

4.2.2 Error Analysis of Thermal Canister

A bias uncertainty analysis was conducted on Eq. 2-55 to determine the amount of error that occurred due to inherent errors in the instrumentation and the devices that were used in the Thermal Canister assembly. A bias describes the difference between the measured value and the actual value of a parameter. This difference between the measured value and actual value of a parameter can be caused by manufacturer-related uncertainties that are outlined in the product documentation of each measurement device. A bias uncertainty analysis calculates the maximum possible difference between the measured value and the actual value for each variable in an equation. The bias of different variables propagates through an equation to produce one value that describes the total uncertainty of that measurement. It should be noted that a bias uncertainty analysis is different from a precision uncertainty analysis where the difference in measurements is between only measured values and is not compared to the actual value. There were fourteen variables in Eq. 2-55, namely ρ, C_p, A_c, V, ΔT_e, A_s, ε, k, W, ΔT_w, σ, $T_2(W,t)$, $T_1(0,t)$, and T_∞, which may have contributed to the uncertainty in the estimated heat release rate. The associated error with variables

such as density of the flue gas, ρ, specific heat capacity of the flue gas, C_p, emissivity of the enclosure wall, ε, and thermal conductivity of the enclosure wall, k, were assumed to be zero even though in practice, these variables would have error. These variables were either assumed or were taken from the studies of other researchers. The ambient temperature, T_∞, was also considered to have zero error as the value assumed was taken to be constant. The Stefan-Boltzmann constant was assumed to have an error of zero because it is a well-known and documented constant. Temperature measurements for ΔT_e, ΔT_w, $T_2(W,t)$, and $T_1(0,t)$ were measured using a Type-J thermocouple that had an associated error of 1.1°C or 0.4% (greater of the two values), as provided by the manufacturer. Error associated with a thermocouple is calculated by the fixed point method or by the comparison method, both yielding the upper limit of error [90]. Therefore, when considering the propagation of uncertainty in the heat release rate calculations, the uncertainty obtained would be conservatively high. Errors associated with the length measurements for variables such as area of cross-section of exhaust pipe A_c, surface area of the enclosure walls A_s, and thickness of the enclosure wall W were determined by considering the accuracy of the measuring tape that was used. The manufacturer indicated that the error for the measuring tape was 1 mm. The error for the anemometer that was used to measure the velocity of the flue gas was 0.1 m/s.

The propagation of uncertainty calculations was conducted by using equations derived from Taylor [91]. The propagated uncertainty in the estimated heat release rate is

$$\left(\frac{\omega_{q'Total}}{q'_{Total}}\right)^2 = 4\left(\frac{\omega_r}{A_c}\right)^2 + \left(\frac{\omega_V}{V}\right)^2 + \left(\frac{\omega_{\Delta T_e}}{\Delta T_e}\right)^2 + \sum_{i=1}^{10}\left\{\begin{array}{l}\left(\frac{\sqrt{\omega_l^2+\omega_b^2}}{A_s}\right)^2 + \left(\frac{\omega_{\Delta Tw}}{\Delta T_w}\right)^2 + \left(\frac{\omega_W}{W}\right)^2 \\ +16\left(\frac{\omega_{T_2(W,t)}}{T_2(W,t)}\right)^2 + 16\left(\frac{\omega_{T_1(0,t)}}{T_1(0,t)}\right)^2\end{array}\right\}_i . \qquad (4\text{-}1)$$

Two time periods, 300 and 500 seconds, were selected from experimental burn, Burn 1 with the Gel Product B-treated fuel bed. The 300-second time period was during the pre-combustion phase of the experimental burn and the 500-second time period was during the combustion phase of the experimental burn. It was found that the errors associated with the two time periods were 47% and 40%, respectively. This large error stems from the error associated with the J-type thermocouple and can be considered as a conservatively high estimate due to the manufacturer associated error of the thermocouples representing the upper limit of error. Therefore, in practice, the error associated with the heat release rate estimates would be much lower than the 47% and 40% for pre-combustion and combustion phases of the experimental burn, respectively. Thirty-one (31) thermocouples were used in the test assembly to obtain temperature readings. The propagation of the error associated with each thermocouple reading forms the largest component of uncertainty in the heat release rate equation. To reduce the errors, the J-type thermocouples could be replaced by the R/S-type thermocouples. The R/S-type thermocouples have a manufacturer-rated error of 0.6°C or 0.25% and would reduce the level of uncertainty in the estimated heat release rates. This option would, however, prove to be a more expensive one.

4.2.3 Evaluation of Functionality of Thermal Canister

The Thermal Canister was able to capture heat released during the combustion process of the fuel bed in five different directions. This methodology eliminates the orientation issues that Anderson [73] faced due to the positioning of the heat flux sensor relative to the burning fuel. Variability due to the orientation of the fuel is also overcome by capturing energy in all directions. Therefore, the fuel orientation, a variable that is difficult to control for fine-fuel fuel beds, is no longer a parameter that influences the measurements of performance of the chemical treatments. External

environmental influences such wind speed and direction, ambient temperature, and relative humidity do not have to be considered since the fuel bed is placed in an enclosure. The methodology is also capable of measuring time-to-ignition. The onset of fluctuations in curves of heat release rates versus time, as seen in Figs. 4-11 to 4-14, indicate that the treated fuels have ignited. However, the time-to-ignition values measured from the onset of fluctuations in the transient heat release rates curves are not accurate. At the time of ignition, energy is released from the fuel and is incident on the walls of the canister. This incident energy and consequent change in the wall temperature is not recorded simultaneously in all the walls due to the location of the fuel within the Thermal Canister device. The fuel is located at the bottom of the Thermal Canister device and is not equidistant from all the walls of the Thermal Canister. Therefore, the temperature change due to the energy released from ignition of the fuel is recorded in each wall at a marginally different time. This marginal time difference in recording temperature data of the walls of the Thermal Canister results in an inaccurate time-to-ignition value deduced from the heat release rate curves. In addition, the issues of measurement resolution and thermal lag of this device (discussed below) add to the inaccuracy of the time-to-ignition measurements. The Thermal Canister is therefore able to provide an estimate of the time-to-ignition but with a lower degree of accuracy, and hence should not be relied upon. This method of measuring time-to-ignition is, however, independent of visual measurements, thereby promoting safe practices.

The Thermal Canister does have drawbacks in measurement resolution, thermal lag, and the lack of a cooling mechanism. If the fuel present in the enclosure has a low heat of combustion or the sample size is too small, the incident heat flux on the walls of the enclosure will be too low to result in a significant temperature difference between the inside and outside faces of each wall. Energy incident on the walls of the enclosure is the sum of energy from the combustion of fuel,

radiative heat transfer from the radiant panel, as well as heat transfer from the heated air that passes through the assembly. If the heat of combustion of the fuel is very low, the energy conducted through the walls of the enclosure will predominantly comprise of radiation from the radiant panel and from the heated air. Therefore, it is necessary that the samples being assessed have large mass or large heat of combustion values. All sensible enthalpy rise systems have been documented to have dynamic errors related to thermal lag, which are difficult to eliminate [74]. The Thermal Canister is based on the concept of sensible enthalpy rise and therefore inherits this issue. The lack of a cooling mechanism for the test assembly has been discussed in the evaluation of repeatability of the test methodology, stating that experimental burns cannot be done at a higher frequency due the time required for the assembly to return to its initial conditions.

The Thermal Canister test methodology can be improved by installing measurement devices that enable the accurate measurement of the exhaust gas properties. This would improve the accuracy of the estimates of the heat release rate, which are currently calculated by assuming that the properties of the exhaust gas in the mathematical calculations are those of dry air. The test methodology should also include precautions to clean the inside walls of the Thermal Canister prior to every new experimental burn. This would enable the removal of remnant residual chemicals that may reside on the inner walls of the Thermal Canister enclosure from previous experimental burns that may influence the surface temperature of inner walls. In addition, accurate temperature measurement of the air column inside the Thermal Canister enclosure would allow for better estimation of the energy lost by radiation from the inner walls of the Thermal Canister enclosure to the air column.

The mathematical model that applied to the Thermal Canister can be improved by accounting for the energy gain/loss experienced by one section of the Thermal Canister wall due to radiation from

other Thermal Canister wall sections in the enclosure. This would include shape factor calculations for the walls as well as the lid of the Thermal Canister.

4.2.4 Evaluation of Capabilities of Thermal Canister

Wildland fire chemicals are manufactured as concentrates, with recommended mixing ratios for these concentrates detailed in the Qualified Products List (QPL) [92] produced by the US Forestry Service. The recommended range of mixing ratios for these chemical concentrates is based on their toxic impact on the environment. However, the QPL does not provide any information about the performance of the fire chemicals at different mixing ratios. Therefore, there exists a need to investigate the performance of each fire chemical for the specified mixing ratio to have a better understanding of the performance of the products and to identify the optimum mixing ratio of these products. The Thermal Canister is a suitable test methodology to conduct this investigation, where a range of mix ratios for different products can be evaluated and their relative performance can be gauged. The methodology also provides control over the quantity of fire chemicals that should be applied on a fuel bed. This control reduces the error that occurs in other test methods such as the ones described by Anderson [73] and Pluscinski *et al.* [63], where the possibility of application of excess fire chemicals can arise. The Thermal Canister test methodology can also be used to study the long term performance of wildfire chemicals. Water-based wildfire chemicals, specifically foams and gels, are expected to experience a reduction in performance over time due to the evaporation of water. However, this reduction in performance has only been a qualitative observation during field experiments and has not been quantified. The Thermal Canister test methodology would enable proper quantification of the change in the performance of the wildfire

chemicals over time. This information would be useful in aerial applications when wildfire chemicals such as foams and gels are being applied in advanced of the fire front.

The Thermal Canister may also enable the study of whether an increase in the mixing ratio of a fire chemical leads to improved performance of the product. Currently, the relationship between mixing ratio and performance of fire chemicals has not been well documented. It was observed during the experimental burns involving Gel Product A that an increase in mixing ratio to 3% resulted in a significant increase in viscosity of the mixed product. As a consequence of increased viscosity, the wetting capabilities of the product decreased, thereby retarding surface exposure. A reduction in surface exposure led to an increase in the size of the thermal blanket formed on the fuel bed. This trade-off between a decrease in surface exposure and an increase in fuel bed protection should be evaluated thoroughly.

The Thermal Canister test methodology can be used to evaluate the heat release rate for broader applications. This test methodology accommodates the use of both foliar and non-foliar samples, and therefore may find applications in testing of building protection material. Sample sizes of the fuel being assessed can also be varied. This test method may be an alternative for experiments such as the bomb calorimeter, where there is minimal flexibility for changes in sample size.

5 CONCLUSIONS

The relationship between fire intensity, fuel load, and coverage level was explored using three different types of fuel beds: pine needle fuel bed, feather moss fuel bed, and a mixed fuel bed of pine needles and feather moss. An experimental assembly was fabricated where a radiant panel was used to simulate radiant energy from a forest fire. Coverage level and fuel load values were individually varied in separate experiments for each fuel type. The fire intensities were calculated using Byram's Fireline Intensity formula. An analysis of variance (ANOVA) test was conducted to verify if the mean fire intensities obtained were statistically different. A Tukey's HSD (honestly significant difference) Post Hoc Test was done to further study the differences in mean fire intensities.

It was found that the relationship between the coverage level and fire intensity for different types of fuel bed resembled a negative exponential curve. The resultant fire behavior obtained when coverage levels was varied for different fuel beds was dependent on the water retention characteristics of the fuel. The fire behavior observed in the experimental burns involving pine needle and feather moss fuel beds were relatively straightforward and were discussed based on water retention characteristics of the respective fuels. The fire behavior observed in the mixed fuel bed was also interpreted based on the water retention characteristics of the fuel bed but was found to be more complicated due to the coexistence of two vegetative fuels with significantly different water retention characteristics. It was observed that the pine needle layer in the mixed fuel bed had a higher rate of spread than the feather moss layer since the feather moss was able to retain more water, and thus required more energy to ignite. Since the fire was predominantly in the pine needle

layer of the mixed fuel bed, the fire behavior that was observed closely resembled that of the pine needle fuel bed.

The investigation of the relationship between fuel load and fire intensity saw a positive relationship for the three different vegetative fuel beds. Based on the information gathered from the fuel load variation experimental burns, it was inferred that there exists a quantifiable fuel load for which the effects of applied coverage level and fuel load equally influence the fire resultant fire behavior. This quantifiable fuel load was found to be different for the different vegetative fuel beds that were used in the experimental burns.

Information from the coverage level variation experimental burns was used to select the fuel type used in a custom built-thermal calorimeter. The calorimeter, known as the "Thermal Canister" was developed by Anderson [76] using a one-dimensional heat conduction model based on uniform heating of a rectangular-shaped body. The purpose of the Thermal Canister was to estimate the heat release rate produced during the combustion of vegetative fuels, which would be used as a means to evaluate the performance of the fire chemicals. Modifications to the mathematical model and experimental design were made in order to generate accurate estimates of the heat release rate.

Five different fuel treatments were selected to validate the repeatability of the experimental assembly as well as evaluate the relative performance of the treatments. The names of the products used as treatments were intentionally excluded for proprietary reasons. The different fuel treatments selected were: untreated fuel (no water/chemicals), water at coverage level 0.8, Foam Product at coverage level 0.8, Gel Product A at coverage level 0.8, and Gel Product B at coverage level 0.8. The mixing ratios used in preparation of the fire chemicals were selected as per the specifications that were provided by the manufacturers. Experimental burns for each treatment

type were carried out three times to examine the validity of the test methodology as well as evaluate the repeatability of the Thermal Canister. The performance characteristic of the test methodology was identified as the heat release rate and was used to evaluate the relative performance of the fire chemicals. By comparing the average heat release rates measured by the device at different times, the test methodology was able to characterize the performance of the different fire chemical treatments. Narrow standard deviation, coefficient of variation, and repeatability standard deviation values suggested that the test methodology was repeatable. The test methodology may be used as an alternative method to evaluate the performance of wildland fire chemicals.

A discussion on the functionalities and capabilities of the Thermal Canister was presented. The test methodology was found to be capable of evaluating the performance of fire chemicals at different mixing ratios on both foliar and non-foliar samples. The test methodology also addressed several deficiencies in other test methodologies such as orientation dependent capture of heat released during combustion, control cover the volume of fire chemicals used in experiments, and protection against external environmental factors such as wind. The Thermal Canister may also be used for a wide range of applications where the heat release rates of other types of non-vegetative fuels are required.

6 RECOMMENDATIONS FOR FUTURE WORK

Coverage Level and Fire Intensity Experiments

The fire behavior observed in the coverage level experiments showed that the resultant fire intensities were dependent on the water retention characteristics of the vegetative fuels. Interpreting fire behavior for experimental fuel burns involving pine needle and feather moss fuel beds was relatively easy due to the presence of only one vegetative fuel type in the fuel bed. However, interpreting fire behavior in the mixed fuel bed was found to be more complex due to the presence of different vegetative fuel types in the fuel bed, each with different water retention characteristics. The different water retention characteristics of the vegetative fuels present in the mixed fuel bed made it difficult to develop an analytical approach to this problem. Therefore, it will be necessary to conduct further experimental burns with mixed fuel beds to understand the relationship between coverage level and fire intensity better. Experimental burns with mixed fuel beds represent surface fires more accurately than fuel beds with only one vegetative fuel type. Results and observations obtained from mixed fuel bed experimental burns would therefore be more applicable in real life surface fire scenarios. Addition of other vegetative fuels such as grass and leaves would improve the accuracy of the fuel bed representation of surface fuels, thereby providing a more accurate representation of fire behavior in surface fires. An alternate approach can be taken to understand how coverage levels affect ignition and fire intensity. The application of coverage level directly affects the moisture content of a vegetative fuel. A study can be conducted to evaluate the impact of varying moisture content of the fuel on ignition and combustion of the fuel. This research would build on several existing studies that focus on ignition probability based on the information from wildland fire information systems that rely on fine fuel moisture content (FFMC) as a key indicator of fire danger in their fire forest prediction models.

This study would be divided into two main components: studying the impact of moisture variation on ignition and relating changes in fuel moisture content based on the applied coverage. The results of this study would be beneficial since the focus of moisture content as the primary parameter of interest would enable the information from this research to build on current forestry prediction models that also use moisture content in the determination of the flammability of vegetative fuel.

Fuel Load and Fire Intensity Experiments

The information gathered from the experimental burns involving fuel load variations at constant coverage levels suggested that there exists a quantifiable fuel load for which the applied coverage level and the fuel load equally influence the resultant fire behavior. This experiment can therefore be expanded to map the relationship between fuel load and fire intensity for different fuel types at different coverage levels to find this quantifiable fuel load. By creating an information database using the different parameters and results from this experiment, a coverage level can be suggested based on the fuel type and fuel load such that significant increases in fire intensity are avoided in practice. This information can find practical field applications where dispatch can rely required coverage level information to aerial tankers based on the fuel load and fire intensity of an advancing fire.

Thermal Canister Methodology

The Thermal Canister was shown to be capable of estimating the heat release rate that was used to gauge the relative performance of fire chemicals. However, the transient response time of the Thermal Canister in relation to the response of the thermocouples was not studied in great detail. The transient response is a crucial parameter in improving the accuracy of estimated time-to-ignition measurements using the Thermal Canister device. Investigating the transient response

time would involve modelling the thermocouples as embedded into the walls of the Thermal Canister.

The error analysis conducted in Section 4.2.2 determined the quantitative error that could occur in the heat release rate estimates that were obtained using the Thermal Canister. However, these errors were determined using the manufacturer's stated limit of error. The use manufacturer's stated limit of error in the error analysis leads to the most conservative scenario. Therefore, the errors in the heat release rate estimates may actually be significantly lower. Determining the actual thermocouple errors would be required to determine the actual heat release rate estimates. This process would involve developing a rigorous industry-standard calibration procedure to determine the actual errors in the temperature values from the thermocouples used in the Thermal Canister. In addition, calibration of the Thermal Canister device would be required if the device is intended for commercial use. This calibration process may be developed alongside the calibration process of the thermocouples. Accuracy of the heat release rates estimates can be further improved by determining the properties of the fuel gas and incorporating those properties into the heat release rate calculations. Comparing the performance of the Thermal Canister with other calorimeters using similar materials is also required to test the accuracy of the heat release rate measurements. Further, an energy balance assessment to investigate the existence of any unaccounted energy losses or leaks that may occur during the experimental burns would help improve the accuracy of the Thermal Canister methodology.

The Thermal Canister test methodology was found to be effective in characterizing the relative performance of fire chemicals. If industrial practitioners intend to employ this test methodology, a standard test produce must be developed for the preparation of the vegetative fuel, fire chemicals, and test assembly as well as for the proper execution of the experiment. Furthermore, additional

experiments would have to be conducted where parameters such as fuel type, fuel load, and coverage level are varied to determine the ideal parameters help determine the relative performance of the fire chemicals. Developing a suitable cooling mechanism for the Thermal Canister would help increase the frequency of the experimental burns, which would be highly beneficial for industrial use where the performance several samples of fire chemicals would need to be frequently evaluated.

7 REFERENCES

[1] A. Shlisky, J. Waugh, et al. “Fire, Ecosystems and People: Threats and Strategies for Global Biodiversity Conservation,” GFI Technical Report 2007-2, The Nature Conservancy, Arlington, VA, 2007.

[2] S. H. Doerr, C. Santin, “Global trends in wildfire and its impacts: preceptions vervus realities in a changing wold,” *Phil. Trans. R. Soc. B*, 371 20150345, 2016.

[3] R. C. Balling, G. A. Meyer, S. G. Wells, "Relation of surface climate and burned area in Yellowstone National Park," *Agricultural and Forest Meteorology,* Vol. 60, no. 3-4, pp. 285-293, 1992.

[4] E. K. Heyerdahl, L. B. Brubaker, J. K. Agee, "Annual and decadal climate forcing of historical fire regimes in the interior Pacific Northwest, USA," *Holocene,* Vol. 12, no. 5, pp. 597-604, 2002.

[5] A. L. Westerling, H. G. Hidalgo, D. R. Cayan, T. W. Swetnam, "Warming and Earlier Spring Increase Western U.S. Forest Wildfire Activity," *Science,* Vol. 313, no. 5789, pp. 940-943, 2006.

[6] X. Wang, D. K. Thompson, G. A. Marshall, C. Tymstra, R. Carr, M. D. Flannigan, “Increasing frequency of extreme fire weather in Canada with climate change,” *Climatic Change*, Vol. 130 (4), 2015.

[7] B. J. Stocks *et al*., “Large forest fires in Canada, 1959-1997,” *J. Geophysc. Res.*, 107, 8149, 2002.

[8] S. W. Running, “Is global warming causing more, larger wildfires?” *Science*, Vol. 313, pp. 927–928, 2006.

[9] P. N. Omi, “Forest Fires: A Reference Handbook,” Santa Barbara: ABC-CLIO, 2005, p. 102.

[10] W. W. Knorr, T. T. Kaminski, A. A. Arneth, U. U. Weber, "Impact of human population density on fire frequency at the global scale," *Biogeosciences Discussions,* Vol. 10, no. 10, pp. 15735-15778, 2013.

[11] M. A. Moritz, M. Parisien, E. Batllori, M. A. Krawchuk, J. Van Dorn, D. J. Ganz, K. Hayhoe, “Climate change and disruptions to global fire activity,” *Ecosphere*, Vol. 3 (6), http://dx.doi.org/10.1890/ES11-00345.1, 2012.

[12] G. D. Haddow, J. A. Bullock, D. P. Coppola, “Introduction to Emergency Management (4th ed.),” Elsevier, Burlington, MA, USA, 2011.

[13] OIG (Office of the Inspector General), "Audit report: Forest Service large fire suppression costs," San Francisco, USDA Office of the Inspector General Western Region, Report No 08601-44-SF, 2006, p. 4.

[14] D. Gavin, D. Hallett, F. Hu, K. Lertzman, S. Pichard, K. Brown, J. Lynch, P. Bartlein, D. Peterson, "Forest fire and climate change in western North America: insights from sediment charcoal recoards," *Frontiers in Ecology and the Environment,* Vol. 5, pp. 449-506, 2007.

[15] Alberta Government, “Recovery after the Wood Buffalo Wildfire”, https://www.alberta.ca/documents/Wildfire-Home-Again-Report.pdf (accessed on 13th April 2017).

[16] V. Brusentsev, W. Vroman, “Wildfires in the United States,” Research Report, Urban Institute, http://www.urban.org/sites/default/files/publication/77201/2000593-Wildfires-in-the-United-States-A-Primer.pdf, (accessed on 13th April 2017).

[17] S. J. Pyne, P. L. Andrews, R. D. Laven, “Introduction to wildland fire,” New York: Wiley, 1996, p. 66.

[18] J. Barrows, "Fire behaviour in Northern Rocky Mountain forests," Missoula, USDA Forest Service Station Pap. 29, 1951, pp. 1-120.

[19] J. R. Holton, J. A. Curry, J. A. Pyle, “Encyclopedia of Atmospheric Sciences, Volumes 1-6 – Wildfire Weather,” Elsevier ISBN 978-0-12-227090-1, 2003.

[20] M. E. Alexander, “Calculating and interpreting forest fire intensities,” *Can. J. Bot.*, Vol. 60, pp. 349-357, 1982.

[21] R. Kremens, A. Smith and M. Dickinson, "Fire Metrology: Current and Future Directions in Physics-Based Measurements," *Fire Ecology,* vol. 6, no. 1, pp. 13-35, 2010.

[22] G. M. Byram, “Combustion of forest fuels,” In: K. P. Davis (editor) “Forest fire: control and use,” McGraw-Hill, New York, NY, pp. 61-89, 1959.

[23] F. Morandini, Y. Perez-Ramirez, V. S. P. Tihay and T. Barboni, "Radiant, convective and heat release characterization of vegetation fire," International Journal Of Thermal Sciences, vol. 70, pp. 83-91, 2013.

[24] J. E. Keeley, "Fire intensity, fire severity and burn severity: a brief review," International Journal of Wildland Fire, vol. 18, pp. 116-126, 2009.

[25] S. W. Taylor, M. E. Alexander and R. G. Pike, Field guide to the Canadian Forest Fire Behavior Prediction (FBP) System, Victoria: Canadian Forest Service, 1996, pp. 9-33.

[26] D. Swanson, T. Helvig, “Effectiveness of direct and indirect attack on wildfire with air-delivered retardants,” Report no. WSCI 0173-14, Northern Forest Fire Laboratory, Missoula.

[27] R. Ault, C. Mooney, J. Thomasson, “Drop patterns for the Bambi-Max bucket and the Bell 212 helitanker, FPInnvoations, Hinton, August 2012.

[28] R. G. Newstead, R.J. Liewskovsky, “Air tanker and fire retardant drop patterns”, Information Report NOR-X-273, Northern Forestry Centre, Canadian Forestry Service, Edmonton, 1985.

[29] G. Lovellette, “How to conduct drop tests of aerial retardant delivery systems”, Aerial Devliery-0E01P06, Technology and Development Program, USDA Forest Service, Missoula, July 2004.

[30] J. E. Grigel, R. G. Newstead, R.J. Liewskovsky, “Air drop tests with helitankers”, Information Report NOR-X-77, Northern Forest Research Centre, Edmonton, February 1974.

[31] G. Johnson, “Ground pattern performance of the marsh turbo thrush”, Report 0057-2835-MTDC, Technology and Development Program, USDA Forest Service, Missoula, April 2000.

[32] A. Suter, “Ground pattern performance of the Griffith Big Dipper Model 100 helibucket”, Report 0057-2829-MTDC, Technology and Development Program, USDA Forest Service, Missoula, April 2000.

[33] C. W. George, “Improving the performance of fire retardant delivery systems on fixed wing aircraft”, Research Note INT-400, Intermountain Research Station, USDA Forest Service, Missoula, February 1992.

[34] C. W. George, “Determining airtanker delivery performance using a simple slide chart-retardant coverage computer”, General Technical Report INT-113, Intermountain Research Station, USDA Forest Service, Missoula, April 1981.

[35] J. E. Grigel, R. G. Newstead, R. J. Liewskovsky, "A review of retardant delivery systems used in fixed-wing airtankers", Information Report NOR-X-134, Northern Forest Reseaerch Centre, Edmonton, May 1975.

[36] A. M. Taber, A. E. Mary, Elenz, Lisa M., P. G. Langowski, "Decision Making for Wildfires: A Guide for Applying a Risk Management Process at the Incident Level," General Technical Report RMRS-GTR-298WWW, Rocky Mountain Research Station, USDA Forest Service, Missoula, 2013.

[37] P. Thomas, R. McAlpine, "Fire in the Forest," Cambridge University Press, Cambridge, United Kingdom, p. 172, November 2010.

[38] G. S. Ramsey, "Forest Fire Management in Canada," Ibero - Americano Fire Fighting Seminar, Brasilia, Brazil, September 1986.

[39] Edward Goldberg, "Use of Fire Chemicals in Aerial Fire Fighting", http://airtanker.org/wp-content/uploads/2012/12/Fire-Chemical-Use-Eddie-Goldberg.pdf (accessed on 13th April 2017).

[40] K. D. Kalabokidis, "Effects of wildfire suppression chemicals on people and the environment—a review," *Global Nest: Int J*, Vol. 2, pp. 129–137, 2000.

[41] A. D. Blakely, "Combustion recovery of flaming pine needle fuel beds sprayed with water/MAP mixtures," Report SD 11.A257 - No. 421, Intermountain Research Station, USDA Forest Service, Utah, USA, May 1990.

[42] Fire and Aviation Management, "Implementation guide for aerial application of fire retardant," Fire and Avition Management, USDA Forest Service, https://www.fs.fed.us/fire/aviation/references/implementation_guide_aerial_application_retardant.pdf, (accessed on 17th April, 2017).

[43] Augeda A, Pastor E, Planas E. “Different scales for studying the effectiveness of long-term forest fire retardants,” *Prog. Energy Combust. Sci.*, Vol. 34, pp. 782-796, 2008.

[44] R. C. Rothermal, C. E. Hardy, “Influence of moisture on effectiveness of fire retardants,” Report no. INT-18, Intermountain Research Station, United States Department of Agriculture (USDA) Forest Service, Ogden, Utah, 1965.

[45] A. Gimenez, E. Pastor, L. Zarate, E. Planas and J. Arnaldos, "Long-term forest fire retardants: a review of quality, effectiveness, application and environmental considerations," *International Journal of Wildland Fire,* Vol. 13, pp. 1-15, 2004.

[46] E. Stechishen, W. G. Murray, “Effectiveness of foam as a fire suppressant,” The Art and Science of Fire Management, Petawawa National Forestry Institute, Ontario, 1990.

[47] USDA Forest Service, “Specification for fire suppressant foam for wildland firefighting (Class A foam),” Specification 5100-307a, United States Department of Agriculture (USDA) Forest Service, Missoula, Montana, 2007.

[48] B. S. Gardiner, B. Z. Dlugogorski, G. J. Jameson, “Rheology of fire-fighting foams,” *Fire Saf. J*, Vol. 31, pp. 61-75, 1998.

[49] W. Drenckhan, A. S. Jalmes, “The science of foaming,” *Adv. Colloid Interface Sci.* Vol. 222, pp. 228-259, 2015.

[50] USDA Forest Service, “Specification for water enhancers (gels) for wildland firefighting”, Specification 5100-306a, United States Department of Agriculture (USDA) Forest Service, Missoula, Montana, 2007.

[51] M.P. Plucinski, G. J. McCarthy, J.J. Hollis, et al., “The effect of aerial suppression on the containment time of Australian wildfires estimated by fire management personnel,” *Int. J. Wildland Fire*, Vol. 21, pp. 219–229, 2012.

[52] M. P. Plucinski, E. Pastor, “Criteria and methodology for evaluating aerial wildfire suppression,” *Int. J. Wildland Fire,* Vol. 22, pp. 1144–1154, 2013.

[53] M.P. Plucinski, J.S. Gould, G.J. McCarthy, et al., “The effectiveness and efficiency of aerial firefighting in Australia,” Report no. A0701, Department of Environment and Conservation, Melbourne, June 2007.

[54] NWCG Fire Equipment Working Team, “Foam vs fire: Class A foam for wildland fires,” Report no. NFES 2246/PMS 446-1, United States Department of Agriculture, USA, October 1993.

[55] NWCG Fire Equipment Working Team, “Foam vs fire: Aerial applications,” Report no NFES 1845/ PMS 446-3, United States Department of Agriculture, USA, October 1995.

[56] S. Liodakis, D. Bakirtzis, A. P. Dimitrakopoulos, “Auto ignition and thermogravimetric analysis of forest species treated with fire retardants,” *Thermochim Acta*, Vol. 399, pp. 31–42, 2003.

[57] J. W. Lyons, “The chemistry and uses of fire retardants,” Malabar, FL: RE Krieger Publishing Company, 1987.

[58] Q. Wang, J. Li, E. Winandy, “Chemical mechanism of fire retardance of boric acid on wood,” *Wood Sci Technol*, Vol. 38, pp. 375–389, 2004.

[59] I. A. Isa, S.W. Jodeh, “Thermal properties of automotive polymers III – thermal characteristics and flammability of fire retardant polymers,” *Mater Res Innov*, Vol.4, pp. 135–143, 2001.

[60] A. D. Pouwels, G. B. Eijkel, J. J. Boon, “Curie-point pyrolysis–capillary gas chromatography high resolution mass spectrometry of micro crystalline cellulose,” *J Anal Appl Pyrol*, Vol. 14, pp. 237–280, 1989.

[61] S. Liodakis, I. Antonopoulos, T. Kakardakis, “Evaluating the use of minerals as forest fire retardants,” *Fire Safety J*, Vol. 45, pp. 98–105, 2010.

[62] A. D. Blakely, “Flammability reduction comparisons of four forest fire retardants,” Research Note INT-381, Intermountain Research Station, Department of Agriculture (USDA) Forest Service, Ogden, Utah, April 1988.

[63] M. P. Plucinski, A. L. Sullivan, R.J. Hurley, “A methodology for comparing the relative effectiveness of suppressant enhancers designed for the direct attack of wildfires”. *Fire Safety J*, Vol. 87, pp. 71-79, 2017.

[64] O. Grexa, H. Lubke, “Flammability parameters of wood tested on a cone calorimeter” *Polym Degrad Stabil*, Vol. 74, pp. 427–432, 2001.

[65] ISO 5660-1:1993. Fire tests—reaction to fire. Part 1—rate of heat release for building products (cone calorimeter method).

[66] ASTM E1321-12, Standard test method for determining material ignition and flame spread properties. ASTM International, West Conshohocken, PA, 2013.

[67] United States Department of Agriculture (USDA) Forest Service, Wildland Fire Chemical Systems, Standard test procedure, Section 2: Fire Tests, STP 2.1-2.2, https://www.fs.fed.us/rm/fire/wfcs/tests/index.htm (2007, accessed on 20 February 2017).

[68] A. M. Tafreshi, M. Di Marzo, “Foams and gels as fire protection agents,” *Fire Safety J*, Vol. 33, pp. 295–305, 1999.

[69] M. A. Dietenberger, A. Shalbafan, J. Welling, et al. “Treated and untreated foam core particleboards with intumescent veneer: comparative analysis using a cone calorimeter,” *J. Therm Anal Calorim*, Vol. 114, pp. 979–987, 2013.

[70] D. K. Shen, M. X. Fang, W. K. Chow, "Ignition of wood based materials by thermal radiation," *Int. J. Eng Perform Based Fire Code*, Vol. 8(2), pp. 69–83, 2006.

[71] J. L. Beverly, B. M. Wotton, "Modelling the probability of sustained flaming: predictive value of fire weather index components compared with observations of site weather and fuel moisture conditions," *Int. J. Wildland Fire*, Vol. 16, pp. 161-173, 2007.

[72] NFPA 2113, Standard on selection, care, use, and maintenance of flame-resistant garments for protection of industrial personnel against short- duration thermal exposures, Quincy, MA, 2015.

[73] S. Anderson, A. McDonald, "Performance testing of wildland fire chemicals using a custom-built heat flux sensor," *J. Fire Sci*, Vol. 33 pp. 473-492, 2015.

[74] M. L. Janssens, "Methods and Equations of Fire Calorimetry," In M. M. Hirschler, R. E. Lyon (eds.), Special Symposium on Fire Calorimetry, Gaithersburg, MD, July 27-28, 1995, pp.11-22.

[75] W. M. Thornton, "The Relation of Oxygen to the Heat of Combustion of Organic Compounds," Philos. Mag., Ser. 6 (33), 196-203 (1917).

[76] S. Anderson, "Quantification of performance of wildfire chemicals using custom-built heat flux sensors," University of Alberta, MSc. Thesis, 2015.

[77] L. Jiji, "Heat Conduction," 3rd ed., Springe-Verlag Berlin Heidelberg, Inc., pp. 72–83, 120–128, 2009.

[78] J. Bray, "Aluminum Mill and Engineered Wrought Products, Properties and Selection: Nonferrous Alloys and Special-Purpose Materials," in ASM Handbook, vol. 2, ASM International, pp. 29-61, 1990.

[79] E. Sullivan, A. McDonald, "Mathematical Model and Sensor Development for Measuring Energy Transfer from Wildland Fires", *Int. J. Wildland Fire*, Vol. 23, pp. 995–1004, 2014.

[80] R. W. Powel, C. Y. Ho, P. E. Liley, "Thermal Conductivity of Selected Materials", National Standard Reference Data Series – National Bureau of Standards – 8 (Category 5 – Thermodynamic and Transport Properties), Issued November 25, 1966.

[81] Y. A. Çengel, A. J. Ghajar, "Heat and Mass Transfer: Fundamentals & Applications," 4th ed., New York: McGraw-Hill, 2011, pp. 12 – 14, 237, 249, 527, 753, 884.

[82] S. Anderson, R. Refai, A. McDonald, "Error reduction in the 'thermal cube' heat flux sensor used in wildland forest fires," #TFESC-12598, In: ASTFE *1st Thermal and Fluids Engineering Summer Conference*, New York, USA, 9 August-12 August 2015.

[83] ASTM D4442-07, Standard Test Methods for Direct Moisture Content Measurement of Wood and Wood-Base Materials, ASTM International, West Conshohocken, PA, 2007.

[84] J.A. Beck, M.E. Alexander, S.D. Harvey, A.K. Beaver, "Forecasting diurnal variations in fire intensity to enhance wildland firefighter safety", *Int. J. of Wildland Fire*, Vol. 11, pp. 173-182, 2002.

[85] ASTM D240-17, Standard Test method for Heat of Combustion of Liquid Hydrocarbon Fuels by Bomb Calorimeter.

[86] Kundu P, Cohen I, Dowling D. *Fluid Mechanics.* 5th ed. California: Academic Press, 2012, p. 803.

[87] ASTM E177-14, Standard Practice for Use of the Terms Precision and Bias in ASTM Test Methods, ASTM International, West Conshohocken, PA, 2013.

[88] ASTM E456-13, Standard Terminology Relating to Quality and Statistics, ASTM International, West Conshohocken, PA, 2013.

[89] R. A. Fisher, "The Arrangement of Field Experiments," *Jrnl of the Ministry of Agric.,* Vol. 33, pp. 504.

[90] G.W. Burns GW and M.G. Scroger, "The calibration of thermocouples and thermocouple materials," NIST Special Publication 250-35, NIST Measurement Services, 1989.

[91] J. R. Taylor, "An Introduction to Error Analysis: The Study of Uncertainties in Physical Measurements," 2nd ed., Sausalito, California: University Science Books, pp. 13, 60-66, 1996.

[92] USDA Forest Service - Wildland Fire Chemicals, https://www.fs.fed.us/rm/fire/wfcs/ (accessed on 21 March 2017)

[93] Omegalux QF, QG, QC, and QH Series Infrared Radiant Panel, Operator's Manual, Omega Engineering Incorporated, 1991.

8 APPENDIX

1. Modified Heat Flux Sensor Block Engineering Drawing [76]

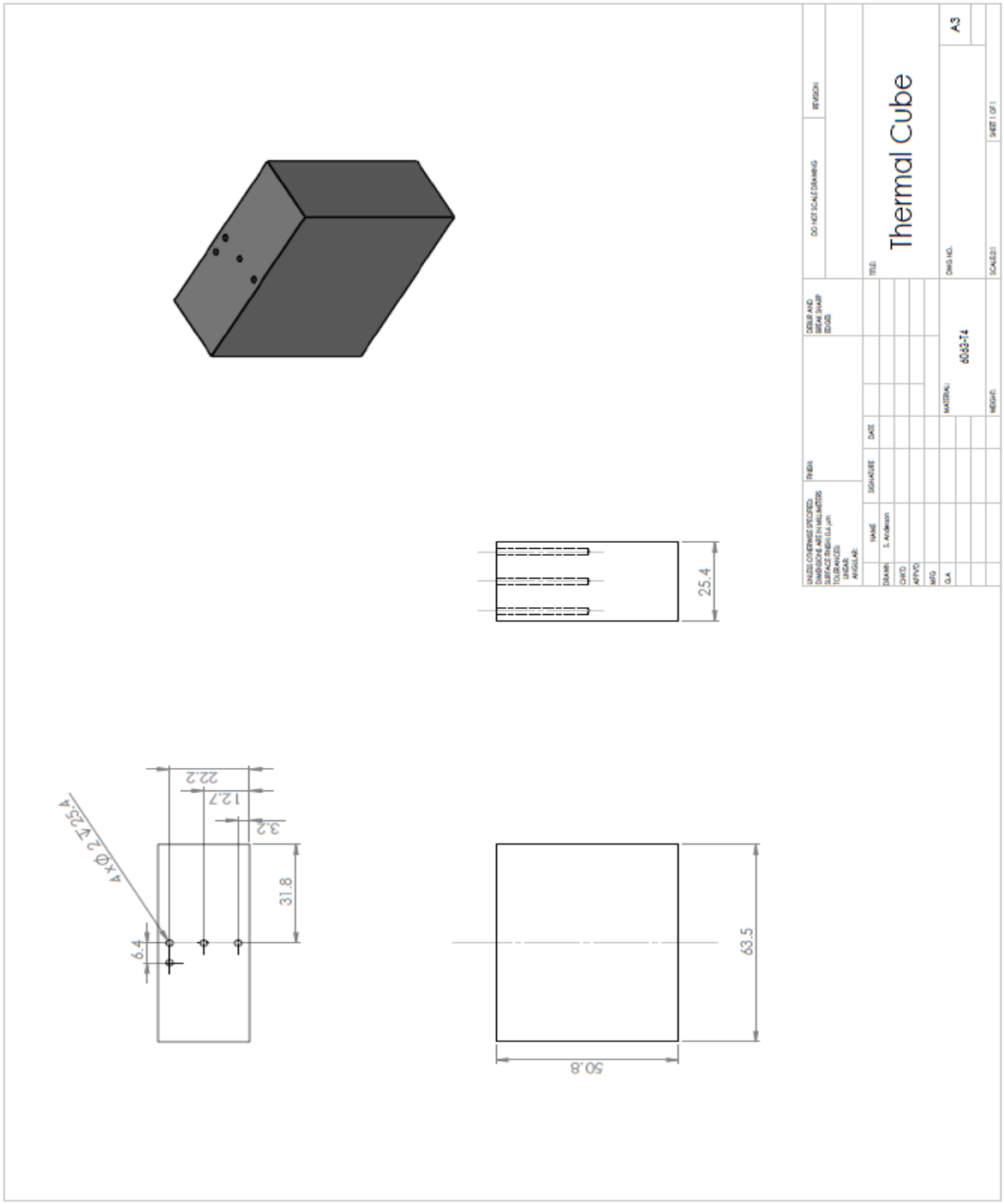

2. Omega Radiant Heater Specifications [93]

SECTION 5 SPECIFICATIONS

5.1 GENERAL SPECIFICATIONS

VOLTAGE:

QF SERIES:	120 VAC, 480 VAC, 1 and 3 phase 120/240, 240/480 VAC dual voltage, 1 phase
QG SERIES:	120, 240 and 480 VAC, 1 phase 120/240, 240/480 VAC dual voltage, 1 phase
QC, QH SERIES:	240 VAC, 1 phase 240/480 VAC dual voltage, 1 phase

WATTAGE:

QF SERIES:	720 - 21,600 watts
QG SERIES:	720 - 8640 watts
QC, QH SERIES:	1660 - 8640 watts

MAXIMUM OPERATING TEMPERATURE:

QF, QG SERIES:	1600°F
QC, QH SERIES:	1800°F

DIMENSIONS: See specific Series specifications in Sections 5.2 through 5.4.

Omega Radiant Heater Specifications [93]

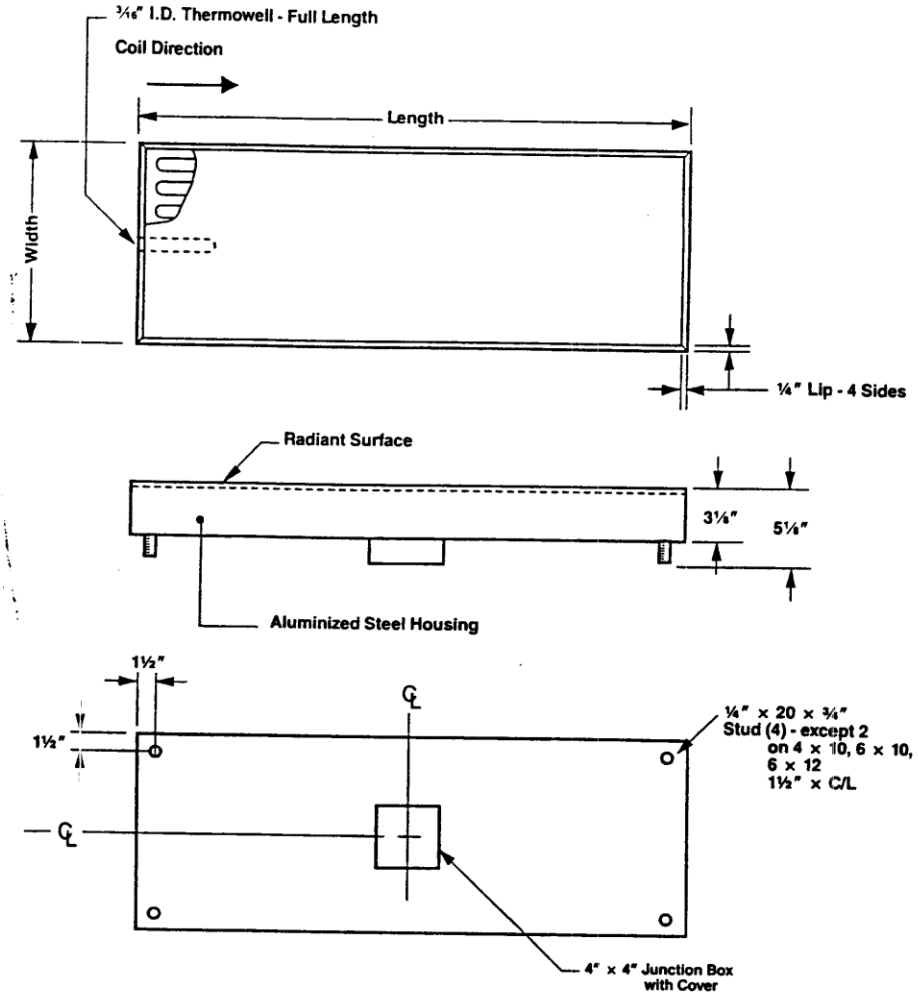

Width (in.)	Length (in.)	Wattage	Voltage	Phase	Without Thermowell Model No.	With Thermowell Model No.
40 W/in² QC Series						
4	10	1600	240	1	QC-041040	QC-041040-T
6	10	2400	240/480	1	QC-061040	QC-061040-T
8	10	3200	240/480	1	QC-081040	QC-081040-T
10	10	4000	240/480	1	QC-101040	QC-101040-T
12	10	4800	240/480	1	QC-121040	QC-121040-T
6	12	2880	240/480	1	QC-061240	QC-061240-T
12	12	5760	240/480	1	QC-121240	QC-121240-T
60 W/in² QH Series						
4	10	2400	240/480	1	QH-041060	QH-041060-T
6	10	3600	240/480	1	QH-061060	QH-061060-T
8	10	4800	240/480	1	QH-081060	QH-081060-T
10	10	6000	240/480	1	QH-101060	QH-101060-T
12	10	7200	240/480	1	QH-121060	QH-121060-T
6	12	4320	240/480	1	QH-061260	QH-061260-T
12	12	8640	240/480	1	QH-121260	QH-121260-T

3. Thermal Canister Engineering Drawings [76]

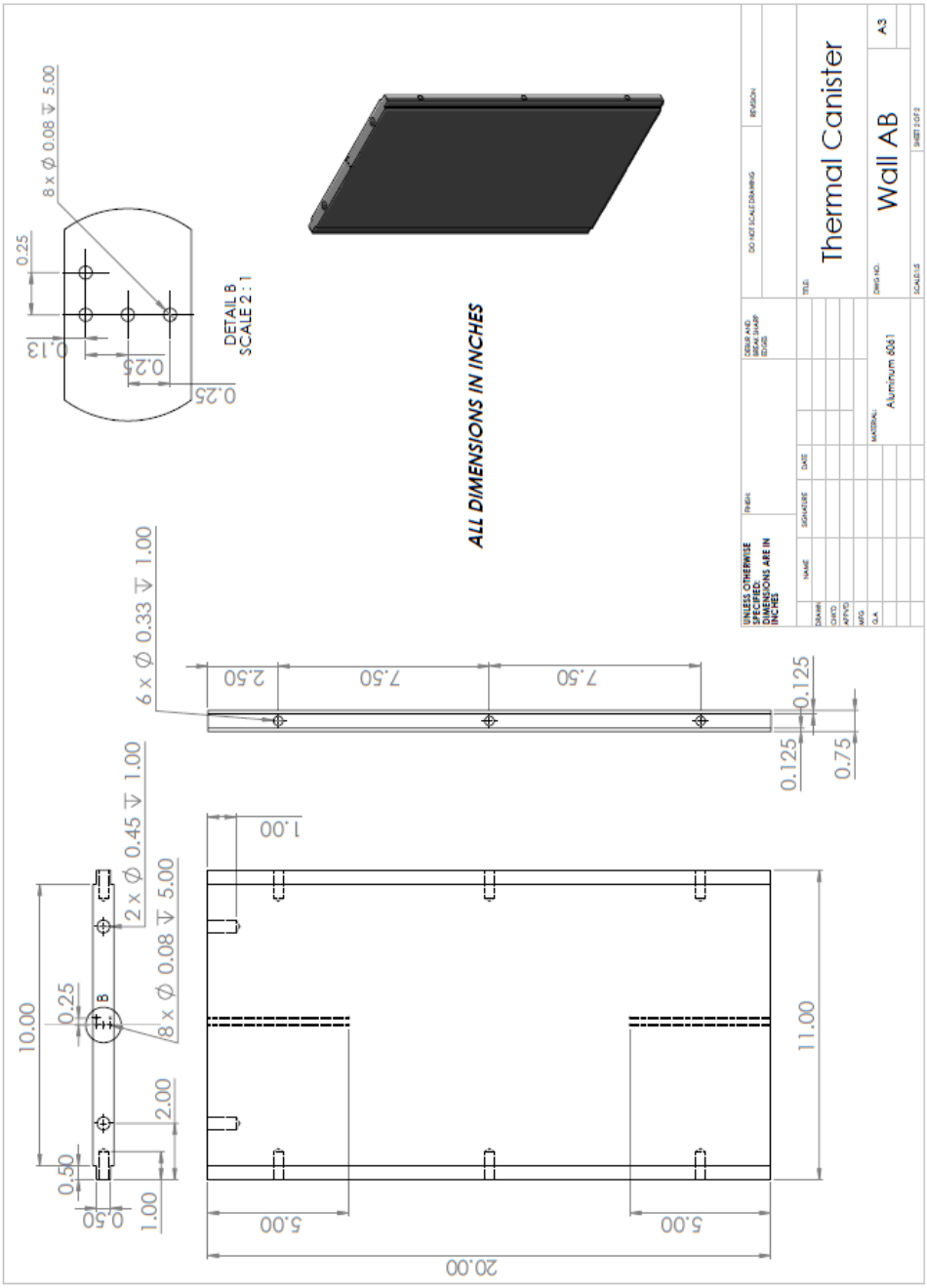

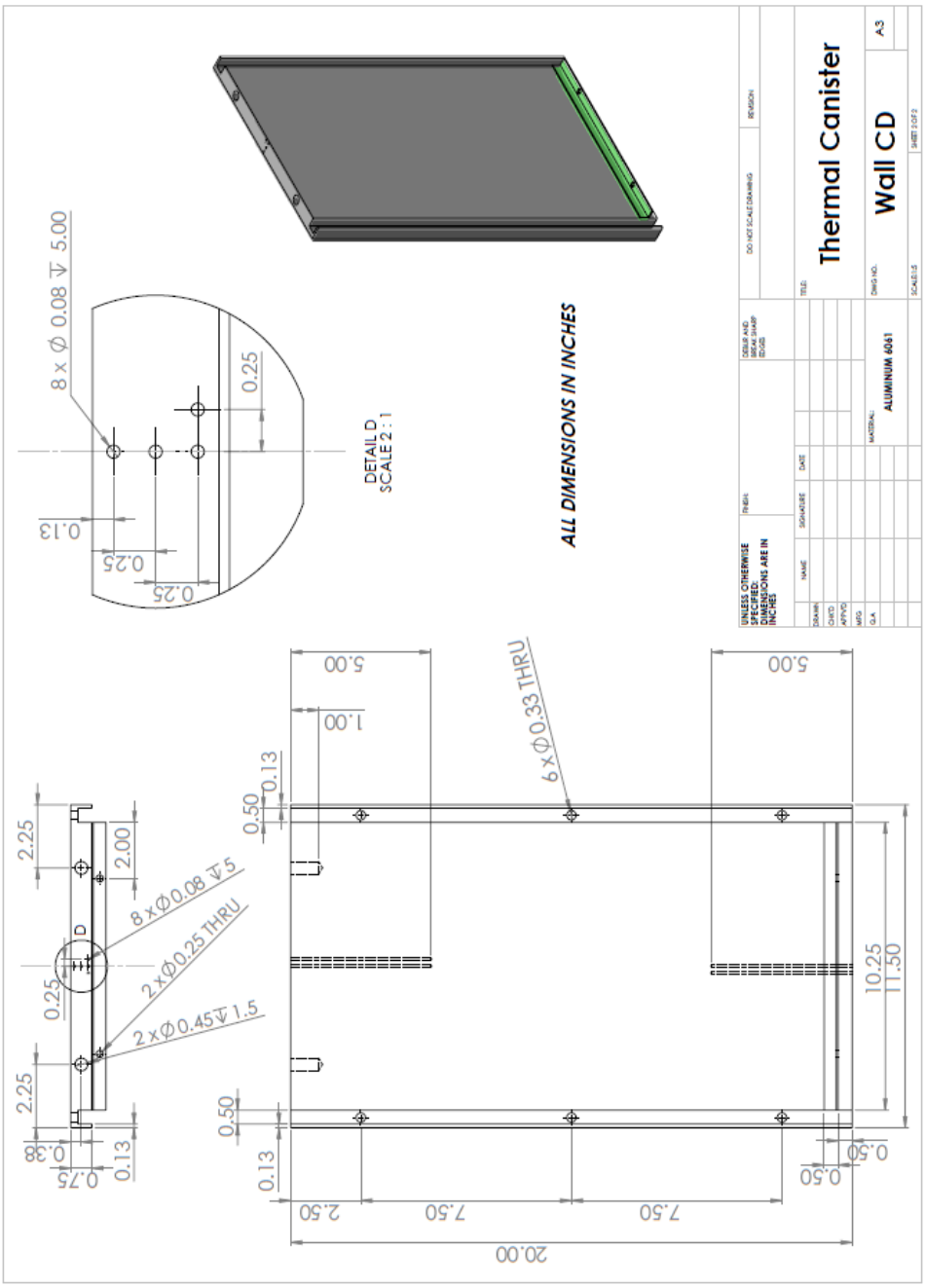
Thermal Canister
Wall CD
A3
ALUMINUM 6061
ALL DIMENSIONS IN INCHES
DETAIL D
SCALE 2 : 1
8 x Ø 0.08 Ⓜ 5.00
0.25
0.13
0.25
0.25
5.00
1.00
0.13
0.50
6 x Ø0.33 THRU
5.00
2.25
2.00
8 x Ø0.08 Ⓜ 5
2 x Ø0.25 THRU
2 x Ø0.45 Ⓜ 1.5
0.25
2.25
0.38
0.75
0.13
0.50
0.13
10.25
11.50
0.50
2.50
7.50
7.50
20.00

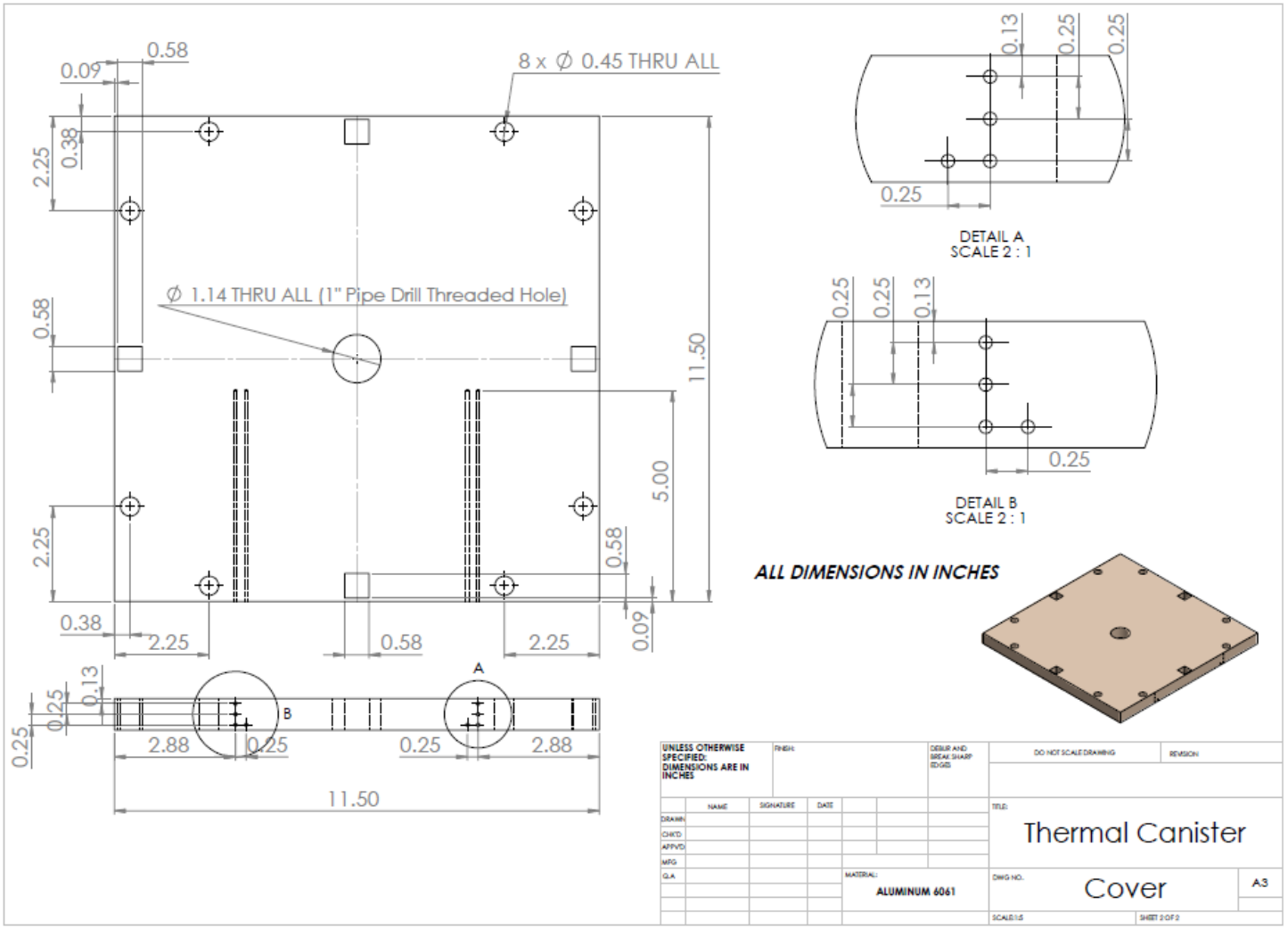
8 x ∅ 0.45 THRU ALL
∅ 1.14 THRU ALL (1" Pipe Drill Threaded Hole)
0.09
0.58
0.38
2.25
0.58
11.50
5.00
2.25
0.58
0.09
0.38
2.25
0.58
2.25
0.13
0.25
0.25
A
B
2.88
0.25
0.25
2.88
11.50
0.13
0.25
0.25
0.25
DETAIL A
SCALE 2 : 1
0.25
0.25
0.13
0.25
DETAIL B
SCALE 2 : 1
ALL DIMENSIONS IN INCHES
UNLESS OTHERWISE SPECIFIED: DIMENSIONS ARE IN INCHES
FINISH:
DEBUR AND BREAK SHARP EDGES
DO NOT SCALE DRAWING
REVISION
NAME
SIGNATURE
DATE
DRAWN
CHKD
APPVD
MFG
Q.A
MATERIAL:
ALUMINUM 6061
TITLE:
Thermal Canister
Cover
DWG NO.
A3
SCALE:1:5
SHEET 2 OF 2

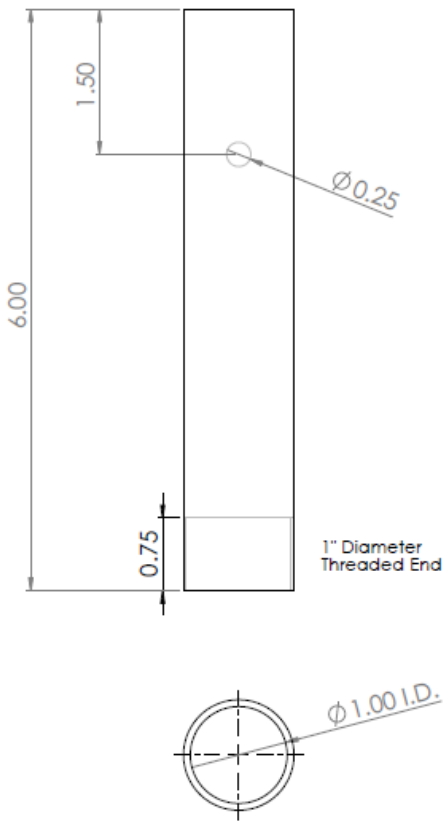

ITEM NO.	DESCRIPTION	MTL	QTY.
1	1" Diameter Tube	Aluminum	1

ALL DIMENSIONS IN INCHES

UNLESS OTHERWISE SPECIFIED: DIMENSIONS ARE IN INCHES		FINISH:		DEBUR AND BREAK SHARP EDGES		DO NOT SCALE DRAWING	REVISION
	NAME	SIGNATURE	DATE				
DRAWN						TITLE: Thermal Canister	
CHK'D							
APPV'D							
MFG							
QA				MATERIAL: Aluminum Tube		DWG NO. Exhaust Pipe	A3
						SCALE:1:2	SHEET 1 OF 1